National Library of Canada
Bibliothèque nationale du Canada

Canadian Theses Service
Service des thèses canadiennes

Ottawa, Canada
K1A 0N4

NOTICE

The quality of this microform is heavily dependent upon the quality of the original thesis submitted for microfilming. Every effort has been made to ensure the highest quality of reproduction possible.

If pages are missing, contact the university which granted the degree.

Some pages may have indistinct print especially if the original pages were typed with a poor typewriter ribbon or if the university sent us an inferior photocopy.

Reproduction in full or in part of this microform is governed by the Canadian Copyright Act, R.S.C. 1970, c. C-30, and subsequent amendments.

AVIS

La qualité de cette microforme dépend grandement de la qualité de la thèse soumise au microfilmage. Nous avons tout fait pour assurer une qualité supérieure de reproduction.

S'il manque des pages, veuillez communiquer avec l'université qui a conféré le grade.

La qualité d'impression de certaines pages peut laisser à désirer, surtout si les pages originales ont été dactylographiées à l'aide d'un ruban usé ou si l'université nous a fait parvenir une photocopie de qualité inférieure.

La reproduction, même partielle, de cette microforme est soumise à la Loi canadienne sur le droit d'auteur, SRC 1970, c. C-30, et ses amendements subséquents.

NL-339 (r. 88/04) c

Canada

UNIVERSITY OF ALBERTA

A CLASS OF VISCOELASTIC WAVES IN RODS AND FLUID FILLED TUBES

BY

YANNING PENG

A thesis submitted to the Faculty of Graduate Studies and Research in partial fulfillment of the requirements for the degree of MASTER OF SCIENCE.

DEPARTMENT OF MATHEMATICS

EDMONTON, ALBERTA

FALL 1991

National Library of Canada
Bibliothèque nationale du Canada

Canadian Theses Service
Service des thèses canadiennes

Ottawa, Canada
K1A 0N4

The author has granted an irrevocable non-exclusive licence allowing the National Library of Canada to reproduce, loan, distribute or sell copies of his/her thesis by any means and in any form or format, making this thesis available to interested persons.

The author retains ownership of the copyright in his/her thesis. Neither the thesis nor substantial extracts from it may be printed or otherwise reproduced without his/her permission.

L'auteur a accordé une licence irrévocable et non exclusive permettant à la Bibliothèque nationale du Canada de reproduire, prêter, distribuer ou vendre des copies de sa thèse de quelque manière et sous quelque forme que ce soit pour mettre des exemplaires de cette thèse à la disposition des personnes intéressées.

L'auteur conserve la propriété du droit d'auteur qui protège sa thèse. Ni la thèse ni des extraits substantiels de celle-ci ne doivent être imprimés ou autrement reproduits sans son autorisation.

ISBN 0-315-70184-6

Canada

UNIVERSITY OF ALBERTA

RELEASE FORM

NAME OF AUTHOR: YANNING PENG

TITLE OF THESIS: A CLASS OF VISCOELASTIC WAVES IN RODS AND FLUID FILLED TUBES

DEGREE FOR WHICH THESIS WAS PRESENTED: MASTER OF SCIENCE

YEAR THIS DEGREE GRANTED 1991

Permission is hereby granted to the UNIVERSITY OF ALBERTA LIBRARY to reproduce single copies of the thesis and to lend or sell such copies for private, scholarly or scientific research purposes only.

The author reserves other publication rights, and neither the thesis nor extensive extracts from it may be printed or otherwise reproduced without the author's written permission.

Yanning Peng

SIGNED

PERMANENT ADDRESS:

Department of Alberta

University of Alberta

Edmonton, Alberta T6G 2G1

Date Aug. 15, 1991

UNIVERSITY OF ALBERTA

THE FACULTY OF GRADUATE STUDIES AND RESEARCH

The undersigned certify that they have read, and recommend to the Faculty of Graduate Studies and Research, for acceptance, a thesis entitled A CLASS OF VISCOELASTIC WAVES IN RODS AND FLUID FILLED TUBES submitted by YANNING PENG in partial fulfillment of the degree of Master of Science.

R.J. Tait
Supervisor

M. Kovalyov

Y.S. Wong

M.G. Faulkner

Date Aug. 15, 1991

To My Parents and Jidong

ABSTRACT

In this thesis, one dimensional wave propagation in linear viscoelastic rods and fluid filled viscoelastic tubes is studied. The wall displacement function for a fluid filled viscoelastic tube is obtained as an inverse Laplace transform. This differs from the expression obtained by Pipkin [19] for longitudinal displacement in a viscoelastic rod by a term containing η which is related to the radial inertia of the tube. A class of viscoelastic relaxation functions are considered in [19] for which the wave generated by a step input at $t = 0$ approaches a constant shape at large distances. These shapes can be tabulated as probability distribution functions. The classification depends on the behavior of the apparent viscosity of the viscoelastic material. For fluid filled viscoelastic tubes, using the same classification, we investigate the behavior of the wall displacement and the fluid mean pressure analytically and numerically for two types of initial inputs. The step function input is used to compare and contrast the results with [19] and a smooth input is used to compare the results with experiment. Depending on the type of the viscoelasticity and on the radial inertia term η, the result may be a probability distribution function or may be oscillatory.

Acknowledgement

I wish to express my sincere thanks to my supervisor, Professor R.J. Tait. I am deeply indebted to him for his invaluable guidance and great amount of effort spent on this thesis.

I would also like to thank Drs. Y.S. Wong, M. Kovalyov and M.G. Faulkner for their careful proofreading and helpful comments on this thesis.

I am very grateful for the financial support from Dr. R.J. Tait and the Department of Mathematics, University of Alberta. I am very thankful to the advise from Mrs. M. Benedict for the use of *TeX* and her constant help.

Finally, special thanks are due to my husband and my overseas family for their limitless love and continuous encouragement.

TABLE OF CONTENTS

		Page
Abstract		
Acknowledgement		
List of Figures		
Chapter 1.	Introduction	1
Chapter 2.	Viscoelasticity	5
Chapter 3.	Governing Equations for Fluid Filled Viscoelastic Tubes	16
Chapter 4.	Reduction to Probability Distributions for Rod Problem	23
Chapter 5.	Transformed Solution and the Steepest Descents for Tube Problems	56
Chapter 6.	Numerical Procedures and Conclusions	73
Bibliography		106

LIST OF FIGURES

Figure — Page

Fig.[2-1]. Variation of stress-relaxation modulus $G(t)$ $(--)$ and storage modulus $G_1(\omega)$ $(—)$ for (I) PMMA and (II) Hevea. 9

Fig.[2-2]. Variation of loss tangent with frequency for (I) PMMA and (II) Hevea. 10

Fig.[2-3]. [2-3.1]. Variation of stress-relaxation modulus $(--)$ and storage modulus $(—)$, [2-3.2] Variation of loss tangent with frequency for (1) Kelvin-Voigt, (2) Maxwell, (3) Standard linear model. 11

Fig.[2-4]. [2-4.1] Constant slope of stress-relaxation modulus and storage modulus, [2-4.2] Constant loss tangent of power-law solid. 12

Fig.[4-1]. The contour of integration for the inverse Laplace transform of $\dfrac{1}{\sqrt{s\overline{G}(s)}}$. 38

Fig.[5-1]. The graph of $\dfrac{t}{x} = \dfrac{1+\frac{\tau}{2}s}{(1+\tau s+\hat{\eta}s^2)^{3/2}}$. 59

Fig.[5-2]. The nonuniformity behavior of $\dfrac{t}{\hat{x}} = \dfrac{(1-p/2)s^p}{(s^p+\hat{\eta}s^2)^{3/2}}$. 64

Fig.[5-3]. The graph of $\dfrac{t}{\hat{x}} = \dfrac{G_\infty+(1-\frac{1}{2}p)s^p}{(G_\infty+s^p+\eta s^2)^{3/2}}$. $G_\infty = 0.05$, $p = 0.05$, $\eta = 0.173125$, $\hat{x} = 6$. 68

Fig.[5-4]. Plots of equation (5.42), $W(\hat{x},t)$ for the case $s\overline{G}(s) = \hat{c}s^p$. Fig.[5-4.1] shows that the maximum point happens at $K_0 < 1$, so that $\hat{x}/t < 1$. The wave is faster than the purely elastic case with $\hat{\eta}$ omitted. Fig.[5-4.2] shows that for $\hat{\eta} = 0$, the viscoelastic wave $(p > 0)$ is faster than the pure elastic case $(p = 0)$. 71

Fig.[5-5]. Plots of equation (5.53), $W(\hat{x},t)$ when $s\overline{G}(s) = G_\infty + \hat{c}s^p, G_\infty > 0$. Fig.[5-5.1] shows that wave is faster at $\eta = 0$ then at $\eta > 0$. Fig.[5-5.2] shows that wave goes faster with the incresing of G_∞. 72

Fig.[6-1]. The graph of $p_m(x,t)$ with $\Omega(s) = \dfrac{s}{\sqrt{1+\tau s+\eta s^2}}$ at $x = 6cms$, $\tau = 9*10^{-5}$, $\eta = 0.173125$. 80

Fig.[6-2]. The graph of $p_m(x,t)$ with $\Omega(s) = \frac{s}{\sqrt{1+\tau s+\eta s^2}}$ at $x = 11cms$, $\tau = 9 * 10^{-5}$, $\eta = 0.173125$. 81

Fig.[6-3]. The graph of $p_m(x,t)$ with $\Omega(s) = \frac{s}{\sqrt{1+\tau s}}$ at $x = 6cms$, $\tau = 9 * 10^{-5}$. 82

Fig.[6-4]. The graphs of $p_m(x,t)$ with $\Omega(s) = \frac{s}{\sqrt{1+\tau s+\eta s^2}}$ at $x = 6cms$, $\tau = 9 * 10^{-5}$, and different choices of η. 83

Fig.[6-5]. The graph of $p_m(x,t)$ with $\Omega(s) = \frac{s}{\sqrt{\hat{c}s^p}}$ at x=6cms, $\hat{c}$=1, p=0.05. 84

Fig.[6-6]. The graphs of $p_m(x,t)$ with $\Omega(s) = \frac{s}{\sqrt{\hat{c}s^p+\eta s^2}}$ at x=6cms, $\hat{c}$=1, p=0.05 for various η. 85-86

Fig.[6-7]. The graphs of $p_m(x,t)$ with $\Omega(s) = \frac{s}{\sqrt{\hat{c}s^p+\eta s^2}}$ at x=6cms, $\hat{c}$=1, η=0.173125 for various p. 87-88

Fig:[6-8]. The graphs of $p_m(x,t)$ with $\Omega(s) = \frac{s}{\sqrt{\hat{c}s^p+\eta s^2}}$ at x=6cms, p=0.05, η=0.173125 for various $\hat{c}$. 89-90

Fig.[6-9]. The graph of $p_m(x,t)$ with $\Omega(s) = \frac{s}{\sqrt{G_\infty+s^p+\eta s^2}}$ at x=6cms, p=0.05, G_∞=0.1, η=0. 91

Fig.[6-10]. The graphs of $p_m(x,t)$ with $\Omega(s) = \frac{s}{\sqrt{G_\infty+s^p+\eta s^2}}$ at x=6cms, p=0.05, η=0.1 and various G_∞. 92-93

Fig.[6-11]. The graphs of $p_m(x,t)$ with $\Omega(s) = \frac{s}{\sqrt{G_\infty+s^p+\eta s^2}}$ at x=6cms, p=0.05, G_∞=0.1 and various η. 94-95

Fig.[6-12]. Figs.[6-3], [6-5] & [6-9] on one axis of coordinates. 96

Fig.[6-13]. W(x,t) with step input and $s\overline{G}(s) = 1 + s$, at $x = 6$. 97

Fig.[6-14]. W(x,t) with step input and $s\overline{G}(s) = 1 + s^2$, at $x = 6$. 98

Fig.[6-15]. W(x,t) with step input and $s\overline{G}(s) = 1 + s + \frac{1}{4}s^2$, at $x = 6$. 99

Fig.[6-16]. W(x,t) with step input and $s\overline{G}(s) = s^p$, at $x = 6$, $p = 0.05$. 100

Fig.[6-17]. W(x,t) with step input and $s\overline{G}(s) = s^p + s^2$, at $x = 6$, $p = 0.05$. 101

Fig.[6-18]. W(x,t) with step input and $s\overline{G}(s) = 1 + s^p$, at $x = 6$, $p = 0.05$. 102

Fig.[6-19]. W(x,t) with step input and $s\overline{G}(s) = 1 + s^p + s^2$, at $x = 6$, $p = 0.05$. 103

Fig.[6-20]. W(x,t) with step input and $s\overline{G}(s) = s$, at $x = 6$, $p = 0.05$. 104

Fig.[6-21]. W(x,t) with step input and $s\overline{G}(s) = s + s^2$, at $x = 6$, $p = 0.05$. 105

Chapter 1. Introduction

The study of waves in fluid-filled flexible tubes appears to date from Euler [1], who studied blood flow in arteries using a one-dimensional model. Since then, depending on the wall properties, the fluid properties and the dominant effects being considered, the basic concept has been extended and two main routes for modeling the problem have emerged.

If large variation in cross sectional area occurs, as in studying collapsible tubes, Euler's one-dimensional model has been extended to a quasi-linear hyperbolic system, and the continuity and momentum equations are written as

$$\frac{\partial}{\partial t}(\rho A) + \frac{\partial}{\partial x}(\rho A u) + \Psi = 0 \tag{1.1}$$

$$\rho(\frac{\partial u}{\partial t} + \frac{\partial}{\partial x}\frac{u^2}{2}) + \frac{\partial p_r}{\partial x} + \Phi = 0 \tag{1.2}$$

together with a relation of the form

$$\begin{aligned} p_r &= \Lambda(A, x, t) \\ u &= \Omega(A, x, t) \end{aligned} \tag{1.3}$$

where $A(x,t)$ is the cross-sectional area of the tube, ρ,u are the density and axial velocity of the fluid respectively, and p_r is the excess pressure in the fluid measured from a suitable reference p_0. Φ and Ψ are correction terms introduced to allow for leakage and frictional effects, t and x denote time and axial coordinates respectively.

The constitutive equation for the wall is given by the first of equations (1.3). For a review of the problems treated in this way, especially with a view to biological applications, we refer to the articles by Skalak et al [2], [3], Fung [4], and the book of Caro et al [5].

In particular, Lighthill [6] discusses the equations and their linearisation in the form

$$\begin{aligned}\frac{\partial^2 p_r}{\partial x^2} &= \frac{1}{A_0}\Big(\frac{\partial(\rho A)}{\partial p_r}|_{p_r=0}\Big)\frac{\partial^2 p_r}{\partial t^2} \\ &= \frac{1}{A_0}\Big(A\frac{\partial \rho}{\partial p_r} + \rho\frac{\partial A}{\partial p_r}\Big)|_{p_r=0}\,\frac{\partial^2 p_r}{\partial t^2},\end{aligned} \tag{1.4}$$

where A_0 is the reference value of the cross-sectional area.

In the simplest case, assume the thickness of the wall is fixed. Along with the changes in diameter, a circumferential stress or hoop stress exists. Under this condition, we get the following expression

$$\frac{A - A_0}{A_0} = \frac{2R\rho}{hE}(1-\sigma^2), \tag{1.5}$$

where R is the mean radius of the tube, h the wall thickness, E the Young's modulus of the wall material and σ the Poisson's ratio. We assume here that the wall is made of isotropic material, the factor $(1-\sigma^2)$ being introduced due to the assumption that the wall is longitudinally tethered. Equation (1.4) then becomes

$$\frac{\partial^2 p_r}{\partial x^2} = \Big(\frac{1}{c_s^2} + \frac{1}{c_0^2}\Big)\frac{\partial^2 p_r}{\partial t^2}, \tag{1.6}$$

with c_s the speed of the sound in the fluid, and

$$c_0^2 = \frac{hE}{2R\rho(1-\sigma^2)}.$$

Since $c_s = 1400 m/s$ for water, while the pulse speeds to be considered below have $c_0 = 10 m/s$, the compressibility effects may be neglected. Thus for many cases a linear theory of the type discussed below is adequate. For recent advances in considering nonlinear effects, we refer to [7], [8].

The second approach is to deal with the linearised equations. A good survey is given by Rubinow and Keller [9], [10] for propagation of a simple harmonic wave, and details for pulse propagation may be found in [11]. Certain effects, such as

shock wave propagation, can not be predicted by linear theory. Nevertheless, when the main effect is that of dispersion, a linearisation may well be effective. [12] gives a good example of a linear, one-dimensional model for impulse wave propagation by taking account of the dispersion relation. The speed and amplitude of the wave in a water filled latex tube, obtained experimentally by Greenwald and Newmann [13] are adequately described by this simple viscoelastic model.

In the linear theory of fluid filled flexible tubes, it is clear that the viscoelasticity of the wall plays an important part. The difficulty is in finding a suitable relaxation function valid for different materials. Pipkin [14] has suggested a way around this difficulty using an idea of Kolsky's [15] who discovered the phenomenon of a universal pulse shape in experiments on three polymers. Based on this idea, in Chapter 2, we show that these kinds of materials have the properties of near constant loss angle over a broad range of frequency and the initial precursor wave is negligible compared with the main contribution of the wave form at large t. We use both the Laplace and Fourier transforms. In Chapter 3, we introduce the governing equations and the general solutions of the wave propagation in a fluid filled viscoelastic tube. In Chapter 4, we consider in detail the results by Pipkin [19] that the pulse propagation in a linear viscoelastic rod approaches a constant shape, and the shape functions can be tabulated as stable probability distribution functions. In Chapter 5, we concentrate on the asymptotic discussion of wave propagation in a fluid filled viscoelastic tube by considering three relaxation functions which are of the same classes as those considered in Chapter 4 so that the results can be compared. Finally in Chapter 6, we explain the numerical methods used and display the graphs of the mean pressure function for the various choices of the coefficients. Furthermore, we show the relations between the displacement and mean pressure functions, and illustrate that in the case of a fluid filled viscoelastic tube, which differs from a rod by the presence of a factor η, the mean

pressure function may have oscillation, and therefore the displacement function can not in general be tabulated as a probability distribution function.

Chapter 2. Viscoelasticity

Since we confine our attention to a one-dimensional model in which the stress $\sigma(x,t)$ and the strain $\varepsilon(x,t)$ depend on a single material coodinate x and time t, we assume a constitutive stress history of linear viscoelasticity

$$\sigma(x,t) = \int_{-\infty}^{t} G(t-s)\, d\varepsilon(x,s), \tag{2.1}$$

where the integral is a Stieltje's integral, together with the other basic equations

$$\begin{aligned} \frac{\partial \sigma}{\partial x} &= \frac{\partial^2 u}{\partial t^2}, \\ \varepsilon &= \frac{\partial u}{\partial x}, \\ v &= \frac{\partial u}{\partial t}, \end{aligned} \tag{2.2}$$

where u and v are displacement and velocity respectively, and $G(t)$ represents the particular material stress relaxation modulus with $G(t) = 0$ for $t < 0$. In general, for a solid, $G(t)$ will have an instantaneous modulus $G_0 = G(t = 0^+)$ and a relaxed modulus $G_\infty = G(t = \infty)$, and is a monotone decreasing function.

The above equations are in nondimensional form, and are obtained from the dimensional ones by setting

$$\begin{aligned} (\hat{G},\ \hat{\sigma}) &= (G,\ \sigma)/G_r, \\ (\hat{x},\ \hat{u}) &= (x,\ u)/L, \\ \hat{t} &= tc_0/L, \end{aligned} \tag{2.3}$$

where L is a reference length, $c_0^2 = G_r/\rho$, G_r is a suitable reference modulus and ρ the density of the fluid. The hats are dropped in the final version.

We consider the initial and boundary value problem with

$$u(x,0) = v(x,0) = 0, \quad v(0,t) = f(t). \tag{2.4}$$

There are advantages to both the Fourier and Laplace transform approaches. Assuming $\int_0^t G(t)dt < \infty$, $t > 0$, we begin with the Fourier transform

$$\tilde{\varphi} = \int_0^\infty \varphi(x,t)e^{-i\omega t}\,dt, \tag{2.5}$$

and set

$$G^*(\omega) = G_\infty + i\omega \int_0^\infty [G(t) - G_\infty]e^{-i\omega t}dt. \tag{2.6}$$

Then assuming quiescent condition for $t < 0$, we have

$$\tilde{\sigma} = G^*(\omega)\tilde{\varepsilon}, \tag{2.7}$$

$$\tilde{\varepsilon} = \tilde{u}_x, \tag{2.8}$$

$$\tilde{v} = i\omega\tilde{u}, \tag{2.9}$$

$$\tilde{\sigma}_x = -\omega^2\tilde{u}. \tag{2.10}$$

So that

$$\tilde{v}(x,\omega) = \tilde{f}(\omega)e^{-i\omega x/\sqrt{G^*(\omega)}}, \tag{2.11}$$

and

$$v(x,t) = \frac{1}{2\pi}\int_{-\infty}^{\infty} \tilde{f}(\omega)e^{i\omega t - i\omega x/\sqrt{G^*(\omega)}}\,d\omega, \tag{2.12}$$

$$\tilde{f}(\omega) = \int_0^\infty f(t)e^{-i\omega t}\,dt.$$

The deduction of equation (2.7) is as follows.

$$\begin{aligned}\sigma(x,t) &= \varepsilon_0 G(t) + \int_0^t G(t-s)\,d\varepsilon(x,s) \\ &= G_\infty\varepsilon(t) + \varepsilon_0[G(t) - G_\infty] + \int_0^t [G(u) - G\infty]\varepsilon'(t-u)\,du.\end{aligned}$$

So that

$$\begin{aligned}
\tilde{\sigma} &= G_\infty \tilde{\varepsilon} + \varepsilon_0(\tilde{G} - \tilde{G_\infty}) + \int_0^\infty e^{-i\omega t}\,dt \int_0^t [G(u) - G_\infty]\varepsilon'(t-u)\,du \\
&= G_\infty \tilde{\varepsilon} + \varepsilon_0(\tilde{G} - \tilde{G_\infty}) + \int_0^\infty [G(u) - G_\infty]e^{-i\omega u}\,du \int_0^\infty \varepsilon'(p)e^{-i\omega p}\,dp \\
&= G_\infty \tilde{\varepsilon} + \varepsilon_0[\tilde{G} - \tilde{G_\infty}] + \int_0^\infty [G(u) - G_\infty]e^{-i\omega u}du \\
&\left[\varepsilon(p)e^{-i\omega p}|_o^\infty + i\omega \int_0^\infty \varepsilon(p)e^{-i\omega p}dp\right] \\
&= G^*(\omega)\tilde{\varepsilon}.
\end{aligned}$$

The Laplace transform on the other hand leads to the results

$$\overline{\varphi}(s) = \int_0^\infty \varphi(t)e^{-st}\,dt, \tag{2.13}$$

$$\overline{v}(x,s) = \overline{f}(s)e^{-xs/\sqrt{s\overline{G}(s)}}, \tag{2.14}$$

$$v(x,t) = \frac{1}{2\pi i}\int_{Br} \overline{f}(s)e^{st - xs/\sqrt{s\overline{G}(s)}}\,ds. \tag{2.15}$$

Where

$$\overline{G}(s) = \int_0^\infty e^{-st}G(t)\,dt, \quad \Re(s) > 0, \tag{2.16}$$

$$\overline{f}(s) = \int_0^\infty e^{-st}G(t)\,dt,$$

If we have a sinusoidal input $\varepsilon(t) = \varepsilon_0 e^{-i\omega t}$, $t > 0$, with amplitude ε_0 and radian frequency ω, then

$$\begin{aligned}
\sigma(t) &= G(t)\varepsilon(0) + \int_0^t G(t-s)\varepsilon'(s)\,ds \\
&= G(t)\varepsilon(t) + \int_0^t [G(s) - G(t)]\varepsilon'(t-s)\,ds \\
&= G(t)\varepsilon_0 e^{i\omega t} + \varepsilon_0 i\omega e^{i\omega t}\int_0^t [G(s) - G(t)]e^{-i\omega s}\,ds \\
&\to G^*(\omega)\varepsilon_0 e^{i\omega t} = G^*(\omega)\varepsilon(t), \quad \text{as} \quad t \to \infty.
\end{aligned} \tag{2.17}$$

Assuming the integral (2.6) converges, the constant $G^*(\omega)$ is called the complex or dynamic modulus. $G^*(\omega)$ can be computed in terms of the Laplace transform and

$$G^*(\omega) = \lim_{r \to 0^+} (r + i\omega)\overline{G}(r + i\omega). \tag{2.18}$$

We argue as follows: If $r > 0$

$$\begin{aligned}(r + i\omega)\overline{G}(r + i\omega) &= (r + i\omega)\int_0^\infty e^{-(r+i\omega)t}G(t)\,dt \\ &= (r + i\omega)\int_0^\infty e^{-(r+i\omega)t}[G(t) - G_\infty]\,dt + G_\infty.\end{aligned}$$

Note that as $r \to 0^+$, we retrieve equation (2.18).

By (2.18), we can see that the results (2.12) and (2.15) agree if in (2.15) the Bromwich contour can be moved to concide with the imaginary axis, so that the Laplace and Fourier transforms are equivalent .

From the dynamic modulus, we introduce more concepts. Since $G^*(\omega)$ is a complex number, we can write it as

$$G^*(\omega) = G_1(\omega) + iG_2(\omega) = |G^*(\omega)|e^{i\delta(\omega)}. \tag{2.19}$$

The quantity $G_1(\omega)$ is known as the storage modulus, $G_2(\omega)$ as the loss modulus, and $\delta(\omega)$ the loss angle. The tangent of loss angle $\tan\delta(\omega)$ is called the loss tangent,

$$\tan\delta(\omega) = \frac{G_2(\omega)}{G_1(\omega)} \tag{2.20}$$

From (2.6) and (2.19), we have

$$G_1(\omega) = G_\infty + \omega\int_0^\infty [G(t) - G_\infty]\sin\omega t\,dt, \tag{2.21}$$

$$G_2(\omega) = \omega\int_0^\infty [G(t) - G_\infty]\cos\omega t\,dt. \tag{2.22}$$

At zero frequency,

$$G_1(0) = G_\infty, \quad G_2(0) = 0. \tag{2.23}$$

To discuss the behaviors of different materials, we consider two typical materials as given in Lockett [17].

(I) PMMA: polymethyl methacrylate, representative of an amorphous polymer of high molecular weight below its glass transition temperature reduced to a reference temperature of $-22°C$.

(II) Hevea Rubber: representative of the rubbery behavior of a lightly crosslinked amorphous polymer, which has a reference of $25°C$.

Since the quantities vary rapidly, they are usually shown on a log / log scale

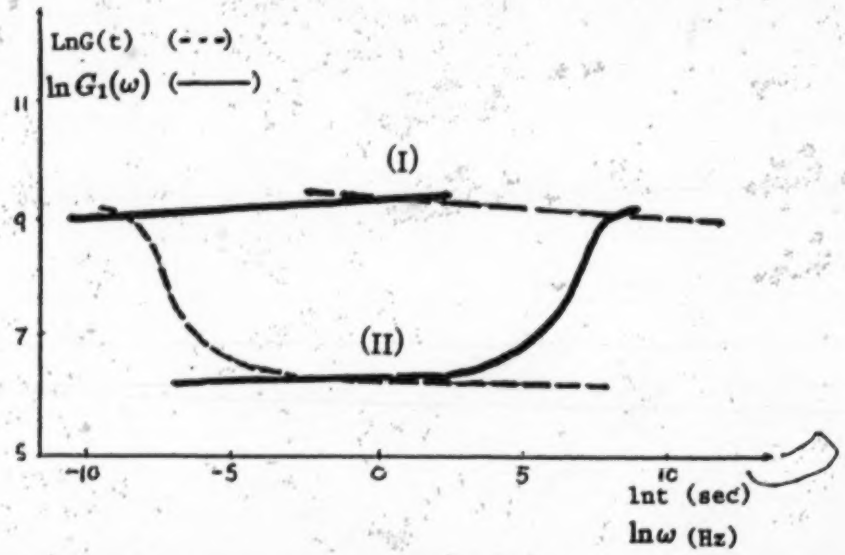

Fig.[2-1]. Variation of stress-relaxation modulus $G(t)$ (– –) and storage modulus $G_1(\omega)$ (—) for (I) PMMA and (II) Hevea.

Fig.[2-1]

Fig.[2-1] shows values of stress-relaxation modulus $G(t)$ (broken curves) and storage modulus $G_1(\omega)$ (unbroken curves).

Similarly, we have Fig.[2.2] showing the variation of the loss tangent with the frequency for the two typical materials.

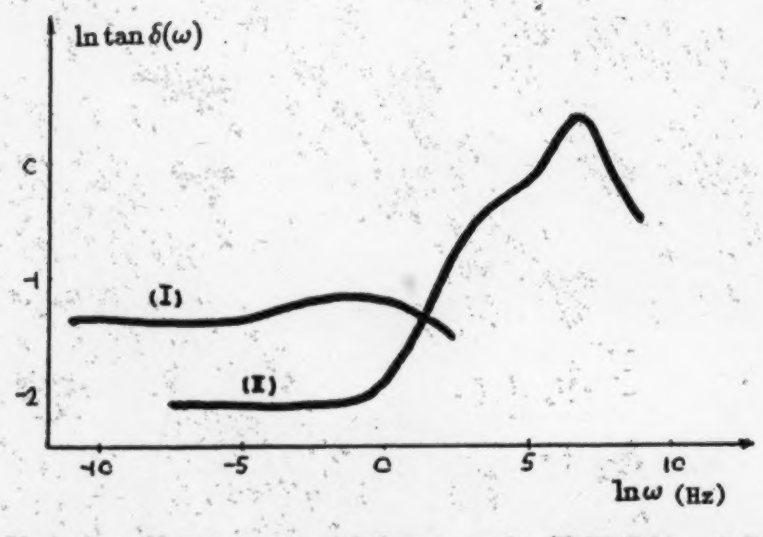

Fig.[2-2]. Variation of loss tangent with frequency for (I) PMMA and (II) Hevea.

Fig[2-2]

It can be seen that the curve for PMMA shows little dependence on frequency whereas that for the rubber varies by two orders of magnitude having a loss peak at approximately 10^5 hz.

Typical examples of simple viscoelastic models are as follows:

1) Kelvin-Voigt:

$$\begin{aligned} G(t) &= G_\infty[\tau\delta(t) + H(t)], \\ \overline{G}(s) &= G_\infty(\tau + \frac{1}{s}), \\ G^*(\omega) &= G_\infty(1 + i\omega\tau), \\ \tan\delta(\omega) &= \omega\tau. \end{aligned} \tag{2.24}$$

2) Maxwell:

$$\begin{aligned} G(t) &= G_0 e^{-t/\tau_1}, \quad \tau_1 = \frac{\tau}{G_0}, \\ \overline{G}(s) &= G_0 \frac{1}{s + 1/\tau_1}, \\ G^*(\omega) &= G_0 \frac{i\omega\tau_1}{1 + i\omega\tau_1} = G_0 \left(\frac{\omega^2\tau_1^2}{1 + \omega^2\tau_1^2} + i \frac{\omega\tau_1}{1 + \omega^2\tau_1^2} \right), \\ \tan\delta(\omega) &= \frac{1}{\omega\tau_1} = \frac{G_0}{\omega\tau} \end{aligned} \tag{2.25}$$

3) Standard Linear Solid:

$$
\begin{aligned}
G(t) &= G_\infty + (G_0 - G_\infty)e^{-t/\tau_1}, \\
\overline{G}(s) &= \frac{G_\infty}{s} + \frac{G_0 - G_\infty}{s + 1/\tau_1}, \\
G^*(\omega) &= G_\infty + (G_0 - G_\infty)\frac{i\omega\tau_1}{1 + i\omega\tau_1}. \\
&= G_0\frac{\omega^2\tau_1^2}{1+\omega^2\tau_1^2} + G_\infty\frac{1}{1+\omega^2\tau_1^2} + i(G_0 - G_\infty)\frac{\omega\tau_1}{1+\omega^2\tau_1^2} \\
\tan\delta(\omega) &= \frac{(G_0 - G_\infty)\omega\tau_1}{G_\infty + G_0\omega^2\tau_1^2}.
\end{aligned}
\tag{2.26}
$$

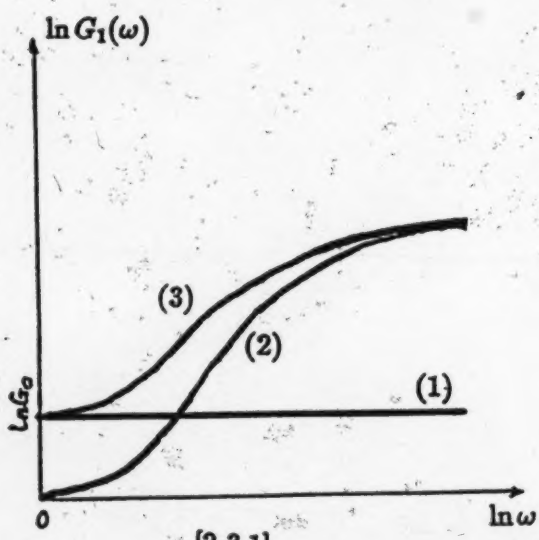

[2-3.1].

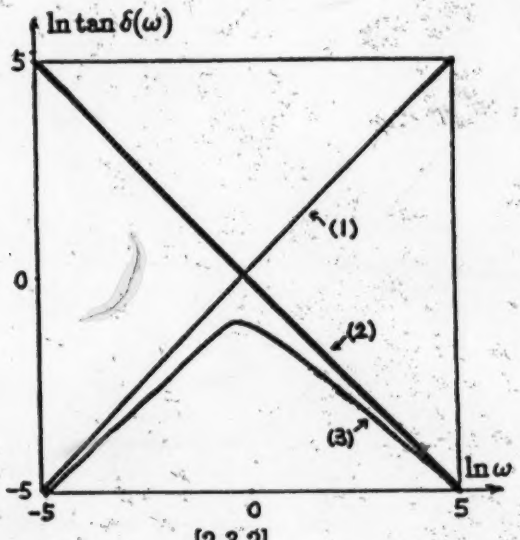

[2-3.2].

Fig.[2-3]. [2-3.1]. Variation of storage modulus, [2-3.2]. Variation of loss tangent with frequency for (1)Kelvin-Voigt, (2) Maxwell, (3) Standard linear model.

Fig.[2-3] show that these models can be used to approximate the behavior of PMMA or rubber only on part of the interval of the frequency range, but not over the whole range.

4) Power-law solid:

$$
\begin{aligned}
G(t) &= ct^{-p}, \quad 0 < p < 1, c > 0, \\
s\overline{G}(s) &= \hat{c}s^{p}, \quad \hat{c} = c\int_0^\infty u^{-p}e^{-u}\,du, \\
G^*(\omega) &= \hat{c}(i\omega)^{p}, \\
G_1(\omega) &= \hat{c}\omega^{p}\cos\frac{p\pi}{2}, \\
\tan\delta &= \tan\frac{p\pi}{2}.
\end{aligned}
\tag{2.27}
$$

It is evident that over a broader range PMMA or rubber shows little dependence on frequency. It can be well approximated by a power-law solid, since log /log value of G_1 as a function of ω is a constant,

$$
\frac{d\ln G_1(\omega)}{d\ln\omega} = p, \tag{2.28}
$$

$$
\text{and} \quad \frac{d\ln\tan\delta(\omega)}{d\ln\omega} = 0,
$$

where p is positive, generally small compared to 1. The log / log plot of the variation of stress-relaxation modulus with time, the storage modulus and loss tangent

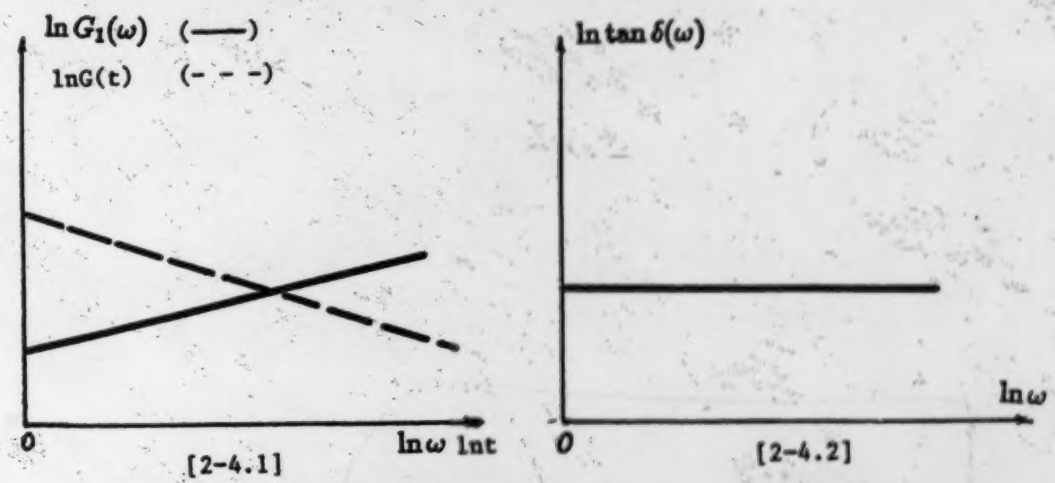

Fig.[2-4]. [2-4.1]. Constant slope of stress-relaxation modulus and storage modulus, [2-4.2]. Constant loss tangent of power-law solid.

Next, we concentrate on the generalised solution corresponding to an input $u(0,t) = H(t)$, or $v(0,t) = \delta(t)$ so that we consider (2.12) or (2.15) with $\overline{f} = 1$. Since our interest is in the behavior of $v(x,t)$ for large t, the dominant part of the signal comes from the saddle point of the integral (2.12) or (2.15), normally in the neighbourhood of origin of ω or s. If $G^*(\omega)$ or $\overline{G}(s)$ is analytic in this neighbourhood, we can expand in power of ω or s. But for power-law solid, as well as a large number of real materials, this is not the case. According to Pipkin [14], $v(x,t)$ can be written in the form of the inverse Fourier transform

$$v(x,t) = \frac{1}{\pi}\Re\int_0^\infty exp\{i\omega(t - \frac{x}{c(\omega)}) - \omega x\tau(\omega)\}\, d\omega, \tag{2.29}$$

where for a small loss angle $\delta(\omega)$,

$$\begin{aligned} c(\omega) &\approx [G_1(\omega)/\rho]^{1/2}, \\ \tau(\omega) &= c^{-1}(\omega)\tan\frac{1}{2}\delta(\omega) \approx c^{-1}(\omega)p\pi/4. \end{aligned} \tag{2.30}$$

It follows that if there is a stationary point at ω_0, it is determined as the solution of the equation

$$\frac{d}{d\omega}\left[\omega(t - \frac{x}{c(\omega)})\right] = 0.$$

Since we can prove that

$$\frac{d}{d\omega}c^{-1} \approx -\frac{p}{2\omega c},$$

We then can get that ω_0 satisfies

$$c(\omega_0) = \frac{x}{t}(1 - \frac{p}{2}).$$

Expanding the exponent of the integrand in equation (2.29) about ω_0, we have

$$\begin{aligned}
& i\omega(t-\frac{x}{c})-\omega x\tau \\
& \sim i\omega t\left(1-\frac{x}{tc_0}-\frac{x}{t}(c^{-1}(\omega_0))'(\omega-\omega_0)\right)-\omega t(1-\frac{p}{2})^{-1}\frac{p\pi}{4} \\
& \approx i\omega t\left(1-\frac{1}{1-p/2}(1-\frac{p}{2}\ln\frac{\omega}{\omega_0})\right)-\omega t\frac{p\pi}{(1-p/2)4} \\
& \approx \frac{i\omega t}{1-p/2}(1-\frac{p}{2}-1+\frac{p}{2}\ln\frac{\omega}{\omega_0}+i\frac{p\pi}{4}) \\
& = -\frac{i\omega tp/2}{1-p/2}(1-\ln\frac{\omega}{\omega_0}-i\frac{\pi}{2}). \qquad (2.31)
\end{aligned}$$

Noting that the integral (2.29) along the negative half of the axis is the complex conjugate of that along the positive half, the imaginary parts of the two integrals cancel each other. (2.29) can also be written as

$$\begin{aligned}
v(x,t) &= \frac{1}{2\pi}\int_0^\infty \exp\{-\frac{i\omega tp/2}{1-p/2}(1-\ln\frac{\omega}{\omega_0}-i\frac{\pi}{2})\}\,d\omega \\
&\quad + \frac{1}{2\pi}\int_{-\infty}^0 \exp\{\frac{i\omega tp/2}{1-p/2}(1-\ln\frac{\omega}{\omega_0}+i\frac{\pi}{2})\}\,d\omega \qquad (2.32) \\
&\overset{s=i\omega}{=} \frac{1}{2\pi i}\int_{Br} \exp\{-\frac{stp/2}{1-p/2}(1-\ln\frac{s}{i\omega_0})\}\,ds.
\end{aligned}$$

This result is the asymptotic form generated by a relaxation function $G(t) = ct^{-p}$, $0 < p < 1$. We can get the same result by inverting the Laplace transform (2.14). Since $s\overline{G}(s) = \hat{c}s^p$,

$$v(x,t) = \frac{1}{2\pi i}\int_{Br} \exp\{st - \frac{x}{\hat{c}^{1/2}}s^{1-p/2}\}\,ds, \qquad (2.33)$$

with saddle point s_0 satisfying

$$s_0^{-p/2} = \frac{1}{1-p/2}\frac{t}{x}\hat{c}^{1/2}.$$

On expanding the integrand about s_0 as $p \ll 1$,

$$(\frac{s}{s_0})^{-p/2} \sim 1-\frac{p}{2}\ln\frac{s}{s_0}, \qquad (2.34)$$

and

$$v(x,t) \sim \frac{1}{2\pi i}\int_{Br} \exp\{-\frac{stp/2}{1-p/2}(1-\ln\frac{s}{s_0})\}\,ds. \tag{2.35}$$

(2.32) and (2.35) are identical if $s_0 = i\omega_0$. Furthermore, let $z = \dfrac{stp/2}{1-p/2}$,

$$v(x,t) \sim \frac{1-p/2}{(p/2)t}\frac{1}{2\pi i}\int_{Br} e^{z\ln(z/z_0)-z}\,dz. \tag{2.36}$$

Although we have discussed the asymptotic form of the pulse for large t, we have to know the effect of the precursor wave, i.e. the behavior of the pulse ahead of the main contribution. We then consider its Laplace transform for large s.

First, we suppose that $G(0^+) \neq 0$. It will be shown later in Chapter 4 that if $G(0^+) \neq 0$, then $s\overline{G}(s) \to G(0^+)$ as $|s| \to \infty$ in the right half plane so that as $|s| \to \infty$, $\overline{v}(x,s) \to e^{-xs/\sqrt{G(0^+)}}$, therefore

$$v(x,t) \sim \delta(t - \frac{x}{\sqrt{G(0^+)}}). \tag{2.37}$$

The precursor wave travels out with velocity $c^2 = G(0^+)$. Pipkin extends this argument. Later result shows that $s\overline{G}(s)$ is analytic in the s plane cut along the negative real axis so that as $|s| \to \infty$,

$$s\overline{G}(s) = G(0^+) + s^{-1}G'(0^+) + \ldots,$$

Normally $G'(0^+) < 0$ and we assume $G'(0^+)/G(0^+) << 1$. Then

$$\overline{v}(x,s) \sim \exp\{-xs/\sqrt{G(0^+)}(1 - \frac{1}{2}s^{-1}\frac{G'(0)}{G(0)} + \ldots)\}, \quad s \to \infty, \tag{2.38}$$

so that

$$v(x,t) \sim e^{-x\tau/2c}\delta(t - \frac{x}{c}), \quad \tau = -\frac{G'(0)}{G(0)} > 0. \tag{2.39}$$

The precursor wave is then exponentially damped as it travels out, so that the majority of the signal is in the part given by the saddle point. We then can conclude that, although the form ct^{-p}, $p > 0$ for $G(t)$ is unbounded and unrealistic at $t = 0$, the actual precursor wave is of no great importance and the asymptotic result for $v(x,t)$ reflects accurately the contribution for a large class of real materials.

Chapter 3. Governing Equations for Fluid Filled Viscoelastic Tubes

For an incompressible Newtonian fluid in a circular cylindrical tube of constant wall thickness, with an axially symmetric motion, the linearised Navier Stokes equations are

$$\frac{\partial w}{\partial t} = -\frac{1}{\rho}\frac{\partial p_r}{\partial r} + \nu\Big(L(w) - \frac{w}{r^2}\Big), \tag{3.1}$$

$$\frac{\partial u}{\partial t} = -\frac{1}{\rho}\frac{\partial p_r}{\partial x} + \nu L(u), \tag{3.2}$$

$$\frac{\partial w}{\partial r} + \frac{w}{r} + \frac{\partial u}{\partial x} = 0, \tag{3.3}$$

where r,x are radial and axial coordinates respectively, and t denotes time, w and u are the radial and axial velocities, ρ the fluid density and ν its kinematic viscosity, p_r denotes the excess pressure in the fluid measured relative to a fixed reference pressure usually taken as the ambient pressure external to the tube. L is the operator

$$L(\phi) = \frac{\partial^2 \phi}{\partial r^2} + \frac{1}{r}\frac{\partial \phi}{\partial r} + \frac{\partial^2 \phi}{\partial x^2}.$$

The effects of the viscosity term have been considered by Sawatzky [16].

For the study of waves in an elastic thin-wall tube, shell theory based on the Herrman-Mirsky formulation is adopted. Details may be found in [11]. The radial displacement W of a tethered tube is given by the equation of motion

$$D\frac{\partial^4 W}{\partial x^4} + \frac{E_p}{R^2}W = P - \gamma h\frac{\partial^2 W}{\partial t^2} + \gamma I\frac{\partial^4 W}{\partial x^2\,\partial t^2}, \tag{3.4}$$

where

$$D = \frac{Eh^3}{12(1-\sigma^2)},\ E_p = \frac{Eh}{(1-\sigma^2)},\ I = \frac{h^3}{12} \tag{3.5}$$

are refered as the flexural modulus, the compressive modulus and the rotatory inertia of the tube wall respectively. Assuming the wall is isotropic, E and σ denote the Young's modulus and Poisson's ratio, γ is the density of the tube material, h

the wall thickness, R the radius of the tube and P denotes transmural pressure. Experience with calculations of the model indicates that the effect of the terms D and I are small and may be neglected compared with the main disturbance. Then (3.4) can be simplified as

$$\frac{E_p}{R^2}W = P - \gamma h \frac{\partial^2 W}{\partial t^2}. \tag{3.6}$$

We now assume that this equation is also suitable for the viscoelastic case. With this assumption, the viscoelastic analogue of eqation (3.6) is

$$\frac{4h}{R^2}G * W = P - \gamma h \frac{\partial^2 W}{\partial t^2} \tag{3.7}$$

where $*$ denotes convolution, that is

$$G * W = \int_{-\infty}^{t} G(t-s)\, dW(s), \tag{3.8}$$

where the integral is a Stieltjes Integral.

In general, $G(t) = 0$, for $t < 0$, and is to be considered as a distribution or generalised function, called the relaxation function.

The Euler equations for the incompressible Newtonian fluid are

$$\rho \frac{\partial^2 U_x}{\partial t^2} = -\frac{\partial p_r}{\partial x}, \tag{3.9}$$

$$\rho \frac{\partial^2 U_r}{\partial t^2} = -\frac{\partial p_r}{\partial r}, \tag{3.10}$$

where U_x and U_r are axial and radial fluid displacements.

The continuity equation is

$$\frac{1}{r}\frac{\partial (rU_r)}{\partial r} + \frac{\partial U_x}{\partial x} = 0. \tag{3.11}$$

Before solving the equations, we nondimensionalize them by setting

$$(\hat{W}, \hat{x}, \hat{r}, \hat{U}_x, \hat{U}_r) = (W, x, r, U_x, U_r)/R,$$

$$(\hat{t}, \hat{s}) = (t, s)c_0/R,$$

$$(\hat{u}, \hat{w}) = (u, w)/c_0, \tag{3.12}$$

$$(\hat{p_r}, \hat{P}) = (p_r, P)/\rho c_0^2,$$

$$\hat{G} = G/G_r,$$

$$\alpha = h/R,$$

$$\eta = \frac{\gamma\alpha}{2\rho} + \frac{1}{8}. \tag{3.13}$$

The reference speed c_0 is given by

$$c_0^2 = \frac{2G_r h}{\rho R} = \frac{2G_r \alpha}{\rho} \tag{3.14}$$

where G_r is a suitable reference stress.

In all the following, we use nondimensionalized variables, but omit the hats for convenience. Then the governing equations become

$$G * W = \frac{P}{2} - (\eta - \frac{1}{8})\frac{\partial^2 W}{\partial t^2}, \tag{3.15}$$

$$\frac{\partial^2 U_x}{\partial t^2} = -\frac{\partial p_r}{\partial x}, \tag{3.16}$$

$$\frac{\partial^2 U_r}{\partial t^2} = -\frac{\partial p_r}{\partial r}, \tag{3.17}$$

$$\frac{U_r}{r} + \frac{1}{r}\frac{\partial U_r}{\partial r} + \frac{\partial U_x}{\partial x} = 0. \tag{3.18}$$

Transforming (3.16) and (3.17) by setting

$$w = \frac{\partial U_r}{\partial t}, \; u = \frac{\partial U_x}{\partial t},$$

and taking the derivative w.r.t t on both sides of (3.18), (3.16)–(3.18) can be changed to

$$\frac{\partial u}{\partial t} = -\frac{\partial p_r}{\partial x}, \tag{3.19}$$

$$\frac{\partial w}{\partial t} = -\frac{\partial p_r}{\partial r}, \tag{3.20}$$

$$\frac{w}{r} + \frac{1}{r}\frac{\partial w}{\partial r} + \frac{\partial u}{\partial x} = 0. \tag{3.21}$$

Typical values for water in a rubber latex tube are $c_0 = 860cm/s$, $R = 0.4cm$, $h = 0.035cm$, $\gamma/\rho = 1.1$, then $\alpha = 0.0875$, $\eta = 0.173125$.

In addition, boundary and initial conditions in linearized form must be specified:

$$\begin{aligned} w(1,x,t) &= \frac{\partial W(x,t)}{\partial t}, \\ p_i(x,t) &= p_r(1,x,t), \\ P &= p_i(x,t) - p_e(x,t), \end{aligned} \tag{3.22}$$

where $p_i(x,t)$ is the excess internal fluid pressure at the wall and $p_e(x,t)$ the excess external pressure.

Since our main interest is the comparison of the choice of the form of $G(t)$ and the effect of radial inertia, we further simplify the equations by taking

$$\begin{aligned} U &= U_x(x,t), \\ p_m &= 2\int_0^1 r' p_r(r',x,t)\,dr' \\ &= \frac{1}{A}\iint_A r' p_r(r',x,t)\,dr'\,d\theta. \end{aligned}$$

We then have

$$\begin{aligned} \frac{\partial^2 U}{\partial t^2} &= -\frac{\partial p_m}{\partial x}, \\ \frac{1}{8}\frac{\partial^3 U}{\partial x \partial t^2} &= P - p_m, \\ W &= -\frac{1}{2}\frac{\partial U}{\partial x}. \end{aligned} \tag{3.23}$$

If U is eliminated, we obtain

$$\begin{aligned} \frac{\partial^2 W}{\partial t^2} &= \frac{1}{2}\frac{\partial^2 p_m}{\partial x^2}, \\ P &= p_m - \frac{1}{8}\frac{\partial^2 p_m}{\partial x^2}, \\ G * W &= \frac{P}{2} - (\eta - \frac{1}{8})\frac{\partial^2 W}{\partial t^2}. \end{aligned} \tag{3.24}$$

Finally, we can write an equation for W from (3.24)

$$\begin{aligned} G * \frac{\partial^2 W}{\partial x^2} &= \frac{1}{2}\frac{\partial^2 P}{\partial x^2} - (\eta - \frac{1}{8})\frac{\partial^4 W}{\partial x^2\,\partial t^2} \\ &= \frac{1}{2}\Big(\frac{\partial^2 P}{\partial x^2} + \frac{1}{8}\frac{\partial^4 p_m}{\partial x^4}\Big) - \eta\frac{\partial^4 W}{\partial x^2\,\partial t^2} \\ &= \frac{1}{2}\frac{\partial^2 p_m}{\partial x^2} - \eta\frac{\partial^4 W}{\partial x^2\,\partial t^2} \\ &= \frac{\partial^2 W}{\partial t^2} - \eta\frac{\partial^4 W}{\partial x^2\,\partial t^2}, \end{aligned}$$

so that the governing equations can be finally simplified as

$$G * \frac{\partial^2 W}{\partial x^2} = \frac{\partial^2 W}{\partial t^2} - \eta\frac{\partial^4 W}{\partial x^2\,\partial t^2}, \tag{3.25}$$

$$G * W = \int_{-\infty}^{t} G(t-s)\,dW(s), \tag{3.26}$$

$$\frac{\partial^2 p_m}{\partial x^2} = 2\frac{\partial^2 W}{\partial t^2}. \tag{3.27}$$

To these equations, we must add some suitable initial and boundary conditions. We suppose for the moment that $G(t)$, $t \geq 0$ is given, $W(x,t)$ is subject to quiescent initial conditions and boundary condition

$$W(0,t) = \Phi(t). \tag{3.28}$$

Although the dispersive nature of the wave is easier to identify using Fourier Transforms, it is advantageous here to proceed with the Laplace Transform

$$\overline{G(s)} = \int_0^\infty e^{-st} G(t)\,dt, \quad \Re(s) > 0. \tag{3.29}$$

Let

$$\ddot{W} = \frac{\partial^2 W}{\partial t^2}, \; W'' = \frac{\partial^2 W}{\partial x^2}, \quad L : \text{Laplace Transform.}$$

By quiescent initial conditions

$$\begin{aligned} L(\ddot{W}) &= s^2 \overline{W}, \\ L(\eta \ddot{W}'') &= \eta s^2 \overline{W_{xx}}, \\ L(G * W'') &= s\overline{G}\,\overline{W_{xx}}, \end{aligned} \tag{3.30}$$

and so equation (3.25) can be written as

$$s\overline{G}\,\overline{W_{xx}} = s^2 \overline{W} - \eta s^2 \overline{W_{xx}},$$

that is

$$\overline{W_{xx}} - \frac{s^2}{s\overline{G} + \eta s^2} \overline{W} = 0. \tag{3.31}$$

The solution is

$$\overline{W}(x,s) = B(s)e^{-\Omega(s)x} + A(s)e^{\Omega(s)x}, \tag{3.32}$$

where

$$\Omega(s) = \left(\frac{s^2}{s\overline{G} + \eta s^2} \right)^{1/2} > 0.$$

Since $\overline{W}$ is bounded as $x \to \infty$, it can be shown that $A(s)$ has to be zero, so that

$$\overline{W}(x,s) = B(s)e^{-\Omega(s)x}, \tag{3.33}$$

where

$$B(s) = \overline{W}(0,s) = \overline{\Phi}(s), \quad \overline{\Phi}(s) = L\{\Phi(t)\},$$

and we then have

$$W(x,t) = \frac{1}{2\pi i} \int_{Br} \overline{\Phi}(s) exp\{st - \frac{sx}{\sqrt{s\overline{G} + \eta s^2}}\}\, ds, \tag{3.34}$$

where Br denotes the standard Bromwich contour.

It is now clear that equation (3.34) differs from the wave propagation in a viscoelastic rod by the term containing the factor η. One would then conjecture that the techniques which have been proven useful for the discussion of wave propagation in rods would be of value in discussing the present problem of wave propagation in fluid filled tubes.

Chapter 4. Reduction to Probability Distributions for Rod Problem

As we had mentioned in Chapter 3, wave propagation in a fluid filled viscoelastic tube is different from those in a viscoelastic rod by the factor η. For the latter case, Pipkin [19] has shown that for all viscoelastic materials satisfying certain conditions, the waves approach a steady shape at sufficiently large distance, and is a probability distribution. In this chapter, we will detail the proofs of the properties.

From (3.33) in Chapter 3, we can see that the one-dimensional pulse propagation problem in a viscoelastic material can be reduced to inverting the expression of the form

$$\overline{W}(x,s) = \overline{\Phi}(s)e^{-\Omega(s)x} \tag{4.1}$$

where $\Omega(s) = \dfrac{s}{\sqrt{s\overline{G(s)}}}$, $\overline{G(s)}$ denotes the Laplace transform of a relaxation function $G(t)$, and the basic problem has $\overline{\Phi}(s) = \dfrac{1}{s}$.

It turns out that under certain conditions on $G(t)$, the signal generated by the inversion of (4.1) is non-negative for all t, and is closely related to certain stable probability distributions.

We start with some definitions and theorems which will be used later in the chapter, and refer to Feller [20] for details of the proofs.

DEFINITION 1. *A point function $F(t)$ on $[0,\infty)$ is a distribution function if*

(1) $F(t)$ is nondecreasing and right continuous,

(2) $F(0) = 0$, . $F(\infty) < +\infty$.

$F(t)$ is a probability distribution function on $[0,\infty)$, if it is a distribution function and $F(\infty) = 1$.

$F(t)$ is defective, if $F(\infty) < 1$.

DEFINITION 2. *A completely monotone function $w(s)$ on $(0,\infty)$ is such that it possesses derivatives $w^{(n)}(s)$ of all orders and*

$$(-1)^n w^{(n)}(s) \geq 0, \quad s > 0. \tag{4.2}$$

THEOREM 1. *A function $w(s)$ on $(0,\infty)$ is the Laplace transform of a probability distribution $F(t)$.*

$\Longleftrightarrow$ *$w(s)$ is completely monotone, and $w(0) = 1$.*

THEOREM 2. *$w(s)$ is the Laplace transform of a measure $F(t)$, ($F(t)$ is not necessarily finite,)*

$\Longleftrightarrow$ *$w(s)$ is completely monotone on $(0,\infty)$.*

Here the Laplace transform is defined as

$$w(s) = \int_0^\infty e^{-st}\, dF(t).$$

We call it Feller's Laplace transform to distinguish it from the one we used in the previous chapters.

THEOREM 3. *If $F(t)$ is a probability distribution, then it has the Lesbegue decomposition:*

$$F(t) = pF_1(t) + qF_2(t) + rF_{a.c}(t) \tag{4.3}$$

where $F_1(t)$ is singular distribution which can be considered as jumps in $F(t)$, and $F_{a.c}$ is an absolutely continuous part. $F_2(t)$ is a singular distribution of the anomalous type which is not absolutely continuous.

THEOREM 4. *If φ is completely monotone and ψ a positive function with completely monotone derivative, then $\varphi(\psi)$ is completely monotone.*

THEOREM 5. *If φ and ψ are completely monotone, so is their product $\varphi\psi$.*

To prove that (4.1) with $\overline{\Phi}(s) = \frac{1}{s}$ is the Laplace transform of a probability distribution function $F(t)$, we have to prove that (4.1) is a completely monotone function by Theorem 1. Since $e^{-\mu}$ is completely monotone function of μ for $\mu > 0$, by Theorem 4 & 5, we can concentrate on the proofs that $\Omega(s) \geq 0$, $\Omega'(s)$ is completely monotone for $s > 0$.

We begin by assuming that

$$G(t) = \tau_0\delta(t) + G_1(t), \quad \tau_0 > 0, \tag{4.4}$$

where $G_1(t)$ is completely monotone, and G_∞ denotes both $\lim_{t\to\infty} G(t)$ and $\lim_{t\to\infty} G_1(t)$, and $G_1(t) - G_\infty$ is normalized such that $G_1(0^+) - G_\infty = 1$.

Since $G_1(t) - G_\infty$ is completely monotone by Theorem 1, it is the Laplace transform of a probability distribution function $P(\mu)$. Then taking the following integral as a Stieltje's integral, we have

$$G_1(t) = G_\infty + \int_0^\infty e^{-\mu t}\, dP(\mu), \quad 0 < t < \infty. \tag{4.5}$$

Furthermore, by Theorem 3, (4.5) can be modified such that

$$G(t) = \tau_0\delta(t) + G_\infty + \sum_k a_k e^{-\mu_k t} + \int_0^\infty e^{-\mu t} p(\mu)\, d\mu, \tag{4.6}$$

where $a_k \geq 0$ denote the jumps in P at points μ_k. We assume that the number of components is finite, $0 < \mu_1 < \mu_2 < \cdots < \mu_k < \ldots$, and that F_2 does not occur in the expression for $G(t)$. Further $p(\mu)$ is a non-negative integrable function satisfying the conditions that

$$\int_0^x p(\mu)d\mu < +\infty, \quad x < +\infty, \tag{4.7}$$

$$\text{and} \quad \int_x^\infty \frac{p(\mu)}{\mu}\, d\mu < +\infty, \quad x > 0, \tag{4.8}$$

with the understanding that as $x \to \infty$ in (4.7), the integral may diverge, and similarly for (4.8), as $x \to 0^+$.

Equations (4.7) and (4.8) are necessary and sufficient conditions that

$$G_1(t) - G_\infty < +\infty, \quad \int_0^t (G_1(t) - G_\infty)dt < +\infty, \quad t > 0. \tag{4.9}$$

(4.9) implies that both $G(t)$ and $\int_0^t G(t)dt$ exist for $t > 0$. It also allows us to apply the Laplace transform to $G(t)$ by noting that

$$\overline{G(s)} = \tau_0 + \frac{G_\infty}{s} + \sum_k \frac{a_k}{\mu_k + s} + \int_0^\infty \frac{p(\mu)}{\mu + s} d\mu. \tag{4.10}$$

The last integral in (4.10) exists for $s \geq s_0 > 0$, since

$$\begin{aligned} \int_0^\infty \frac{p(\mu)}{\mu + s_0} d\mu &= \int_0^A \frac{p(\mu)}{\mu + s_0} d\mu + \int_A^\infty \frac{p(\mu)}{\mu + s_0} d\mu \\ &< \frac{1}{s_0} \int_0^A p(\mu) d\mu + \int_A^\infty \frac{p(\mu)}{\mu} d\mu < \infty. \end{aligned}$$

THEOREM 6. *If* $\int_0^\infty \frac{p(x)}{x + s} dx$ *exists for some* $s_0 > 0$, *then it is well defined and analytic in the complex s-plane cut along the negative real axis.*

By Theorem 6, which is from Widder [22], we obtain the analytic continuation properties of $\overline{G(s)}$ into the complex s-plane cut along the negative real axis.

Let $R(s) = s\overline{G(s)}$, the following shows that $R(s)$ is positive and $R'(s)$ is completely monotone for s real and positive. We have

$$\begin{aligned} &G(t) = \tau_0 \delta(t) + G_\infty + \{G_1(t) - G_\infty\}, \\ &\overline{G(s)} = \tau_0 + \frac{G_\infty}{s} + \int_0^\infty e^{-st} \{G_1(t) - G_\infty\} dt > 0, \quad s > 0, \end{aligned} \tag{4.12}$$

It then follows that

$$R(s) = s\overline{G(s)} > 0,$$

and

$$R'(s) = s(\overline{G(s)})' + \overline{G(s)}$$
$$= \tau_0 - \int_0^\infty e^{-st} tG'(t)dt \geq 0, \tag{4.13}$$

since

$$G'(t) < 0, \quad \text{and} \quad tG'(t) \to 0, \quad \text{as } t \to 0. \tag{4.14}$$

Equation (4.14) follows from the integrability of $G(t)$ at zero. This also implies the existence of the integral of $tG'(t)$, such that

$$0 \leq \int_0^t t(-G'(t))dt < +\infty. \tag{4.15}$$

Now, it is obvious that $R'(s)$ satisfies the condition that $(-1)^n \frac{d^n\{R'(s)\}}{ds^n} \geq 0$, $s > 0$. So $R(s) > 0$, and $R'(s)$ is completely monotone for $s > 0$. Then by Theorem 4, we get that $\frac{1}{\sqrt{R(s)}}$ is completely monotone function for $s > 0$.

The result for $R(s)$ can also be easily obtained directly from (4.10) for $s > 0$. Note that the completely monotone property of $G_1(t)$ has not been used other than in obtaining the representation (4.10).

Since $\frac{1}{\sqrt{s\overline{G(s)}}}$ is completely monotone for $s > 0$ by Theorem 2, there exists a measure $H(t)$, such that

$$\frac{1}{\sqrt{s\overline{G(s)}}} = \int_0^\infty e^{-st} dH(t). \tag{4.16}$$

However we have no knowledge of $H(t)$ except that it is nondecreasing and so can not repeat our argument above on $\frac{s}{\sqrt{s\overline{G(s)}}}$.

To further investigate the possible properties of the inverse transform of $\frac{1}{\sqrt{s\overline{G(s)}}}$, we introduce another theorem from Widder [22].

THEOREM 7. *If*

(1). $f(s) = \int_0^\infty e^{-st} d\alpha(t), \quad s < s_0,$

(2) $a > s_0 \geq 0$, *then*

$$\lim_{R\to\infty} \frac{1}{2\pi i} \int_{a-iR}^{a+iR} f(s)\frac{e^{st}}{s} ds = \begin{cases} \dfrac{\alpha(t^+)+\alpha(t^-)}{2}, & t > 0, \\ \dfrac{\alpha(0^+)}{2}, & t = 0, \\ 0, & t < 0. \end{cases}$$

Returning to (4.16) and Theorem 7, we get that

$$\lim_{R\to\infty} \frac{1}{2\pi i} \int_{a-iR}^{a+iR} \frac{1}{s} \frac{1}{\sqrt{s\overline{G(s)}}} e^{st} ds = \begin{cases} \dfrac{H(t^+)+H(t^-)}{2}, & t > 0, \\ \dfrac{H(0^+)}{2}, & t = 0, \\ 0, & t < 0. \end{cases}$$

Clearly, $\overline{G_1(s)} \to 0$, as $|s| \to \infty$ in C, where C is the plane cut along the negative real axis, so that $\overline{G_1(s)}$ can be inverted, and the inversion contour can be deformed into a loop integral around the branch cut.

Similarly, to prove the existence of the inverse integral of $\dfrac{1}{\sqrt{s\overline{G(s)}}}$, we have to give further discussion on $\dfrac{1}{\sqrt{s\overline{G(s)}}}$, as $|s| \to \infty$.

From (4.10),

$$s\overline{G(s)} = \tau_0 s + G_\infty + \sum_k \frac{a_k s}{\mu_k + s} + s\int_0^\infty \frac{p(\mu)}{\mu + s} d\mu.$$

The effect of the leading term is obvious. If $\tau_0 \neq 0$, then $\dfrac{1}{\sqrt{s\overline{G(s)}}} \to 0$, as $|s| \to \infty$, and we proceed to the inversion. If $\tau_0 = 0$, the other leading terms approach a constant as $|s| \to \infty$, and the behavior depends on the last term which we call $s\overline{G_2(s)}$.

Setting $s = Re^{i\theta}$, if $\Re(s)$ and $\Im(s)$ denote the real and imaginary parts of $R(s)$, we have

$$\begin{aligned} s\overline{G(s)} &= \tau_0 R\cos\theta + G_\infty + \sum_k \frac{a_k(\mu_k R\cos\theta + R^2)}{(\mu_k + R\cos\theta)^2 + R^2\sin^2\theta} \\ &+ \int_0^\infty \frac{p(\mu)(\mu R\cos\theta + R^2)}{(\mu + R\cos\theta)^2 + R^2\sin^2\theta} d\mu \\ &+ i\{\tau_0 R\sin\theta + \sum_k \frac{a_k\mu_k R\sin\theta}{(\mu_k + R\cos\theta)^2 + R^2\sin^2\theta} \\ &+ \int_0^\infty \frac{p(\mu)\mu R\sin\theta}{(\mu + R\cos\theta)^2 + R^2\sin^2\theta} d\mu\}, \end{aligned}$$

so that $\Im(s\overline{G(s)}) \neq 0$, as $\theta \neq 0,\ \pi,\ -\pi$ for all $0 < R < +\infty$. This means that $s\overline{G(s)}$ has no zero in the s-plane except possibly along the negative real axis.

Suppose then $\tau_0 = 0$, the sum $\sum$ is bounded as $R \to \infty$, the discussion will be focused on the integral part. We claim that there are two distinct cases:

(a). $G(t) \to +\infty$ as $t \to 0^+$, then $\int_0^\mu p(\mu)d\mu$ diverges to $+\infty$ as $\mu \to +\infty$ from (4.6), and $|s\overline{G(s)}| \to +\infty$, as $|s| \to +\infty$.

(b). $G(t) \to G(0^+) < +\infty$ as $t \to 0^+$, so that $\int_0^\mu p(\mu)d\mu$ converges to $\{G(0^+) - \tau_0 - G_\infty - \sum_k a_k\}$ as $\mu \to +\infty$. Then $|s\overline{G(s)}|$ is bounded as $|s| \to +\infty$.

Case (a).

This case will be divided into two parts again.

(i). $\int_0^\mu p(\mu)d\mu$ diverges as $\mu \to \infty$, and $R\int_R^\infty \frac{p(\mu)}{\mu}d\mu$ diverges as $R \to \infty$.

(ii). $\int_0^\mu p(\mu)d\mu$ diverges as $\mu \to \infty$, and $R\int_R^\infty \frac{p(\mu)}{\mu}d\mu$ converges as $R \to \infty$.

(a)-(i):

First look at the $\Im$-part of $s\overline{G_2(s)}$ for $0 < \varepsilon_+ \leq \theta \leq \pi - \varepsilon_- < \pi$.

$$\begin{aligned} \Im &= R\sin\theta \int_0^\infty \frac{\mu p(\mu)}{(\mu + R\cos\theta)^2 + R^2\sin^2\theta} d\mu \\ &\geq R\sin\theta \int_R^\infty \frac{\mu^2}{(\mu + R\cos\theta)^2 + R^2\sin^2\theta} \frac{p(\mu)}{\mu} d\mu. \end{aligned} \tag{4.17}$$

Let

$$\varphi = \frac{\mu^2}{(\mu + R\cos\theta)^2 + R^2\sin^2\theta} = \frac{\mu^2}{\mu^2 + 2\mu R\cos\theta + R^2}.$$

Since $\mu \geq R$,

$$\text{for} \quad 0 < \delta_+ \leq \theta \leq \frac{\pi}{2}, \quad \varphi \geq \frac{1}{1 + \frac{2R}{\mu} + \frac{R^2}{\mu^2}} \geq \frac{1}{4},$$

$$\text{for} \quad \frac{\pi}{2} \leq \theta \leq \pi - \varepsilon_-, \quad \varphi \geq \frac{1}{1 + \frac{R^2}{\mu^2}} \geq \frac{1}{2}.$$

So that

$$\Im \geq \frac{1}{4} R\sin\theta \int_R^\infty \frac{p(\mu)}{\mu} d\mu \to +\infty, \quad \text{as} \quad R \to \infty,$$

$$\therefore \quad |s\overline{G(s)}| \to +\infty, \quad \text{as} \quad R \to +\infty.$$

For $-\pi < -\pi + \varepsilon_- \leq \theta \leq \varepsilon_+ < 0$, apply the above argument to $|\Im|$, then $|\Im| \to +\infty$, as $R \to +\infty$. So $|s\overline{R(s)}| \to +\infty$, as $R \to +\infty$.

For $\theta = 0$, $\Im = 0$. To prove that $|s\overline{G(s)}| \to +\infty$, as $R \to +\infty$, we can turn to the real part of the integral.

As $0 \leq \theta < \frac{\pi}{2} - \delta$, $0 < \cos\theta \leq 1$,

$$\begin{aligned} \Re &= \int_0^\infty \frac{(\mu R\cos\theta + R^2)\mu}{\mu^2 + 2\mu R\cos\theta + R^2} \frac{p(\mu)}{\mu} d\mu \\ &\geq R\cos\theta \int_R^\infty \frac{\mu^2}{\mu^2 + 2\mu R + R^2} \frac{p(\mu)}{\mu} d\mu \qquad (4.18) \\ &\geq \frac{1}{4} R\cos\theta \int_R^\infty \frac{p(\mu)}{\mu} d\mu \to \infty, \quad \text{as} \quad R \to \infty. \end{aligned}$$

$$\therefore \quad |s\overline{G(s)}| \to \infty, \quad \text{as} \quad R \to \infty.$$

Overall in (a)-(i), $|s\overline{G(s)}| \to +\infty$, as $R \to +\infty$, $-\pi + \varepsilon \leq \theta \leq \pi - \varepsilon$, $\varepsilon > 0$.

(a)-(ii):

Look at the real part.

If $0 \le \theta \le \frac{\pi}{2}$, $0 \le \cos\theta \le 1$,

$$\begin{aligned}\Re &\ge \int_0^R \frac{R^2}{(\mu+R)^2} p(\mu)\, d\mu \\ &\ge \frac{1}{4}\int_0^R p(\mu)\, d\mu \to +\infty, \quad \text{as} \quad R \to +\infty.\end{aligned}$$

If $\frac{\pi}{2} < \theta \le \pi - \varepsilon$, $-1 < \cos\theta < 0$,

$$\begin{aligned}\Re &= \int_0^{R/|\cos\theta|} \frac{R(R+\mu\cos\theta)}{(\mu+R\cos\theta)^2 + R^2\sin^2\theta} p(\mu) d\mu \\ &\quad + \int_{R/|\cos\theta|}^{\infty} - \frac{R(R+\mu\cos\theta)}{(\mu+R\cos\theta)^2 + R^2\sin^2\theta} p(\mu) d\mu \\ &= \mathrm{Pos}(\Re) + \mathrm{Neg}(\Re).\end{aligned}$$

$\mathrm{Pos}(\Re)$ and $\mathrm{Neg}(\Re)$ denote the integral in which $R+\mu\cos\theta$ are positive and negative.

Then

$$\begin{aligned}\mathrm{Pos}(\Re) &\ge \int_0^R \frac{R(R+\mu\cos\theta)}{(R+\mu)^2} p(\mu) d\mu \\ &\ge \frac{1}{2}\int_0^R \frac{R-\mu\cos\varepsilon}{R+\mu} p(\mu) d\mu \\ &\ge \frac{1}{4}\int_0^R (1-\cos\varepsilon) p(\mu) d\mu \\ &\ge \frac{1}{4}(1-\cos\varepsilon)\int_0^R p(\mu) d\mu \to +\infty, \quad \text{as} \quad R \to +\infty.\end{aligned}$$

$$|\mathrm{Neg}(\Re)| = \int_{R/|\cos\theta|}^{\infty} \frac{R(\mu|\cos\theta| - R)}{(\mu+R\cos\theta)^2 + R^2\sin^2\theta} p(\mu) d\mu.$$

Let

$$y(\mu) = \frac{\mu(\mu|\cos\theta| - R)}{(R\cos\theta+\mu)^2 + R^2\sin^2\theta}, \quad \mu \ge \frac{R}{|\cos\theta|},$$

then as $\mu = \dfrac{R}{|\cos\theta| - \sin\theta}$, $y(\mu)$ gets the maximum, and

$$y_{\max} = \frac{1}{2\sin\theta} \le \frac{1}{2\sin\varepsilon}.$$

So that

$$|\mathrm{Neg}(\Re)| \le R\int_{R/|\cos\theta|}^{\infty} y_{\max}\frac{p(\mu)}{\mu}d\mu$$
$$\le R\int_{R}^{\infty}\frac{1}{2\sin\varepsilon}\frac{p(\mu)}{\mu}d\mu$$
$$= \frac{R}{2\sin\varepsilon}\int_{R}^{\infty}\frac{p(\mu)}{\mu}d\mu \quad \text{converges,} \quad \text{as } R\to\infty.$$

$\therefore$ In case (a)-(ii), $|s\overline{G(s)}| \to +\infty$, as $R\to+\infty$, $0\le\theta\le\pi-\varepsilon$, $\varepsilon>0$.

In case (a) that $G(t)\to+\infty$, as $R\to+\infty$, we have proven that $|s\overline{G(s)}|\to+\infty$, as $|s|\to+\infty$, then

$$\lim_{|s|\to+\infty}\frac{1}{\sqrt{s\overline{G(s)}}} = 0. \tag{4.19}$$

so that the inverse Laplace transform of $\dfrac{1}{\sqrt{s\overline{G(s)}}}$ exists.

Case (b).

$$G(t)\to G(0^+) < +\infty, \quad \text{as} \quad t\to 0^+,$$

then

$$\int_0^{\infty} p(\mu)d\mu = G(0^+) - G_\infty - \sum_k a_k = G_2(0^+). \tag{4.20}$$

As $0\le\theta\le\pi-\varepsilon$,

$$|s\overline{G_2(s)}| = \left|\int_0^{\infty}\frac{sp(\mu)}{\mu+s}d\mu\right|$$
$$\le \int_0^{\infty}\left|\frac{s}{\mu+s}\right|p(\mu)d\mu$$
$$= \int_0^{\infty}\frac{R}{\sqrt{(\mu+R\cos\theta)^2+(R\sin\theta)^2}}p(\mu)d\mu.$$

Let

$$y(\mu) = \frac{R^2}{\mu^2+R^2+2R\mu\cos\theta}, \quad \mu\ge 0,$$

then $y(\mu)$ approaches the maximum as $\mu = -R\cos\theta$.

Since

$$\mu \geq 0,\ R \geq 0,$$

$$\therefore \quad \cos\theta \leq 0, \quad \frac{\pi}{2} \leq \theta \leq \pi - \varepsilon,$$

$$\text{and} \quad y_{\max} = \frac{R^2}{R^2 \sin^2\theta} = \frac{1}{\sin^2\theta} \leq \frac{1}{\sin^2\varepsilon}.$$

So that

$$|s\overline{G_2(s)}| \leq \int_0^\infty \frac{1}{\sin\varepsilon} p(\mu)\, d\mu = \frac{G_2(0^+)}{\sin\varepsilon}.$$

We claim that

$$|s\overline{G_2(s)}| \to G_2(0^+), \quad \text{as} \quad |s| \to +\infty \tag{4.21}$$

To get this result, we introduce a theorem from Boas [24].

THEOREM 8. *Let f be analytic and bounded in the closed angle between the rays $\arg z = \alpha$ and $\arg z = \beta$, $|\alpha - \beta| < 2\pi$, and suppose that $f(z) \to L$ as $r \to \infty$ along both rays. Then $f(z) \to L$ uniformly in the angle as $|z| \to \infty$.*

(4.21) can be proven as follows.

(1). On $\theta = 0$,

$$s\overline{G_2(s)} = \int_0^\infty \frac{R}{\mu + R} p(\mu) d\mu.$$

$$\text{For } n > 0, \quad s\overline{G_2(s)} = \int_0^{R/n} \frac{R}{\mu + R} p(\mu) d\mu + \int_{R/n}^\infty \frac{R}{\mu + R} p(\mu) d\mu.$$

$$\int_{R/n}^\infty \frac{R}{\mu + R} p(\mu) d\mu \leq \int_{R/n}^\infty \frac{R}{(R/n) + R} p(\mu) d\mu$$

$$= \frac{n}{n+1} \int_{R/n}^\infty p(\mu) d\mu \to 0, \quad \text{as} \quad R \to \infty.$$

$$\int_0^{R/n} \frac{n}{n+1} p(\mu) d\mu \leq \int_0^{R/n} \frac{R}{\mu + R} d\mu \leq \int_0^{R/n} p(\mu) d\mu.$$

$$\therefore \lim_{R\to\infty} \frac{n}{n+1} \int_0^{R/n} p(\mu) d\mu \leq \lim_{R\to\infty} \int_0^{R/n} \frac{R}{\mu + R} p(\mu) d\mu \leq \lim_{R\to\infty} \int_0^{R/n} p(\mu) d\mu.$$

Since this is true for any $n > 0$, then by picking $n = \sqrt{R}$, we get that

$$\lim_{R\to\infty}\int_0^{\sqrt{R}} \frac{R}{\mu+R}p(\mu)d\mu = \lim_{R\to\infty}\int_0^{\sqrt{R}} p(\mu)d\mu = G_2(0^+),$$

$$\lim_{R\to\infty}\int_{\sqrt{R}}^{\infty} \frac{R}{\mu+R}p(\mu)d\mu = \lim_{R\to\infty}\int_{\sqrt{R}}^{\infty} p(\mu)d\mu = 0.$$

So that

$$s\overline{G_2(s)} = \int_0^{\infty} \frac{R}{\mu+R}p(\mu)d\mu = G_2(0^+), \quad \text{as } |s| \to +\infty.$$

(2). On $\theta = \pi - \varepsilon$,

$$s\overline{G_2(s)} = \int_0^{\infty} \frac{R^2 + \mu R e^{i\theta}}{R^2+\mu^2-2R\mu\cos\varepsilon}p(\mu)d\mu.$$

First consider

$$y_1(\mu) = \frac{R^2}{R^2+\mu^2-2R\mu\cos\varepsilon} \quad \text{on } [0,\infty).$$

$y_1(\mu)$ has one critical point which is the maximum point at $\mu = R\cos\varepsilon$, and

$$y_{1\ \max} = \frac{1}{\sin^2\varepsilon}.$$

Choose n, such that $R/n < R\cos\varepsilon$, i.e. $n > \dfrac{1}{\cos\varepsilon}$.

Then on $[0, R/n]$, $y_1(0) \le y_1(\mu) \le y_1(R/n)$, since $y_1(\mu)$ is increasing, and $y_1(0) = 1$, $y_1(R/n) = \dfrac{1}{1-\dfrac{2n\cos\varepsilon-1}{n^2}}$, where $n\cos\varepsilon > 1$, $0 < \dfrac{2n\cos\varepsilon-1}{n^2} < 1$.

On $[R/n, \infty)$, $y_1(\mu) \le y_{1\ \max} \le \dfrac{1}{\sin^2\varepsilon}$,

$$\int_0^{\infty} y_1(\mu)p(\mu)d\mu = \int_0^{R/n} y_1(\mu)p(\mu)d\mu + \int_{R/n}^{\infty} y_1(\mu)p(\mu)d\mu.$$

Since $0 \le \lim_{R\to\infty}\int_{R/n}^{\infty} y_1(\mu)p(\mu)d\mu \le \dfrac{1}{\sin^2\varepsilon}\lim_{R\to\infty}\int_{R/n}^{\infty} p(\mu)d\mu = 0,$

$$\lim_{R\to\infty}\int_{R/n}^{\infty} y_1(\mu)p(\mu)d\mu = 0.$$

Besides

$$y_1(0)\int_0^{R/n} p(\mu)d\mu \le \int_0^{R/n} y_1(\mu)p(\mu)d\mu \le y_1(R/n)\int_0^{R/n} p(\mu)d\mu,$$

$$\lim_{R\to\infty} y_1(0)\int_0^{R/n} p(\mu)d\mu = \lim_{R\to\infty}\int_0^{R/n} p(\mu)d\mu,$$

$$\lim_{R\to\infty} y_1(R/n)\int_0^{R/n} p(\mu)d\mu = \lim_{R\to\infty}\frac{1}{1-\frac{2n\cos\varepsilon-1}{n^2}}\int_0^{R/n} p(\mu)d\mu,$$

$$\text{so}\quad \lim_{R\to\infty}\int_0^{R/n} p(\mu)d\mu \le \lim_{R\to\infty}\int_0^{R/n} y_1(\mu)p(\mu)d\mu$$

$$\le \lim_{R\to\infty}\frac{1}{1-\frac{2n\cos\varepsilon-1}{n^2}}\int_0^{R/n} p(\mu)d\mu.$$

Since this is true for any n greater than $\dfrac{1}{\cos\varepsilon}$, choose $n=\sqrt{R}$, where R is sufficiently large, then

$$\lim_{R\to\infty}\frac{1}{1-\frac{2\sqrt{R}\cos\varepsilon-1}{R}}\int_0^{\sqrt{R}} p(\mu)d\mu = \lim_{R\to\infty}\int_0^{\sqrt{R}} p(\mu)d\mu = G_2(0^+).$$

$$\text{So}\quad \int_0^{\infty} y_1(\mu)p(\mu)d\mu = \lim_{R\to\infty}\int_0^{\sqrt{R}} y_1(\mu)p(\mu)d\mu + \lim_{R\to\infty}\int_{\sqrt{R}}^{\infty} y_1(\mu)p(\mu)d\mu$$

$$= G_2(0^+).$$

Consider

$$y_2(\mu) = \frac{R\mu}{R^2+\mu^2-2R\mu\cos\varepsilon},\quad \text{on } [0,\infty),$$

$y_2(\mu)$ has one critical point which is the maximum point at $\mu = R$, and $y_{2\,\max} = \dfrac{1}{2(1-\cos\varepsilon)}$.

Choose $n > 1$, such that

$$\int_0^{\infty} y_2(\mu)p(\mu)d\mu = \int_0^{R/n} y_2(\mu)p(\mu)d\mu + \int_{R/n}^{\infty} y_2(\mu)p(\mu)d\mu,$$

$$\text{then } 0 \le \lim_{R\to\infty}\int_{R/n}^{\infty} y_2(\mu)p(\mu)d\mu \le \frac{1}{2(1-\cos\varepsilon)}\lim_{R\to\infty}\int_{R/n}^{\infty} p(\mu)d\mu = 0.$$

$$\therefore \quad \lim_{R\to\infty} \int_{R/n}^{\infty} y_2(\mu)p(\mu)d\mu = 0.$$

$$\int_0^{R/n} y_2(\mu)p(\mu)d\mu \leq \frac{\frac{1}{n}}{1-\frac{2n\cos\varepsilon-1}{n^2}} \int_0^{R/n} p(\mu)d\mu.$$

Since this is true for all $n > 1$, by choosing $n = \sqrt{R}$,

$$\lim_{R\to\infty} \frac{\frac{1}{\sqrt{R}}}{1-\frac{2\sqrt{R}\cos\varepsilon-1}{R}} \int_0^{\sqrt{R}} p(\mu)d\mu = 0,$$

$$\therefore \quad \lim_{R\to\infty} \int_0^{R/n} y_2(\mu)p(\mu)d\mu = 0,$$

such that

$$\int_0^{\infty} y_2(\mu)p(\mu)d\mu = 0.$$

Since

$$s\overline{G_2(s)} = \int_0^{\infty} [y_1(\mu) - y_2(\mu)\cos\varepsilon + iy_2(\mu)\sin\varepsilon]p(\mu)d\mu,$$

we get that

$$\lim_{|s|\to\infty} s\overline{G_2(s)} = \int_0^{\infty} y_1(\mu)p(\mu)d\mu = G_2(0^+).$$

Since $s\overline{G_2(s)}$ is uniformly bounded in $L:\ 0 \leq \theta \leq \pi - \varepsilon$ and tends to $G_2(0^+)$ on $\theta = 0,\ \pi - \varepsilon$, we then can conclude by Theorem 8 that

$$s\overline{G_2(s)} \to G_2(0^+)$$

in complete angle L, as $|s| \to \infty$, so

$$s\overline{G(s)} \to G(0^+) \text{ in L as } |s| \to \infty. \tag{4.22}$$

Similarly for $s\overline{G(s)}$ in $L':\ -\pi + \varepsilon \leq \theta \leq 0$.

We have known that

$$\lim_{R\to\infty}\frac{1}{2\pi i}\int_{a-iR}^{a+iR}\frac{1}{s}\frac{1}{\sqrt{s\overline{G(s)}}}e^{st}ds=\begin{cases}\dfrac{H(t^+)+H(t^-)}{2}, & t>0,\\ \dfrac{H(0^+)}{2}, & t=0,\\ 0 & t<0,\end{cases}\tag{4.23}$$

From the estimates above on $s\overline{G(s)}$, it follows that the integral on the left may be converted to a loop along the rays $\theta=\pi-\varepsilon,\ -\pi+\varepsilon$ around the origin.

Since $s\overline{G(s)}$ is analytic , and the integrand $\dfrac{1}{s}\dfrac{1}{\sqrt{s\overline{G(s)}}}\to 0$, as $R\to\infty$ in the cut plane, it follows that the resulting integral represents a continuous function which may be differentiated with respect to t as often as we please for $t>0$, so in (4.23), $H(t)$ is a continuous non-decreasing function for $t>0$, differentiable as often as we please. Then (4.16) can be modified as

$$\frac{1}{\sqrt{s\overline{G(s)}}}=H(0^+)+\int_0^\infty e^{-st}J(t)dt\tag{4.24}$$

where $J(t)\geq 0$ and differentiable as often as we please for $t>0$.

Until now, we have proven the existence of the inverse integral of $\dfrac{1}{\sqrt{s\overline{G(s)}}}$, and we can say that $\dfrac{1}{2\pi i}\displaystyle\int_{Br}\frac{e^{st}}{\sqrt{s\overline{G(s)}}}ds$ exists for both cases.

From (4.24) we can see that the value $H(0^+)$ depends on $\dfrac{1}{\sqrt{s\overline{G(s)}}}$ as $s\to+\infty$, since $H(0^+)=\lim\limits_{|s|\to+\infty}\dfrac{1}{\sqrt{s\overline{G(s)}}}$.

So, for the case $\tau_0\neq 0$, $H(0^+)=0$.

For case (a) where $\int_0^R p(\mu)d\mu$ diverges as $R\to+\infty$, $\int_0^t[G_1(t)-G_\infty]\,dt\to+\infty$, as $t\to+\infty$, and $H(0^+)=0$.

For case (b) where $\int_0^R p(\mu)d\mu$ converges as $R \to +\infty$, $\int_0^t [G_1(t) - G_\infty]\,dt$ converges as $t \to \infty$, and $H(0^+) = \dfrac{1}{\sqrt{G(0^+)}}$.This also implies that $J(t)$ involves a δ function at $t = 0$.

We have known that $s\overline{G(s)}$ is analytic and non-zero in the cut plane, but may have zeros on the cut. The conclusion is that these zero points must be isolated. Because if not, the function $s\overline{G(s)}$ would be analytic in a neighbourhood containing a portion of negative real axis, and hence analytic on that part of the negative real axis. This is contradictory. So for sufficently large R, we can deform the contour down to just above and below the negative real axis , like shown in Figure [4-1], and $\dfrac{1}{\sqrt{s\overline{G(s)}}}$ is analytic in the cut plane C, so that

$$\frac{1}{2\pi i}\int_{a-i\infty}^{a+i\infty} \frac{e^{st}}{\sqrt{s\overline{G(s)}}}ds + \frac{1}{2\pi i}\int_{ABB'CDE'EF} \frac{e^{st}}{\sqrt{s\overline{G(s)}}}ds = 0. \qquad (4.25)$$

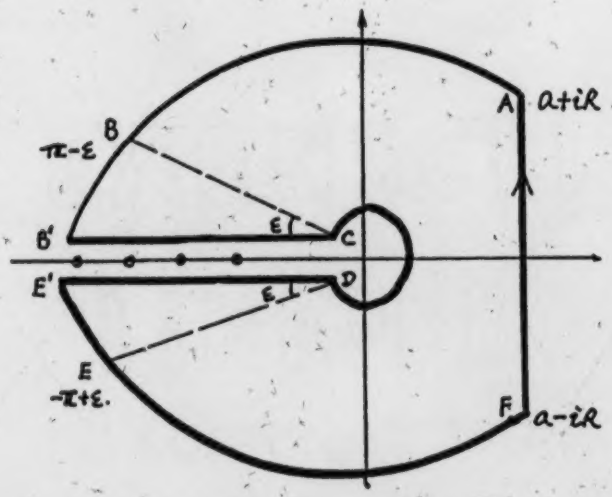

Fig.[4-1]. The contour of integration for the inverse Laplace transform of $\dfrac{1}{\sqrt{s\overline{G}(s)}}$.

Fig.[4-1]

Case (I). $H(0^+) = 0$.

First, we claim that integral along the contours $B'B$ and EE' is zero, since $\dfrac{1}{\sqrt{s\overline{G(s)}}}$ is bounded along them, and that

$$0 \le \frac{1}{2\pi i}\int_{B'B+EE'} \frac{e^{st}}{\sqrt{s\overline{G(s)}}}ds \le \frac{1}{\pi}\int_0^{\varepsilon} \frac{e^{-Rt\cos\varepsilon}R}{|\sqrt{s\overline{G(s)}}|}d\theta \to 0, \text{ as } R \to +\infty.$$

Second, we claim that the integral along the contours FE and BA are zero too, since $\dfrac{1}{\sqrt{s\overline{G(s)}}} \to 0$, as $|s| \to +\infty$.

Next, we claim that the integral along the small circle $\overset{\frown}{CD}$ is zero. That is , no contribution from the loop around the origin. To prove that $\dfrac{1}{2\pi i}\displaystyle\int_{\overset{\frown}{CD}} \frac{e^{st}}{\sqrt{s\overline{G(s)}}}ds \to 0$ as $|s| \to 0$, it is equivalent to prove that $\dfrac{s}{\sqrt{s\overline{G(s)}}} \to 0$ as $|s| \to 0$.

If this is true, then the inverse Laplace transform of $\dfrac{1}{\sqrt{s\overline{G(s)}}}$ will be concentrated along the contour $\overset{\frown}{CB'}$ and $\overset{\frown}{E'D}$, and

$$\frac{1}{2\pi i}\int_{a-i\infty}^{a+i\infty} \frac{e^{st}}{\sqrt{s\overline{G(s)}}}ds = \frac{1}{2\pi i}\int_{CB'+E'D} \frac{e^{st}}{\sqrt{s\overline{G(s)}}}ds.$$

To discuss the integral from the loop around the origin, we claim that $\left|\dfrac{\overline{G(s)}}{s}\right| \to +\infty$ as $|s| \to 0$, $-\pi + \varepsilon \le \theta \le \pi - \varepsilon$, such that $\sqrt{\dfrac{s}{\overline{G(s)}}} \to 0$ as $|s| \to 0$.

First if $-\dfrac{\pi}{2} < \theta < \dfrac{\pi}{2}$,

$$\begin{aligned}
\Re\{s\overline{G(s)}\} &\ge \int_0^{\infty} \frac{(\mu r\cos\theta + r^2)\mu}{\mu^2 + 2\mu r\cos\theta + r^2}\frac{p(\mu)}{\mu}d\mu \quad \text{by (4.18)} \\
&\ge r\cos\theta \int_r^{\infty} \frac{\mu^2}{\mu^2 + 2\mu r\cos\theta + r^2}\frac{p(\mu)}{\mu}d\mu \\
&\ge r\cos\theta \int_r^{\infty} \frac{\mu^2}{\mu^2 + 2\mu^2\cos\theta + \mu^2}\frac{p(\mu)}{\mu}d\mu \\
&= \frac{r\cos\theta}{2(1+\cos\theta)}\int_r^{\infty} \frac{p(\mu)}{\mu}d\mu.
\end{aligned}$$

So that

$$\left|\frac{\overline{G(s)}}{s}\right| = \frac{1}{r^2}\left|s\overline{G(s)}\right| \geq \frac{\cos\theta}{2r(1+\cos\theta)}\int_r^\infty \frac{p(\mu)}{\mu}d\mu.$$

$$\text{If either } \int_r^\infty \frac{p(\mu)}{\mu}d\mu \text{ diverges,} \quad \text{or } 0 < \int_r^\infty \frac{p(\mu)}{\mu}d\mu < +\infty, \quad \text{as } r \to 0, \tag{4.26}$$

we get that $\left|\frac{\overline{G(s)}}{s}\right| \to \infty$, as $r \to 0$, $-\frac{\pi}{2} < \theta < \frac{\pi}{2}$.

Second if $\varepsilon < \theta \leq \pi - \varepsilon$, (or $-\pi + \varepsilon \leq \theta < -\varepsilon$),

$$|\Im(s\overline{G(s)})| \geq r\sin\theta \int_r^\infty \frac{\mu^2}{(\mu + r\cos\theta)^2 + r^2\sin^2\theta}\frac{p(\mu)}{\mu}d\mu \quad \text{by (4.17)}$$

$$\geq \frac{r\sin\theta}{2(1+\cos\theta)}\int_r^\infty \frac{p(\mu)}{\mu}d\mu$$

$$\geq \frac{r\sin\varepsilon}{2(1+\cos\varepsilon)}\int_r^\infty \frac{p(\mu)}{\mu}d\mu,$$

so that

$$\left|\frac{\overline{G(s)}}{s}\right| = \frac{1}{r^2}|s\overline{G(s)}|$$

$$\geq \frac{\sin\varepsilon}{2r(1+\cos\varepsilon)}\int_r^\infty \frac{p(\mu)}{\mu}d\mu \to \infty, \quad \text{as } r \to 0.$$

i.e. $\left|\frac{\overline{G(s)}}{s}\right| \to \infty$, as $|s| \to 0, -\pi + \varepsilon \leq \theta \leq \pi - \varepsilon$.

Then

$$\sqrt{\frac{s}{\overline{G(s)}}} \to 0, \quad \text{as } |s| \to 0. \tag{4.27}$$

Therefore, no contribution exists from the loop around the origin.

In case (I) where $H(0^+) = 0$,

$$J(t) = \frac{1}{2\pi i}\int_{a-i\infty}^{a+i\infty} \frac{1}{\sqrt{s\overline{G(s)}}}e^{st}ds = \frac{1}{2\pi i}\int_{CB'+E'D} \frac{1}{\sqrt{s\overline{G(s)}}}e^{st}ds \tag{4.28}$$

Let $s = -\omega + i\delta$, and $F > 0, 0 < \varphi < \frac{\pi}{2}$ are the complex modulus and angle of $\frac{1}{\sqrt{s\overline{G(s)}}}$, it is easy to see that $\frac{1}{\sqrt{(-\omega+i\delta)\overline{G(-\omega+i\delta)}}}$ and $\frac{1}{\sqrt{(-\omega-i\delta)\overline{G(-\omega-i\delta)}}}$ are complex conjugate each other, then

$$\begin{aligned} J(t) &= \frac{1}{2\pi i}\left[-\int_0^\infty F(-\omega+i\delta)e^{-i\varphi}e^{-\omega t+i\delta t}d\omega + \int_0^\infty F(-\omega-i\delta)e^{i\varphi}e^{-\omega t-i\delta t}d\omega\right] \\ &= \frac{1}{2\pi i}\int_0^\infty \{-F(-\omega+i\delta)[\cos(\varphi-\delta t) - i\sin(\varphi-\delta t)] \\ &\quad + F(-\omega-i\delta)[\cos(\varphi-\delta t) + i\sin(\varphi-\delta t)]\}e^{-\omega t}d\omega \\ &= \frac{1}{\pi}\int_0^\infty F(-\omega+i\delta)\sin(\varphi-\delta t)e^{-\omega t}d\omega \geq 0, \quad t > 0. \end{aligned} \tag{4.29}$$

δ is very small such that the last integral is actually independent of δ, (Otherwise, choose t, such that $\delta t = \frac{\pi}{2}$, Since $0 < \varphi < \frac{\pi}{2}$, $\sin(\varphi - \delta t) < 0$, the integral is less than zero. This is contradicted with $J(t) \geq 0$.)

$$\text{So} \quad J(t) = \frac{1}{\pi}\int_0^\infty F(-\omega)\sin\varphi\, e^{-\omega t}\, d\omega \geq 0, \tag{4.30}$$

where $0 < \varphi < \frac{\pi}{2}$, $F > 0$.

Therefore, $J(t)$ is completely monotone function for $t > 0$, and from (4.24), $J(t)$ is integrable at $t = 0$, so $tJ'(t)$ is integrable at $t = 0$.

Following the reasoning as for $s\overline{G(s)}$, we can get that $\frac{s}{\sqrt{s\overline{G(s)}}}$ is such that

$$\frac{s}{\sqrt{s\overline{G(s)}}} > 0,$$

and

$$\begin{aligned} \left(\frac{s}{\sqrt{s\overline{G(s)}}}\right)' &= \frac{1}{\sqrt{s\overline{G(s)}}} + s\left(\frac{1}{\sqrt{s\overline{G(s)}}}\right)' \\ &= \frac{1}{\sqrt{s\overline{G(s)}}} - s\int_0^\infty tJ(t)e^{-st}dt \\ &= \frac{1}{\sqrt{s\overline{G(s)}}} - \frac{1}{\sqrt{s\overline{G(s)}}} - \int_0^\infty e^{-st}tJ'(t)dt \\ &= -\int_0^\infty e^{-st}tJ'(t)dt \geq 0, \end{aligned} \tag{4.31}$$

and is completely monotone for $s > 0$.

Then by Theorem 4, $\Psi(x,s) = e^{-\frac{sx}{\sqrt{s\overline{G}(s)}}}$ is completely monotone for $s > 0$. Further $\frac{s}{\sqrt{s\overline{G}(s)}} \to 0$, as $s \to 0$ along real axis, so $\Psi(x,0) = 1$.

Case (II)

$$H(0^+) = G(0^+) \neq 0,$$

We have known that

$$\frac{1}{\sqrt{s\overline{G}(s)}} - H(0^+) \to 0, \quad \text{as } |s| \to \infty, \quad -\pi + \varepsilon \leq \theta \leq \pi - \varepsilon.$$

We claim that

$$s\{\frac{1}{\sqrt{s\overline{G}(s)}} - H(0^+)\} \to 0, \quad \text{as } |s| \to 0, \quad -\pi + \varepsilon \leq \theta \leq \pi - \varepsilon.$$

This is true since

$$\frac{s}{\sqrt{s\overline{G}(s)}} - sH(0^+) \to 0 - 0G(0^+) = 0, \quad \text{as } |s| \to 0, \quad -\pi + \varepsilon \leq \theta \leq \pi - \varepsilon.$$

By substitute $\frac{1}{\sqrt{s\overline{G}(s)}}$ everywhere in case (I) with $\frac{1}{\sqrt{s\overline{G}(s)}} - H(0^+)$, we can get the same result.

By (4.24), $J(t)$ is really

$$\tilde{J}(t) = H(0^+)\delta(t) + J(t), \tag{4.32}$$

$J(t)$ is proceeded as case (I) and finished with the same conclusion as case (I). So that

$$\frac{s}{\sqrt{s\overline{G}(s)}} = s\{H(0^+) + \int_0^\infty J(t)e^{-st}dt\} \geq 0, \; s > 0,$$

$$\left(\frac{s}{\sqrt{s\overline{G(s)}}}\right)' = H(0^+) - \int_0^\infty tJ'(t)e^{-st}dt \geq 0,$$

and is completely monotone for $s > 0$.

Therefore $\Psi(x,s) = \exp\{-\frac{sx}{\sqrt{s\overline{G(s)}}}\}$ is completely monotone for $s > 0$, and $\Psi(x,0) = 1$.

By Theorem 1, for both case (I) & (II), $\Psi(x,s)$ is the Laplace transform of a probability distribution $F(x,t)$, it is written as

$$\Psi(x,s) = \int_0^\infty e^{-st}\, dF(x,t) \tag{4.33}$$

Then

$$F(x,t) = \lim_{R\to\infty} \frac{1}{2\pi i} \int_{a-iR}^{a+iR} \frac{1}{s}\Psi(x,s)e^{st}ds, \quad t > 0, \tag{4.34}$$

$$\text{and} \quad F(x,0^+) = \lim_{|s|\to\infty} \Psi(x,s) = 0.$$

(4.33) can also be written as

$$\Psi(x,s) = \int_0^\infty e^{-st} f(x,t)dt,$$

where $f(x,t) = \dfrac{\partial F(x,t)}{\partial t}$ is the probability density function.

Returning to the beginning of this chapter, we note that

$$\overline{W}(x,s) = \frac{1}{s}\Psi(x,s).$$

Under the condition that $G(t)$ is completely monotone, $\overline{W}(x,s)$ is a completely monotone function of s for $s > 0$, and $x > 0$. (4.34) can be written as

$$F(x,t) = W(x,t) = \lim_{R\to\infty} \frac{1}{2\pi i} \int_{a-iR}^{a+iR} e^{st}\overline{W}(x,s)\, ds, \quad x > 0,\ t > 0, \tag{4.35}$$

which is the inverse Laplace transform defined in Chapter 2 & 3. We then can conclude that the inverse Laplace transform of (4.1) exists, and can be interpreted as a probability distribution function.

Next we will discuss the asymptotic behavior of $W(x,t)$ as $t \to \infty$. This is equivalent to the behavior of $\overline{W}(x,s)$ as $s \to 0^+$.

Before doing anything, we introduce some definitions and theorems quoted from Feller [20].

DEFINITION 3. *A positive function $L(t)$ defined on $(0,\infty)$ is slowly varying function at infinity if*

$$\frac{L(ct)}{L(t)} \to 1, \quad \text{for } c > 0, \ t \to +\infty.$$

DEFINITION 4. *A positive function $U(t)$ defined on $(0,\infty)$ is regularly varying function with exponent p if*

$$f(t) = t^p L(t), \ -\infty < p < +\infty,$$

with $L(t)$ slowly varying.

THEOREM 9. *If $-1 < \alpha < +\infty$, and $\Omega(s) = \int_0^\infty e^{-st} f(t)dt$,*

then

$$f(t) = t^\alpha L(t), \ t \to \infty \Longleftrightarrow \Omega(s) \sim s^{-\alpha-1} L(\frac{1}{s})\Gamma(1+\alpha), \ s \to 0^+.$$

THEOREM 10. *(Continuity Theorem). For $n = 1, 2, \ldots$, let F_n be a probability distribution with transform φ_n.*

If $F_n \to F$ where F is a possibly defective distribution with transform φ, then $\varphi_n(s) \to \varphi(s)$, for $s > 0$.

Conversely, if the sequence $\varphi_n(s)$ converges for each $s > 0$ to a limit $\varphi(s)$, then φ is the transform of a possibly defective distribution F, and $F_n \to F$. The limit is not defective iff

$$\varphi(s) \to 1, \qquad \text{as} \quad s \to 0.$$

Since

$$G(t) = \tau_0\delta(t) + G_\infty + \{G_1(t) - G_\infty\},$$

where $\delta(t)$ is excluded from $G_1(t)$,

$$\overline{G(s)} = \tau_0 + \frac{G_\infty}{s} + \int_0^\infty e^{-st}\{G_1(t) - G_\infty\}dt.$$

We introduce the apparent viscosity $\eta(t)$ as

$$\eta(t) = \int_0^t \{G_1(t) - G_\infty\}dt. \tag{4.36}$$

We shall consider two main cases below depending on the behavior of $\eta(t)$.

Case (I).

Suppose $\eta(t)$ diverges rapidly and for $-1 < p \leq 0$,

$$G_1 - G_\infty = t^p L(t), \quad t \to \infty, \tag{4.37}$$

so that $G_1(t) - G_\infty$ is regularly varying for $-1 < p < 0$ and slowly varying for $p = 0$, and

$$G(t) \sim \tau_0\delta(t) + G_\infty + t^p L(t), \quad t \to \infty. \tag{4.38}$$

Then it follows from Theorem 9 that

$$s\overline{G(s)} \sim \tau_0 s + G_\infty + s^{-p}L(\frac{1}{s})\Gamma(1+p), \quad s \to 0^+. \tag{4.39}$$

We also note that

$$\begin{aligned}\eta(t) &\sim \int_0^1 (ut)^p L(ut)t\,du \\ &\sim \frac{1}{1+p}t^{p+1}L(t), \quad t \to \infty,\end{aligned} \tag{4.40}$$

and is regularly varying.

The behavior of $\overline{J}(s) = \dfrac{1}{\sqrt{s\overline{G}(s)}}$ depends on whether G_∞ is zero or not, so we further subdivide Case (I).

Case (IA). $G_\infty = 0$

$$s\overline{G(s)} \sim s^{-p}L(\frac{1}{s})\Gamma(1+p),\ s \to 0^+. \tag{4.41}$$

and

$$\overline{J}(s) \sim s^{p/2}L^{-1/2}(\frac{1}{s})\Gamma^{-1/2}(1+p),\ s \to 0^+. \tag{4.42}$$

$s\overline{G(s)}$ and $\overline{J}(s)$ are regularly-varying function for $s \to 0^+$, $-1 < p < 0$, and slowly varying function for $p = 0$.

Case (IB). $G_\infty \neq 0$

$$s\overline{G(s)} \sim G_\infty \left[1 + \frac{\Gamma(1+p)}{G_\infty}s^{-p}L(\frac{1}{s})\right],\ s \to 0^+. \tag{4.43}$$

$$\overline{J}(s) \sim \frac{1}{\sqrt{G_\infty}}\left[1 - \frac{\Gamma(1+p)}{2G_\infty}s^{-p}L(\frac{1}{s})\right],\quad \text{for } s \to 0^+. \tag{4.44}$$

Case (II)

At this case, $\eta(t)$ satisfies that

$$\eta(t) < \infty,\quad \text{or at most } \eta(t) \sim L(t),\quad \text{as } t \to \infty. \tag{4.45}$$

If $G_1(t) - G_\infty$ is of the form $t^pL(t)$, $p \leq -1$ as $t \to \infty$, $\eta(t)$ will be of this form. Included here are those cases for which $G_1(t) - G_\infty$ behaves exponentially as $t \to \infty$. In a slight misuse of notation we will continue to refer to these cases below as $p \leq -1$.

Since $p \leq -1$, Theorem 9 can not be used for $G_1(t) - G_\infty$, but can be used for $\eta(t)$ by (4.45), with $\alpha = 0$. Then

$$\overline{\eta(s)} \sim s^{-1}L(\frac{1}{s}),\ s \to 0^+, \tag{4.46}$$

$$\text{and}\quad \overline{G_1(s) - G_\infty} = s\overline{\eta(s)}, \tag{4.47}$$

(4.47) is proven as follows.

$$\begin{aligned} s\overline{\eta(s)} &= s\int_0^\infty e^{-st}\int_0^t \{G_1(\tau)-G_\infty\}d\tau\,dt \\ &= \int_0^\infty \Big(\int_\tau^\infty e^{-st}\,d(st)\Big)(G_1(\tau)-G_\infty)d\tau \\ &= \int_0^\infty e^{-s\tau}\{G_1(\tau)-G_\infty\}d\tau \\ &= \overline{G_1(s)-G_\infty}. \end{aligned}$$

So that

$$\overline{G_1(s)-G_\infty} \sim L(\frac{1}{s}), \quad s\to 0^+, \tag{4.48}$$

$$\overline{G(s)} \sim \tau_0 + \frac{G_\infty}{s} + L(\frac{1}{s}), \quad s\to 0^+, \tag{4.49}$$

and

$$s\overline{G(s)} \sim \tau_0 s + G_\infty + sL(\frac{1}{s}), \quad s\to 0^+ \tag{4.50}$$

$$\sim \tau_0 s + G_\infty + s\eta(\frac{1}{s}), \quad s\to 0^+. \tag{4.51}$$

Case (IIA). $G_\infty = 0$

If $\eta(\frac{1}{s}) \to \eta_0$, which is constant, as $s\to 0^+$, then

$$\begin{aligned} &s\overline{G(s)} \sim s(\eta_0+\tau_0), \\ &\overline{J}(s) \sim s^{-1/2}(\eta_0+\tau_0)^{-1/2}, \quad \text{as } s\to 0^+. \end{aligned} \tag{4.52}$$

Otherwise,

$$\begin{aligned} &s\overline{G(s)} \sim s\eta(\frac{1}{s}), \\ &\overline{J}(s) \sim s^{-1/2}\eta^{-1/2}(\frac{1}{s}), \quad \text{as } s\to 0^+. \end{aligned} \tag{4.53}$$

Case (IIB). $G_\infty \neq 0$

If $\eta(\frac{1}{s}) \to \eta_0$, as $s\to 0^+$, then

$$\begin{aligned} &s\overline{G(s)} \sim G_\infty(1+\frac{\tau_0+\eta_0}{G_\infty}s), \\ &\overline{J}(s) \sim \frac{1}{\sqrt{G_\infty}}(1-\frac{\tau_0+\eta_0}{2G_\infty}s), \quad \text{as } s\to 0^+. \end{aligned} \tag{4.54}$$

Otherwise,

$$\begin{aligned} s\overline{G(s)} &\sim G_\infty[1 + \frac{1}{G_\infty} s\eta(\frac{1}{s})], \\ \overline{J}(s) &\sim \frac{1}{\sqrt{G_\infty}}[1 - \frac{1}{2G_\infty} s\eta(\frac{1}{s})], \quad \text{as } s \to 0^+. \end{aligned} \tag{4.55}$$

Until now we have got the asymptotic forms of $\overline{J}(s)$ for all the cases. There are really no difference comparing with Pipkin's [19] results, except with the uniform use of the parameter p.

We now turn to the asymptotic forms taken by the inverse of the expression given in equation (4.1) for the basic problem where $\overline{\Phi}(s) = \frac{1}{s}$. We have

$$W(x,t) = \frac{1}{2\pi i} \int_{r-i\infty}^{r+i\infty} \frac{1}{s} e^{st} e^{-s\overline{J}(s)x}\, ds. \tag{4.56}$$

We first follow the arguments used by Pipkin [19] to obtain the uniform integral representation and then add some comments.

In case (IA) and (IIA) we have

$$\overline{J}(s) = s^{p/2} L^{-1/2}(\frac{1}{s}) \Gamma^{-1/2}(1+p), \ -1 \le p \le 0, \ s \to 0^+, \tag{4.57}$$

where $p = -1$ is used as a short way of describing the cases in case (IIA). When $p = -1$ we interpret

$$L^{-1/2}(\frac{1}{s})\Gamma^{-1/2}(1+p) = \begin{cases} \eta^{-1/2}(\frac{1}{s}) \\ (\eta_0 + \tau_0)^{-1/2} \end{cases}, \quad s \to 0^+, \tag{4.58}$$

depending on the behavior of $\eta(\frac{1}{s})$ as $s \to 0^+$ described in case (IIA).

Consider case (IA) when $p = 0$, and $L(t)$ is constant, in fact it falls in class (II), the case we have labelled $p = -1$. This is a consequence of the lack of uniformity of t^p as $p \to 0$, $t \to \infty$. Nevertheless it is of practical interest to

consider the case p close to zero separately and label the special form we obtain as the class $p = 0$ for later discussion.

So if we rewrite

$$\begin{aligned} L^{-1/2}(\frac{1}{s})\Gamma^{-1/2}(1+p) &= \tilde{L}(\frac{1}{s})\Gamma(1-\frac{p}{2}), \quad -1 < p < 0, \\ \eta^{-1/2}(\frac{1}{s}) \text{ or } (\eta_0+\tau_0)^{-1/2} &= \tilde{L}(\frac{1}{s})\Gamma(1-\frac{p}{2}), \quad p = -1, \end{aligned} \tag{4.59}$$

we have

$$\overline{J}(s) \sim s^{p/2}\tilde{L}(\frac{1}{s})\Gamma(1-\frac{p}{2}), \quad s \to 0^+, \ -1 \le p < 0. \tag{4.60}$$

Following Pipkin [19], we set

$$s = \frac{z}{\omega(x)}, \quad \theta = \frac{t}{\omega(x)}, \tag{4.61}$$

where we choose $\omega(x)$ such that

$$\frac{x\tilde{L}(\omega(x))}{\omega(x)^{1+p/2}} = \frac{1}{|p/2|}, \quad x \to \infty, \tag{4.62}$$

then $\frac{ds}{s} = \frac{dz}{z}$. Equation (4.62) makes it true that $\omega(x) \to \infty$, as $x \to \infty$. Then Substituting (4.61) into $\phi(x,s) = st - s\overline{J}(s)x$ and taking the limit as $x \to \infty$, $t \to \infty$, with $\frac{t}{\omega(x)}$ remaining finite, we have

$$\begin{aligned} \phi(s) &= st - s^{1+p/2}\tilde{L}(\frac{1}{s})\Gamma(1-\frac{p}{2})x \\ &= z\theta - \Gamma(1-\frac{p}{2})z^{1+p/2}\frac{\tilde{L}(\omega(x)/z)x}{\omega(x)^{1+p/2}} \\ &= z\theta - \Gamma(1-\frac{p}{2})z^{1+p/2}\frac{\tilde{L}(\omega(x))x}{\omega(x)^{1+p/2}} \\ &= z\theta - \Gamma(-\frac{p}{2})z^{1+p/2}. \end{aligned} \tag{4.63}$$

Equation (4.56) can then be written as

$$F^*(\theta) = W(x,t) = \frac{1}{2\pi i}\int_{r-i\infty}^{r+i\infty} e^{\theta z}e^{-\Gamma(-p/2)z^{1+p/2}}\frac{dz}{z}, \tag{4.64}$$

Clearly $F^*(\theta)$ is zero for $\theta < 0$ and corresponds to a probability distribution function on $(0, \infty)$.

Next we show that the argument presented above is essentially the Continuity Theorem for a sequence of probability distribution functions.

Defining the sequences $\{x_n\}$ and $\{\omega(x_n)\}$ satisfying that

$$x_n \omega(x_n)^{-1-p/2} \tilde{L}(\omega(x_n)) = \frac{1}{|p/2|}, \quad -1 \le p < 0. \tag{4.65}$$

Then

$$\omega(x_n) = \{\frac{|p|}{2} x_n \tilde{L}(\omega(x_n))\}^{\frac{1}{1+p/2}} \quad -1 \le p < 0. \tag{4.66}$$

Since $1 + \frac{p}{2} > 0$, and $\tilde{L}(\omega(x_n))$ is slowly-varying, $\omega(x_n)$ approaches infinity as $x_n \to \infty$, and (4.65) also infers that $\omega(x_n)$ is an increasing function of x_n, and for fixed z,

$$\tilde{L}(\omega(x_n)/z) \to \tilde{L}(\omega(x_n)), \quad x_n \to \infty. \tag{4.67}$$

Since

$$\Psi(x, s) = e^{-s\overline{J}(s)x},$$

we define a sequence

$$\Phi_n(x_n, z) = \Psi_n(x_n, \frac{z}{\omega(x_n)}) = e^{-\frac{z}{\omega(x_n)}\overline{J}(\frac{z}{\omega(x_n)})x_n}, \tag{4.68}$$

then

$$\begin{aligned} \Phi_n(x_n, z) &= e^{-z^{1+p/2}\Gamma(1-p/2)\frac{\tilde{L}(\frac{\omega(x_n)}{z})x_n}{\omega(x_n)^{1+p/2}}} \\ &\to e^{-z^{1+p/2}\Gamma(1-p/2)x_n\omega(x_n)^{-1-p/2}\tilde{L}(\omega(x_n))} \\ &= e^{-z^{1+p/2}\Gamma(-p/2)} = \Phi(z), \quad x_n \to \infty. \end{aligned} \tag{4.69}$$

Since $\Phi(z)$ is completely monotone, and $\Phi(0) = 1$, $\Phi(z)$ is the Laplace transform of a probability distribution $F^*(\theta)$. Where

$$F^*(\theta) = \frac{1}{2\pi i} \int_{r-i\infty}^{r+i\infty} e^{z\theta} e^{-z^{1+p/2}\Gamma(-p/2)} \frac{dz}{z}, \tag{4.70}$$

where

$$\theta = \frac{t}{\omega(x)}, \quad x \to \infty, \quad t \to \infty. \tag{4.71}$$

For each $\Phi_n(x_n, z)$, Let $\theta = \dfrac{t}{\omega(x_n)}$, $s = \dfrac{z}{\omega(x_n)}$, for $\theta > 0$,

$$\begin{aligned} F_n^*(x_n, \theta) &= \frac{1}{2\pi i} \int_{r-i\infty}^{r+i\infty} e^{z\theta} \Phi_n(x_n, z) \frac{dz}{z} \\ &= \frac{1}{2\pi i} \int_{r-i\infty}^{r+i\infty} e^{st} \Psi_n(x_n, s) \frac{ds}{s}. \end{aligned} \tag{4.72}$$

Since $\Psi(x_n, s)$ is completely monotone for $s > 0$, its inverse Laplace transform $F_n^*(\theta)$ is a probability distribution function. Then by Theorem 10,

$$F_n^*(x_n, \theta) \to F^*(\theta), \quad n \to \infty, \; x_n \to \infty. \tag{4.73}$$

Since $F^*(\theta)$ is a probability distribution function on $(0, \infty)$ in (4.70), the contour may be deformed to the right for $\theta < 0$, so that $F^*(\theta) = 0$, for $\theta < 0$.

We note that Theorem 10 requires $F_n^*(x_n, \theta)$ to be a probability distribution so that $\Phi_n(x_n, z)$ must be completely monotone. Even if $\tilde{\Phi}_n(z)$ is asymptotically equivalent to the form given here for Φ_n, $z \to 0^+$, it may be that $\tilde{\Phi}_n(z)$ is not completely monotone. In that case, as we shall see in Chapter 6 the theorem does not necessarily hold and the resulting function $\tilde{F}(\theta)$ may not be a probability distribution function.

Next we consider case (IB) and (IIB) for $-1 \le p < 0$, and discuss Case $p = 0$ later for the same reason as mentioned above. We have

$$\overline{J}(s) = \frac{1}{\sqrt{G_\infty}} \{1 - \frac{\Gamma(1+p)}{2G_\infty} s^{-p} L(\frac{1}{s})\}; \quad -1 \le p < 0, \; s \to 0^+, \tag{4.74}$$

where again if $p \le -1$, $L(\frac{1}{s})\Gamma(1+p) = \eta(\frac{1}{s})$, or $\eta_0 + \tau_0$, and interpret $p = -1$.

Following Pipkin [19], we set $\tilde{L}(\frac{1}{s}) = L(\frac{1}{s})/2G_\infty$, $j_\infty = \frac{1}{\sqrt{G_\infty}}$, replace s by $\frac{z}{\omega(x)}$, and choose $\omega(x)$ such that

$$j_\infty x \omega(x)^{-(1-p)} \tilde{L}(\omega(x)) \to \frac{1}{|p|}, \quad \text{as } x \to \infty. \tag{4.75}$$

Then

$$\Psi(x,s) = e^{-s\overline{J}(s)x} \to e^{-\frac{zj_\infty x}{\omega(x)}} e^{\frac{1}{|p|}\Gamma(1+p)z^{1-p}} = \Phi(x,z), \quad x \to \infty, \tag{4.76}$$

and

$$\begin{aligned} W(x,t) &= \frac{1}{2\pi i}\int_{r-i\infty}^{r+i\infty} e^{st}\Psi(x,s)\frac{ds}{s} \\ &= \frac{1}{2\pi i}\int_{r-i\infty}^{r+i\infty} e^{zt/\omega(x)}\Phi(x,z)\frac{dz}{z} \\ &= \frac{1}{2\pi i}\int_{r-i\infty}^{r+i\infty} e^{z\frac{(t-j_\infty x)}{\omega(x)}} e^{\frac{1}{|p|}\Gamma(1+p)z^{1-p}}\frac{dz}{z}, \quad x \to \infty. \end{aligned} \tag{4.77}$$

If $p = -1$, $\Gamma(1+p) = 1$, and then

$$W(x,t) = \frac{1}{2\pi i}\int_{r-i\infty}^{r+i\infty} e^{z\frac{(t-j_\infty x)}{\omega(x)}} e^{z^2}\frac{dz}{z}, \quad x \to \infty.$$

In (4.77), since $\Gamma(1+p) > 0$ for $-1 \le p < 0$, the contour can not be deformed to the right, so $W(x,t)$ may not be zero for $t < 0$. This makes sense when we go to the probability distribution interpretation. We have

$$\frac{1}{s}e^{-s\overline{J}(s)x} = \int_0^\infty e^{-st}F(x,t)\,dt \tag{4.78}$$

with $F(x,t)$ a probability distribution function of t on $(0,\infty)$.

Substituting (4.76) into the left hand side of (4.78) and replacing s by $\frac{z}{\omega(x)}$, we have

$$\frac{\omega(x)}{z}e^{-\frac{zj_\infty x}{\omega(x)}} e^{\frac{1}{|p|}\Gamma(1+p)z^{1-p}} = \int_0^\infty e^{-\frac{zt}{\omega(x)}}F(x,t)\,dt, \quad x \to \infty.$$

Set

$$\theta = \frac{t - j_\infty x}{\omega(x)},$$

then

$$\begin{aligned} \frac{1}{z} e^{\frac{1}{|p|}\Gamma(1+p)z^{1-p}} &= \int_0^\infty e^{-z\frac{t - i_\infty x}{\omega(x)}} F(x,t) \frac{dt}{\omega(x)} \\ &= \int_{\frac{-xj_\infty}{\omega(x)}}^\infty e^{-z\theta} F(x, \omega(x)\theta + xj_\infty)\, d\theta \qquad (4.79) \\ &= \int_{-\frac{xj_\infty}{\omega(x)}}^\infty e^{-z\theta} F^*(\theta)\, d\theta, \end{aligned}$$

where $F^*(\theta) = F(x, \omega(x)\theta + xj_\infty)$, $-\dfrac{xj_\infty}{\omega(x)} < \theta < \infty$, therefore $F^*(\theta)$ is a probability distribution function on $(-\dfrac{xj_\infty}{\omega(x)}, \infty)$, which is the shift of $F(x,t)$ to the left by $\dfrac{xj_\infty}{\omega(x)}$.

As $x \to \infty$, by (4.75),

$$\frac{x}{\omega(x)} \sim x^{1 - \frac{1}{1-p}} \to \infty,$$

so that $F^*(\theta)$ is now defined on $(-\infty, \infty)$. As a result we would have to consider a probability distribution on the whole real axis, and a corresponding continuity theorem of the type discussed above. We do not do this but refer to [19] for further discussion.

Case $p = 0$: Suppose we are in class (I) with $p \to 0^-$. We drop the possibility of the extra term $\tau_0 \delta(t)$ for the moment, the effect can be added in later.

We start with case (IA) where $G_\infty = 0$. We have

$$W(x,t) = \frac{1}{2\pi i} \int_{r-i\infty}^{r+i\infty} e^{\frac{tz}{\omega(x)}} e^{-\Gamma(-\frac{p}{2})z^{1+p/2}} \frac{dz}{z}, \quad -1 < p < 0, \qquad (4.79)$$

where

$$\frac{x\tilde{L}(\omega(x))}{\omega(x)^{1+p/2}} = \frac{1}{|p/2|}, \quad x \to \infty.$$

Pipkin then argues as following:

If $p \to 0^-$, then

$$\begin{aligned} \Gamma(-\frac{p}{2}) &\sim -\frac{2}{p}, \\ z^{p/2} &\sim 1 + \frac{p}{2}\ln z, \\ \omega(x) &\sim \frac{|p|}{2} x \tilde{L}(\omega(x)). \end{aligned} \tag{4.80}$$

Substituting these quantities into (4.79) remembering p is small but nonzero, we have

$$\begin{aligned} W(x,t) &= \frac{1}{2\pi i}\int_{r-i\infty}^{r+i\infty} e^{t\frac{z}{\omega(x)}} e^{\frac{2}{p}z(1+\frac{p}{2}\ln z)}\frac{dz}{z} \\ &= \frac{1}{2\pi i}\int_{r+i\infty}^{r+i\infty} e^{z\frac{t-x\tilde{L}(\omega(x))}{\omega(x)}} e^{z\ln z}\frac{dz}{z} \\ &= \frac{1}{2\pi i}\int_{r-i\infty}^{r+i\infty} e^{z\theta + z\ln z}\frac{dz}{z} \\ &= F^*(\theta), \end{aligned} \tag{4.81}$$

where

$$\theta = \frac{t - x\tilde{L}(\omega)}{\omega(x)}. \tag{4.82}$$

This last result is refered to as the case $p = 0$, $G_\infty = 0$.

For case (IB) with $G_\infty > 0$, we have

$$W(x,t) = \frac{1}{2\pi i}\int_{r-i\infty}^{r+i\infty} e^{z(\frac{t-j_\infty x}{\omega(x)})} e^{\frac{1}{|p|}\Gamma(1+p)z^{1-p}}\frac{dz}{z}, \tag{4.83}$$

where

$$\frac{x j_\infty \tilde{L}(\omega(x))}{\theta(x)^{1-p}} = \frac{1}{|p|}, \quad \text{as} \quad x \to \infty.$$

Then as $p \to 0^-$,

$$\begin{aligned} z^{-p} &\sim 1 - p\ln z, \\ \Gamma(1+p) &\sim 1, \\ \omega(x) &\sim x|p| j_\infty \tilde{L}(\omega(x)). \end{aligned} \tag{4.84}$$

So that (4.83) becomes

$$
\begin{aligned}
W(x,t) &= \frac{1}{2\pi i}\int_{r-i\infty}^{r+i\infty} e^{z\left(\frac{t-j_\infty x}{\omega(x)}\right)} e^{\frac{1}{|p|}z(1-p\ln z)}\,\frac{dz}{z} \\
&= \frac{1}{2\pi i}\int_{r-i\infty}^{r+i\infty} e^{z\left(\frac{t-j_\infty x}{\omega(x)}+\frac{1}{|P|}\right)} e^{z\ln z}\,\frac{dz}{z} \qquad (4.85)\\
&= \frac{1}{2\pi i}\int_{r-i\infty}^{r+i\infty} e^{z\theta+z\ln z}\,\frac{dz}{z} \\
&= F^*(\theta),
\end{aligned}
$$

where

$$
\theta = \frac{t-j_\infty x}{\omega(x)}+\frac{1}{|p|} = \frac{t-j_\infty x(1-\tilde{L})}{\omega(x)}. \qquad (4.86)
$$

Since t is changing in the interval $(0,\infty)$, θ is in $(-\frac{(1-\tilde{L})j_\infty x}{\omega},\infty)$. For further discussion, see [19].

Until now we have finished the discussion of the asymptotic behavior of $W(x,t)$ as $x\to\infty$ and $t\to\infty$ for all the cases. The results show that for a viscoelastic rod, under certain conditions, its displacement function $W(x,t)$ approaches a steady shape $F^*(\theta)$, which is a probability distribution.

Chapter 5. Transformed Solution and the Steepest Descents for Tube Problem

In Chapter 3, we derived the general equation of wave propagation in fluid filled viscoelastic tube, and found the wall displacement in the form

$$W(x,t) = \frac{1}{2\pi i}\int_{Br} \overline{\Phi}(s) exp\{st - \frac{sx}{\sqrt{s\overline{G} + \eta s^2}}\}\, ds \qquad (5.1)$$

where $\overline{\Phi}(s)$ is the Laplace transform of the input function. If $G(t)$ is known exactly for the wall material considered, then theoretically $\overline{G(s)}$ can be computed and the integral in (5.1) can be evaluated numerically. In the general case, we do not know the exact form of the function $G(t)$. This prevents this path from being followed, apart from the substantial amount of numerical computation involved.

For integrals of the type given in equation (5.1), we can find the dominant part of their values from the neighborhood of a single point. The method we will use is called the steepest descent method, and the point is called the saddle point which is given by the solution of the equation

$$\frac{d}{dt}\{st - \frac{sx}{\sqrt{s\overline{G(s)} + \eta s^2}}\} = 0 \qquad (5.2)$$

The solution depends on the properties of $s\overline{G(s)}$. In Chapter 4, we consider certain classes of functions $G(t)$, and the asymptotic forms of $s\overline{G(s)}$ for s close to zero. They were divided into four different cases:

(I) $\eta(t) = \int_0^t [G_1(t) - G_\infty]\, dt$ diverges rapidly, $s\overline{G(s)} \sim \tau_0 s + G_\infty + s^p L(\frac{1}{s})\Gamma(1-p)$, $0 < p < 1$.

(IA) If $G_\infty = 0$, $s\overline{G(s)} \sim s^p L(\frac{1}{s})\Gamma(1-p)$.

(IB) If $G_\infty \neq 0$, $s\overline{G(s)} \sim G_\infty + s^p L(\frac{1}{s})\Gamma(1-p)$.

(II) $\eta(t) < \infty$ or slowly varying as $t \to \infty$, $s\overline{G(s)} \sim G_\infty + s(\tau_0 + \eta_0)$, or $G_\infty + s(\tau_0 + \eta(\frac{1}{s}))$.

(IIA) If $G_\infty = 0$, $s\overline{G(s)} \sim s(\tau_0 + \eta_0)$ or $s(\tau_0 + L(\frac{1}{s}))$.

(IIB) As $G_\infty \neq 0$, $s\overline{G(s)} \sim G_\infty + s(\tau_0 + \eta_0)$ or $G_\infty + s(\tau_0 + L(\frac{1}{s}))$.

The solution to equation (5.2), if existing, is in general complex. Assuming that $s\overline{G(s)}$ is analytic, with the exception of possible singularities, then if it is regular near s_0, which is the solution of equation (5.2), we may expand $s\overline{G(s)}$ in a power series in the neighbourhood of s_0. From the asymptotic point of view, for t large, we would expect s_0 to be close to the origin, so that locally an expansion of the form

Case (1):

$$s\overline{G(s)} = a_0 + a_1 s + a_2 s^2 + \ldots. \tag{5.3}$$

would be appropriate. This corresponds to the form of (II) we mentioned above.

On the other hand, if there is a singularity at the origin, we may write $s\overline{G(s)}$ in the form

Case (2):

$$s\overline{G(s)} = s^p(a_0 + a_1 s + a_2 s^2 + \ldots), \quad 0 < p < 1. \tag{5.4}$$

This corresponds to the form (IA) which have a common form as $s\overline{G(s)} = \hat{c}s^p$, $\hat{c} > 0$, $0 < p < 1$. This corresponds to what Pipkin [14] called a power-law solid with $G(t) = ct^{-p}$, $0 < p < 1$.

Extending the second case to $G(t) = G_\infty + ct^{-p}$, where $G_\infty > 0$, $0 < p < 1$, $c > 0$, we get our third case

Case (3):

$$s\overline{G(s)} = G_\infty + \hat{c}s^p, 0 < p < 1. \tag{5.5}$$

This is just the cases (IB) for $0 < p < 1$.

We begin with case (1) at $a_0 \neq 0$, that is regular in the neighbourhood of the origin, and can be written as

$$s\overline{G(s)} = 1 + \tau s + \xi s^2, \tag{5.6}$$

where $s\overline{G(s)}$ has been suitably normalized so that in nondimensional form the leading coefficient is unity. This takes care of the Kelvin-Voigt model and the Standard Linear model for suitable choices of τ and ξ.

Then equation (5.2) becomes

$$\frac{d}{ds}\{st - \frac{sx}{\sqrt{1 + \tau s + \hat{\eta} s^2}}\} = 0, \tag{5.7}$$

$$\text{where} \qquad \hat{\eta} = \xi + \eta,$$

$$\text{i.e.} \qquad t - \frac{x}{2}\frac{2 + \tau s}{(1 + \tau s + \hat{\eta} s^2)^{3/2}} = 0. \tag{5.8}$$

$$\text{then} \qquad \frac{t}{x} = \Psi'(s) = \frac{1 + \frac{\tau}{2}s}{(1 + \tau s + \hat{\eta} s^2)^{3/2}}, \tag{5.9}$$

$$\text{where} \qquad \Psi(s) = \frac{s}{\sqrt{1 + \tau s + \hat{\eta} s^2}}. \tag{5.10}$$

We assume τ, $\hat{\eta}$ positive, and $\tau^2/4\hat{\eta} \ll 1$, so that the appropriate saddle points lie close to the origin.

Given τ and $\hat{\eta}$, we can easily sketch the graph of $\Psi'(s)$, as in Fig.[5-1].

Next we find the point at which the second derivative of $\Psi(s)$ is zero. Then

$$2\tau\hat{\eta}s^2 + (6\hat{\eta} + \frac{1}{2}\tau^2)s + 2\tau = 0,$$

$$s = \frac{-(6\hat{\eta} + \frac{1}{2}\tau^2) \pm \sqrt{(6\hat{\eta} + \frac{1}{2}\tau^2)^2 - 16\tau^2\hat{\eta}}}{4\tau\hat{\eta}}$$

$$\simeq \frac{-(6\hat{\eta} + \frac{1}{2}\tau^2) \pm 6\hat{\eta}[1 - \frac{5}{36}\tau^2/\hat{\eta}]}{4\tau\hat{\eta}}.$$

The point with the maximum value of $\Psi'(s)$ is

$$s_0 \simeq \frac{-(6\hat{\eta} + \frac{1}{2}\tau^2) + (6\hat{\eta} - \frac{5}{6}\tau^2)}{4\tau\hat{\eta}} \qquad (5.11)$$
$$= -\frac{\tau}{3\hat{\eta}}.$$

At this point,

$$\frac{t}{x} = \Psi'(s_0) = \frac{1 - \frac{\tau^2}{6\hat{\eta}}}{(1 - \frac{2\tau^2}{9\hat{\eta}})^{3/2}}$$
$$\sim (1 - \frac{\tau^2}{6\hat{\eta}})(1 + \frac{3}{2}\frac{2\tau^2}{9\hat{\eta}}) \qquad (5.12)$$
$$\sim 1 - \frac{\tau^2}{6\hat{\eta}} + \frac{\tau^2}{3\hat{\eta}}$$
$$= 1 + \frac{\tau^2}{6\hat{\eta}}.$$

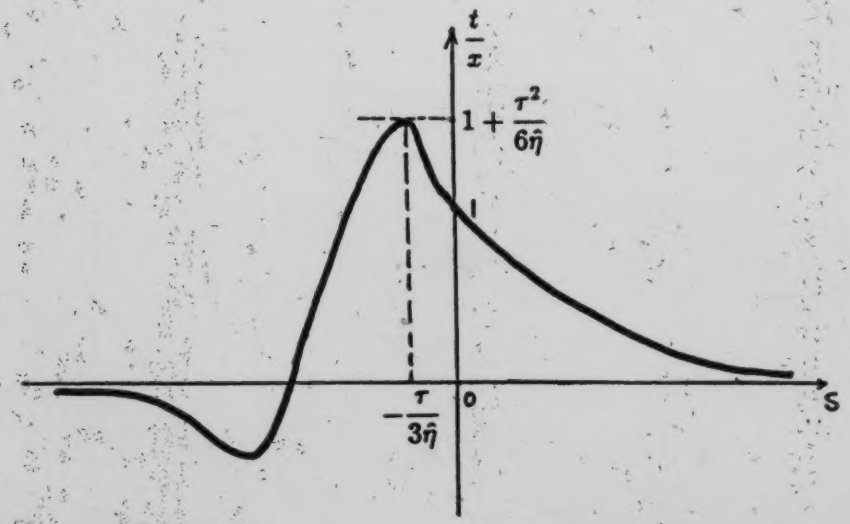

Fig.[5-1]. The graph of $\frac{t}{x} = \frac{1 + \frac{\tau}{2}s}{(1 + \tau s + \hat{\eta}s^2)^{3/2}}$.

Fig.[5-1]

Since both the first and the second derivatives of $st - s\Psi(s)$ equal to zero as $s_0 = -\tau/3\hat{\eta}$ and t/x varies in the neighbourhood of $1 + \tau^2/6\hat{\eta}$, we have a double saddle point at $s_0 = -\tau/3\hat{\eta}$, which is also called the saddle point of order 2.

By replacing $\overline{sG(s)}$ with its approximation $1+\tau s+\xi s^2$ and expanding, we can write (5.1) as the following asymptotic expression

$$\begin{aligned} W(x,t) &= \frac{1}{2\pi i}\int_{Br}\overline{\Phi}(s)\,exp\{st - sx[1-\frac{1}{2}(\tau s+\hat{\eta}s^2)]\}\,ds \\ &= \frac{1}{2\pi i}\int_{Br}\overline{\Phi}(s)\,exp\{s(t-x)+\frac{1}{2}x\tau s^2+\frac{1}{2}x\hat{\eta}s^3\}\,ds. \end{aligned} \tag{5.13}$$

From this expression, we can easily see that as $t/x = 1+\tau^2/6\hat{\eta}$, $s_0 = -\tau/3\hat{\eta}$ is a double saddle point.

Now changing variable to $s = s_0 + l$, and expanding (5.13) at s_0

$$\begin{aligned} W(x,t) &\sim \frac{1}{2\pi i}\overline{\Phi}(s_0)exp\{s_0(t-x)+\frac{1}{2}x\tau s_0^2+\frac{1}{2}x\hat{\eta}s_0^3\} \\ &\int_{Br} exp\{(t-x+x\tau s_0+\frac{3}{2}x\hat{\eta}s_0^2)l+\frac{x\hat{\eta}}{2}l^3\}\,dl \\ &\sim \overline{\Phi}(s_0)exp\{s_0(t-x)+\frac{1}{2}x\tau s_0^2+\frac{1}{2}x\hat{\eta}s_0^3\} \\ &\frac{1}{(\frac{3}{2}x\hat{\eta})^{1/3}}A_i\left(-\frac{1}{(\frac{3}{2}x\hat{\eta})^{1/3}}[t-x+x\tau s_0+\frac{3}{2}x\hat{\eta}s_0^2]\right). \end{aligned} \tag{5.14}$$

where A_i is the standard Airy function of the first kind. We can get this result by choosing a steepest descent path.

Alternatively, we can get a uniform approximation for $W(x,t)$ by using the theorem of Chester, Friedman and Ursell [21]. This result will be more general than the preceeding one, which has some additional flexibility in the choice of $\hat{\eta}$.

Let

$$\tilde{W}(s,t/x) = st/x - \frac{s}{\sqrt{\overline{sG(s)}+\hat{\eta}s^2}}, \tag{5.15}$$

and suppose $\tilde{W}$ is analytic function of s in a suitable domain containing the contour Br and the points $s = s_\pm$, where

$$\begin{aligned} &s_+ \neq s_-, \quad \tilde{W}_s(s_\pm, t/x) = 0, \\ &\tilde{W}_{ss}(s_+, t/x) \neq 0, \quad \tilde{W}_{ss}(s_-, t/x) \neq 0. \end{aligned} \tag{5.16}$$

If these two points coalesce, a double saddle point is produced, such that

$$\begin{aligned} &\tilde{W}_s(s_+, t/x) = \tilde{W}_{ss}(s_+, t/x) = 0, \\ &\tilde{W}_{sss}(s_+, t/x) \neq 0, \quad s_+ = s_-. \end{aligned} \tag{5.17}$$

At the present case, these conditions clearly hold.

Following this theorem, we define $s(\omega)$ by the equation

$$\tilde{W}(s, t/x) = -(\omega^3/3 - \gamma^2\omega) + \rho = U(\omega, t/x) \tag{5.18}$$

where $\gamma(t/x)$ and $\rho(t/x)$ are to be determined.

It can be turned out under certain conditions that

$$\begin{aligned} \frac{4}{3}\gamma^3 &= \tilde{W}(s_+, t/x) - \tilde{W}(s_-, t/x), \\ \rho &= \frac{1}{2}\{\tilde{W}(s_+, t/x) - \tilde{W}(s_-, t/x)\}. \end{aligned} \tag{5.19}$$

Next, defining

$$G_0(\omega) = \Phi(s(\omega))\frac{ds}{d\omega}, \tag{5.20}$$

and setting

$$G_0(\omega) = a_0 + a_1\omega + (\omega^2 - \gamma^2)H_0(\omega). \tag{5.21}$$

It turns out that

$$\begin{aligned} a_0 &= \frac{G_0(\gamma) + G_0(-\gamma)}{2}, \\ a_1 &= \frac{G_0(\gamma) - G_0(-\gamma)}{2\gamma}, \\ H_0 &= \frac{G_0(\omega) - a_0 - a_1\omega}{\omega^2 - \gamma^2}. \end{aligned} \tag{5.22}$$

Finally, the uniform expression of the integral $W(x, t)$ can be written in terms of the Airy function A_i and its derivative A_i' as $x \to \infty$,

$$W(x, t) \sim exp(\rho x)\{a_0 x^{-1/3} A_i(x^{2/3}\gamma^2) + a_1 x^{-2/3} A_i'(x^{2/3}\gamma^2)\}. \tag{5.23}$$

This expansion is uniformly valid as $s_\pm$ varying in a suitable domain.

Applying those results we got from Chester, Friedman and Ursell's theorem to our own case that

$$\tilde{W}(s,t/x) = st/x - \frac{s}{\sqrt{1+\tau s+\hat{\eta}s^2}}.$$

First, find $s_\pm$ which satisfy (5.16). They are also the solutions of the equation (5.9), which can be expanded as

$$\frac{t}{x} - \frac{1}{2}(2+\tau s)(1-\frac{3}{2}\tau s - \frac{3}{2}\hat{\eta}s^2) \simeq 0. \tag{5.24}$$

By omitting the highest order item s^3, (5.24) can be written as

$$(\frac{3}{2}\hat{\eta}+\frac{3}{4}\tau^2)s^2 + \tau s + \frac{t}{x} - 1 = 0.$$

Since $\tau^2/4\hat{\eta} \ll 1$,

$$s_\pm \simeq \frac{-\tau \pm \sqrt{\tau^2 - 6\hat{\eta}(t/x-1)}}{3\hat{\eta}}. \tag{5.25}$$

We can also approximate the transformation (5.18) by

$$\omega = -(\frac{3}{2}\hat{\eta})^{1/3}(s+\frac{\tau}{3\hat{\eta}}). \tag{5.26}$$

We then find γ^2 and ρ by identifying the coefficents of equation (5.18) which is

$$\frac{st}{x} - s(1-\frac{1}{2}\tau s - \frac{1}{2}\hat{\eta}s^2) = -\frac{\omega^3}{3} + \gamma^2\omega + \rho. \tag{5.27}$$

By putting (5.26) into (5.27), we can get

$$\begin{aligned} x^{2/3}\gamma^2 &= -\frac{1}{(\frac{3}{2}\hat{\eta}x)^{1/3}}\{t - x(1+\frac{\tau^2}{6\hat{\eta}})\}, \\ x\rho &= -\frac{\tau}{3\hat{\eta}}\{t - x(1+\frac{\tau^2}{6\hat{\eta}})\} - \frac{1}{2}\hat{\eta}x(\frac{\tau}{3\hat{\eta}})^3 \end{aligned} \tag{5.28}$$

which come from the equations

$$\begin{cases} \dfrac{\tau^2}{6\hat{\eta}} - \gamma^2(\dfrac{3}{2}\hat{\eta})^{1/3} = \dfrac{t}{x} - 1 - \dfrac{\tau^2}{6\hat{\eta}}, \\ \dfrac{\tau^3}{48\hat{\eta}^2} = -\gamma^2(\dfrac{3}{2}\hat{\eta})^{1/3}\dfrac{\tau}{3\hat{\eta}} + \rho. \end{cases}$$

In addition

$$\begin{aligned} a_0 &= -(\frac{2}{3\hat{\eta}})^{1/3}\frac{\overline{\Phi}(s_+) + \overline{\Phi}(s_-)}{2}, \\ a_1 &= (\frac{2}{3\hat{\eta}})^{2/3}\frac{\overline{\Phi}(s_+) - \overline{\Phi}(s_-)}{s_+ - s_-}. \end{aligned} \tag{5.29}$$

$$\begin{aligned} \therefore \quad W(x,t) \sim exp\{&-\frac{\tau}{3\hat{\eta}}[t - (x(1 + \frac{\tau^2}{6\hat{\eta}})] - \frac{1}{2}\hat{\eta}x(\frac{\tau}{3\hat{\eta}})^3\} \\ &\{ a_0 x^{-1/3} A_i(-\frac{1}{(\frac{3}{2}\hat{\eta}x)^{1/3}}[t - x(1 + \frac{\tau^2}{6\hat{\eta}})]) \\ &+ a_1 x^{-2/3} A_i'(-\frac{1}{(\frac{3}{2}\hat{\eta}x)^{1/3}}[t - x(1 + \frac{\tau^2}{6\hat{\eta}})]) \}. \end{aligned} \tag{5.30}$$

The connection to the expression (5.14) is now evident. Equation (5.30) gives the general and uniform asymptotic expression.

There are occasions when the assumption of the analyticity of $s\overline{G(s)}$ about the original may not hold. Pipkin [14] has suggested that the form

$$s\overline{G(s)} = \hat{c}s^p, \ 0 < p < 1, \tag{5.31}$$

which is our second case, may be more appropriate for a broad class of materials, and we now investigate the asymptotic form arising from equation (5.31).

Returning to the expression given by equation (5.1), we now assume the form of equation (5.31) for $s\overline{G}(s)$, and write

$$W(x,t) = \frac{1}{2\pi i}\int_{Br} \overline{\Phi}(s) exp\{E(s,x,t)\}\, ds \tag{5.32}$$

with

$$E(s,x,t) = st - \frac{s\hat{x}}{\sqrt{s^p + \hat{\eta}s^2}} \tag{5.33}$$

where

$$\hat{x} = x/\sqrt{\hat{c}},\ \hat{\eta} = \eta/\hat{c}, \quad \hat{c} > 0,\ \eta > 0,\ 0 \leq p < 1.$$

Using the steepest descents method, we have to find the saddle point which satisfies

$$\frac{dE}{ds} = 0,$$

$$\text{i.e.} \quad \frac{t}{\hat{x}} = \frac{(1 - \frac{p}{2})s^p}{(s^p + \hat{\eta}s^2)^{3/2}}. \tag{5.34}$$

The nonuniformity of the behavior of the right hand side is easily seen by graphing the function (5.34) in Fig.[5-2].

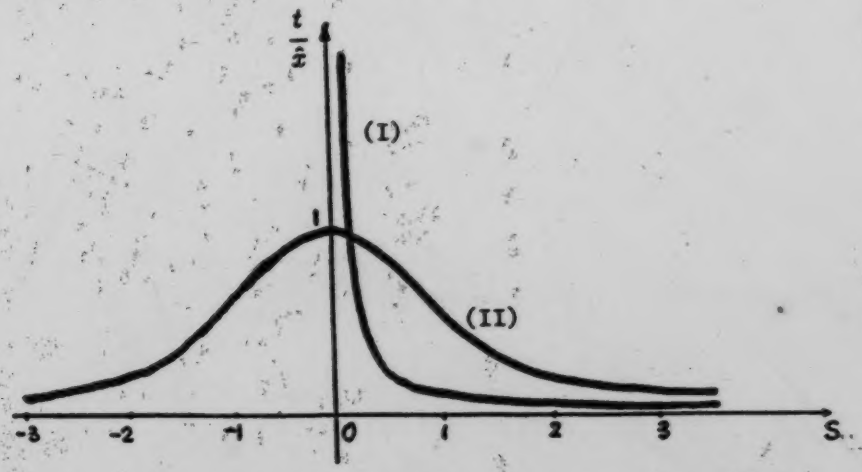

Fig.[5-2]. The nonuniformity behavior of $\frac{t}{\hat{x}} = \frac{(1-p/2)s^p}{(s^p+\hat{\eta}s^2)^{3/2}}$.
(I) $p = 0.05$, (II) $p = 0$.

Fig.[5-2]

Since $p > 0$, there is a simple saddle point in the real line, which occurs at a positive value of s.

If p is small, then for s close to zero, the variation of the value of s with $t/\hat{x}$ is very rapid, and for $t/\hat{x}$ close to 1, s is close to zero. For practical purposes, we

can approximate the value of p by $1/n$, $n \in I^+$, with n large, i.e. $p \doteq 1/n$, and set $s = K^{2n}$.

$$\text{then} \quad E(s, \hat{x}, t) = K^{2n}t - \frac{K^{2n-1}\hat{x}}{\sqrt{1+\hat{\eta}K^{4n-2}}}, \tag{5.35}$$

and the saddle points are given by

$$\frac{t}{\hat{x}} = \frac{2n-1}{2nK(1+\hat{\eta}K^{4n-2})^{3/2}}. \tag{5.36}$$

Then the saddle point K_0 satisfies

$$t = \frac{(2n-1)\hat{x}}{2nK_0(1+\hat{\eta}K_0^{4n-2})^{3/2}}, \tag{5.37}$$

$$E(s(K_0), \hat{x}, t) = -\hat{x}K_0^{2n-1}\frac{1+2n\hat{\eta}K_0^{4n-2}}{2n(1+\hat{\eta}K_0^{4n-2})^{3/2}}, \tag{5.38}$$

$$\frac{\partial E}{\partial K} = 2ntK^{2n-1} - (2n-1)\hat{x}\frac{K^{2n-2}}{(1+\hat{\eta}K^{4n-2})^{3/2}}, \tag{5.39}$$

$$\frac{\partial^2 E}{\partial K^2} = \frac{(2n-1)\hat{x}K_0^{2n-3}(1+(6n-2)\hat{\eta}K_0^{(4n-2)})}{(1+\hat{\eta}K_0^{4n-2})^{5/2}}. \tag{5.40}$$

If n is large, then as $\hat{x}/t$ varies in the neighbourhood of 1, so does K_0, which is the solution of equation(5.37). Assuming this to be the dominant saddle point, we have

$$\begin{aligned} W(\hat{x}, t) \sim \frac{1}{2\pi i}\int \Phi(s(k_0))exp\{E(s(K_0), \hat{x}, t) \\ + \frac{1}{2}E''(s(K_0), \hat{x}, t)(K-K_0)^2\}2nK_0^{2n-1}\,dK \end{aligned} \tag{5.41}$$

with the integral taken along a suitable contour in the vicinity of K_0. Using the standard steepest decent method, we have

$$\begin{aligned} W(\hat{x}, t) &\sim 2n\overline{\Phi}(s(K_0))exp\{E(s(K_0), \hat{x}, t)\}\frac{1}{2\pi i}\int e^{1/2E''(s(K_0),\hat{x},t)(K-K_0)^2}K^{2n-1}\,dK \\ &\sim 2n\overline{\Phi}(s(K_0))exp\{E(s(K_0), \hat{x}, t)\}K_0^{2n-1}\frac{1}{2\pi}\int_{-\epsilon}^{\epsilon} e^{-1/2E''(s(K_0),\hat{x},t)r^2}\,dr \\ &\sim \frac{2n\overline{\Phi}(s(K_0))exp\{E(s(K_0), \hat{x}, t)\}K_0^{2n-1}}{\sqrt{2\pi E''(s(K_0), \hat{x}, t)}} \\ &\sim \frac{2nK_0^{n+1/2}\overline{\Phi}(s(K_0))exp\{E(s(K_0), \hat{x}, t)\}(1+\hat{\eta}K_0^{4n-2})^{5/4}}{\sqrt{2\pi(2n-1)\hat{x}(1+(6n-2)\hat{\eta}K_0^{4n-2})}}. \end{aligned} \tag{5.42}$$

Clearly, if $K_0 \gg 1$ or $K_0 \ll 1$, this quantity is extremely small, and we need only consider it in the neighbourhood of $K_0 = 1$, that is for $\hat{x}/t$ near 1. To examine the behavior, we plot the quantity in equation (5.42) as a function of K_0, dropping the factor $\overline{\Phi}(s(K_0))$ for the moment. The graphs of equation(5.42) for comparison of different parameters are shown at the end of the chapter as Fig.[5-4.1].

The effect of the radial inertia term involving $\hat{\eta}$ can now be seen quite clearly. If p is small, n large, then as $K_0 < 1$, although the terms involving $\hat{\eta}$ are small, they nevertheless have considerable effect on where the maximum value of $W(x,t)$ occurs. Fig.[5-4.1] shows that at the point with the maximum value of $W(\hat{x},t)$, $K_0 < 1$, then as n large, from (5.37) we get that $\hat{x}/t < 1$, so that the wave is slowed down from its purely elastic case with radial inertia $\hat{\eta}$ omitted. Here the purely elastic case is defined as the case that $G(t) = G_0 H(t)$, where $G_0 = G_r \hat{c}$, and $p = 0$. Its maximum point happens at $\hat{x}/t = 1$.

On the other hand, if $\hat{\eta} = 0$, we can follow Pipkin [14] to show that the viscoelastic wave is faster than the purely elastic case. See Fig.[5-4.2].

Thus if $\hat{\eta} = 0$ in (5.36) and (5.42), with $p = 1/n$,

$$K_0 = \frac{2n-1}{2n}\frac{\hat{x}}{t} = \frac{2-p}{2}\frac{\hat{x}}{t}, \tag{5.43}$$

$$W(\hat{x},t) \sim \frac{2}{\sqrt{2\pi p(2-p)\hat{x}}} K_0^{\frac{1}{p}+\frac{1}{2}} exp\{-\frac{p}{2}K_0^{\frac{2}{p}-1}\hat{x}\}. \tag{5.44}$$

Holding $\hat{x}$ fixed and allowing K_0 to vary, we can find a point at which $W(\hat{x},t)$ approaches the maximum value, i.e.

$$\frac{dW}{dK_0} = 0.$$

Then

$$K_0 = (\frac{2+p}{2-p}\frac{1}{p\hat{x}})^{\frac{p}{2-p}}.$$

From (5.43)

$$K_0 = \frac{2-p}{2}\frac{\hat{x}}{t},$$

so that for p very small,

$$\begin{aligned}
\frac{\hat{x}}{t} &= \frac{2}{2-p}\left(\frac{2+p}{2-p}\frac{1}{p\hat{x}}\right)^{\frac{p}{2-p}} \\
&\sim \left(\frac{1}{p\hat{x}}\right)^{\frac{p}{2}} \\
&\sim \left(\frac{1}{p}\right)^{\frac{p}{2}} \\
&\sim e^{\frac{p}{2}ln(\frac{2}{p})} \\
&\sim 1 + \frac{p}{2}ln(\frac{2}{p}) \ > 1,
\end{aligned} \tag{5.45}$$

so that the wave is faster than the elastic case where $\hat{x}/t = 1$.

We notice that the result we got in case (1) is about $a_0 \neq 0$. As $a_0 = 0$, but $a_1 \neq 0$, $s\overline{G}(s) = s(a_1 + a_2 s + \dots)$, we can approximate it by (5.42) with $n = p = 1$.

Consider now an example of the remaining case when $s\overline{G}(s) = G_\infty + \hat{c}s^p$, In order to compare the effect of this relaxation function with the previous one, it is advantageous to normalize it as

$$s\overline{G(s)} = G_\infty + s^p, \quad 0 < p < 1. \tag{5.46}$$

To investigate the asymptotic form of this case, we apply the steepest descent method again. Here

$$E(s, \hat{x}, t) = st - \frac{s\hat{x}}{\sqrt{G_\infty + s^p + \eta s^2}}, \tag{5.47}$$

$$\frac{\partial E}{\partial s} = t - \hat{x}\frac{G_\infty + (1 - \frac{1}{2}p)s^p}{(G_\infty + s^p + \eta s^2)^{3/2}},$$

By setting $\frac{\partial E}{\partial s} = 0$, we get that

$$\frac{t}{\hat{x}} = \tilde{E(s)} = \frac{G_\infty + (1 - \frac{1}{2}p)s^p}{(G_\infty + s^p + \eta s^2)^{3/2}}. \tag{5.48}$$

$$\frac{d\tilde{E(s)}}{ds} = -\frac{p(1+p)G_\infty s^{p-1} + p(1-\frac{p}{2})s^{2p-1} + 6\eta(1-\frac{p}{2})(1-\frac{p}{3})s^{p+1} + 6\eta G_\infty s}{2(G_\infty + s^p + \eta s^2)^{5/2}}$$

$$< 0, \quad \text{for} \quad s > 0, \quad p > 0 \text{ and small.} \tag{5.49}$$

such that the graph of $\tilde{E(s)}$ is strictly decreasing. For very small p, with s approaches zero, $t/\hat{x}$ approaches $\frac{1}{G_\infty^{1/2}}$.

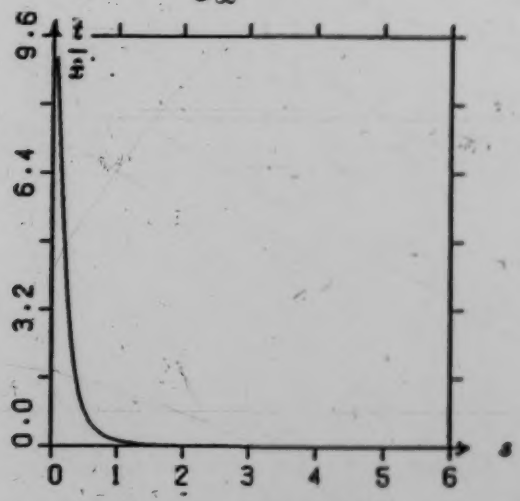

Fig.[5-3]. The graph of $\frac{t}{\hat{x}} = \frac{G_\infty + (1-\frac{1}{2}p)s^p}{(G_\infty + s^p + \eta s^2)^{3/2}}$. $G_\infty = 0.05$, $p = 0.05$, $\eta = 0.173125$, $\hat{x} = 6$.

Fig.[5-3]

The graph of $\tilde{E(s)}$ [Figure 5-3] shows that the function is a strictly decreasing function, without any inflection point. Then given $t/\hat{x}$, which is greater than zero, and not greater than $\frac{1}{G_\infty^{1/2}}$, (5.48) has only one solution for $s > 0$, such that (5.47) has only a simple single saddle point in the real positive line.

For small p, we approximate it by $1/n$, $n \in I^+$, and set $s = K^{2n}$ again, s approaching to zero corresponds to the case that $K < 1$, K is in the neighbourhood of $K = 1$.

Then (5.47) can be written as

$$E(s(K), \hat{x}, t) = K^{2n}t - \frac{K^{2n}\hat{x}}{\sqrt{G_\infty + K^2 + \eta K^{4n}}},$$

the saddle point K_0 satisfies that

$$t = \hat{x}\frac{G_\infty + (1 - \frac{1}{2n})K_0^2}{(G_\infty + K_0^2 + \eta K_0^{4n})^{3/2}}. \tag{5.50}$$

$$E(s(K_0), \hat{x}, t) = -\frac{\hat{x}K_0^{2n+2}(1 + 2n\eta K_0^{4n-2})}{2n(G_\infty + K_0^2 + \eta K^{4n})^{3/2}}. \tag{5.51}$$

Since

$$\frac{\partial E}{\partial K} = \frac{\partial E}{\partial s}\frac{\partial s}{\partial K} = 2nK^{2n-1}\frac{\partial E}{\partial s},$$

$$\frac{\partial^2 E}{\partial k^2} = 2n(2n-1)K^{2n-2}\frac{\partial E}{\partial s} + (2nK^{2n-1})^2\frac{\partial^2 E}{\partial s^2}.$$

At the saddle point,

$$K = K_0,\ s_0 = K_0^{2n},\ \frac{\partial E}{\partial s} = 0,$$

$$\begin{aligned}
&E''(s(K_0), \hat{x}, t) \\
&= \frac{\partial^2 E}{\partial k^2}|_{k=k_0} \\
&= (2nK^{2n-1})^2\frac{\partial^2 E}{\partial s^2}|_{s=s_0} \\
&= 4n^2K_0^{4n-2}(-\hat{x})\frac{dE(s)}{ds}|_{s=s_0} \\
&= \frac{\hat{x}K_0^{2n}[2(n+1)G_\infty + (2n-1)K_0^2 + 2\eta(2n-1)(3n-1)K_0^{4n} + 12G_\infty\eta n^2K_0^{4n-2}]}{(G_\infty + K_0^2 + \eta K_0^{4n})^{5/4}}
\end{aligned} \tag{5.52}$$

Using the steepest descent method to $W(\hat{x},t)$, with the integral taken along a contour in a small neighbourhood of K_0, where $E(s(K_0),\hat{x},t)$ is the maximum on the contour, we get that

$$\begin{aligned}
W(\hat{x},t) &= \frac{1}{2\pi i}\int_{Br}\overline{\Phi}(s)exp\{E(s)\}\,ds, \quad t\to\infty,\ x\to\infty,\\
&= \frac{1}{2\pi i}\int_{Br}\overline{\Phi}(s(K_0))exp\{E(s(K_0),\hat{x},t)\\
&+ \frac{1}{2}E''(s(K_0),\hat{x},t)(K-K_0)^2\}2nK^{2n-1}\,dk\\
&\sim 2nK_0^{2n-1}\overline{\Phi}(s(K_0))exp\{E(s(K_0),\hat{x},t)\}\,\frac{1}{2\pi}\int_{-\varepsilon}^{\varepsilon}e^{-\frac{1}{2}E''r^2}\,dr\\
&\sim \frac{2nK_0^{2n-1}\overline{\Phi}(s(K_0))exp\{E(s(K_0),\hat{x},t)\}}{\sqrt{2\pi E''(s(K_0),\hat{x},t)}}\\
&\sim \frac{2s_0^{\frac{1-p}{2}}\overline{\Phi}(s_0)exp\{E(s_0,\hat{x},t)\}(G_\infty+s_0^p+\eta s_0^2)^{5/4}}{\sqrt{2\pi\hat{x}[2p(1+p)G_\infty+p(2-p)s_0^p+2\eta(2-p)(3-p)s_0^2+12G_\infty\eta s_0^{2-p}]}}.
\end{aligned} \tag{5.53}$$

In the case that $G_\infty = 0$, equation (5.53) is coincident with equation (5.41), the case that $sG(s) = s^p$.

The graphs of equation (5.53) for the different choices of G_∞ and η with small p are shown in Fig.[5-5].

The numerical solutions show us that

(1). At $\eta = 0$, the wave is faster than the case when $\eta \neq 0$.

(2). As G_∞ increases, the wave goes faster.

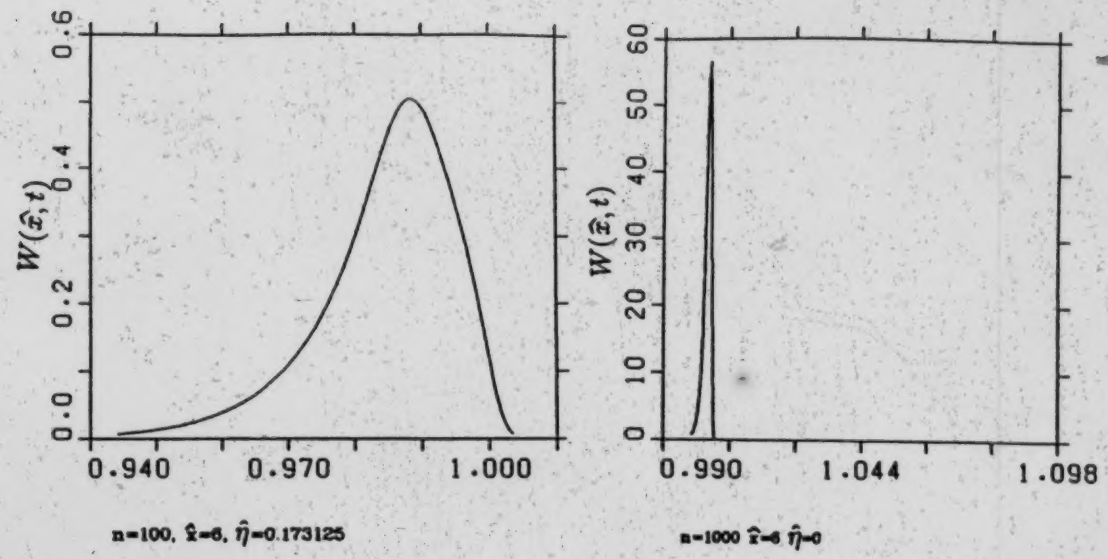

Fig.[5-4.1]

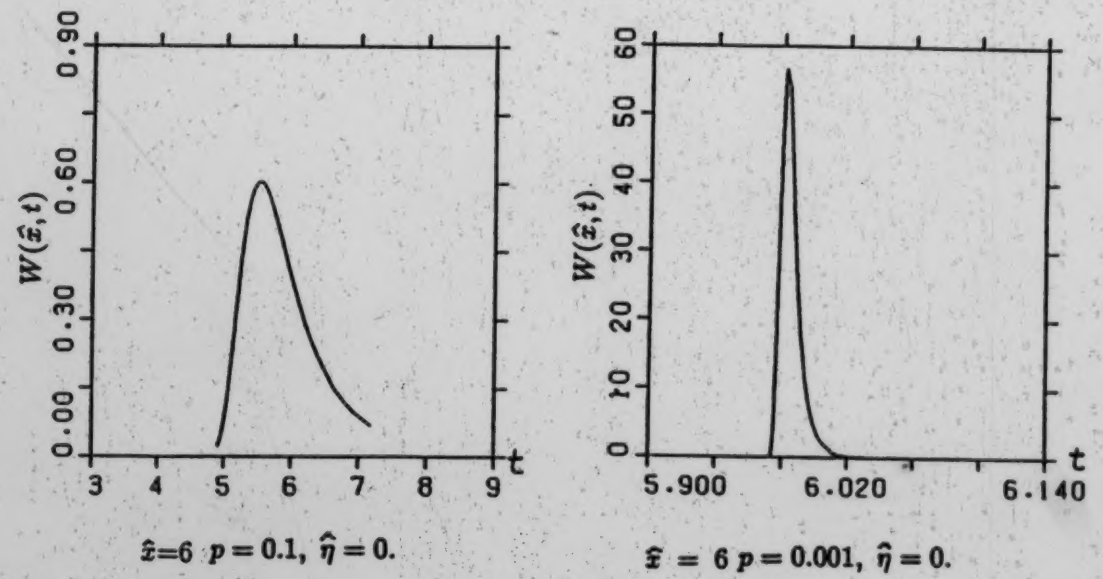

Fig.[5-4.2]

Fig.[5-4]. Plots of equation (5.42), $W(\hat{x},t)$ for the case $s\overline{G}(s) = \hat{c}s^p$. Fig.[5-4.1] shows that the maximum point happens at $K_0 < 1$, so that $\hat{x}/t < 1$. the wave is faster than the purely elastic case with $\hat{\eta}$ omitted. Fig.[5-4.2] shows that for $\hat{\eta} = 0$, the viscoelastic wave ($p > 0$) is faster than the pure elastic case ($p = 0$).

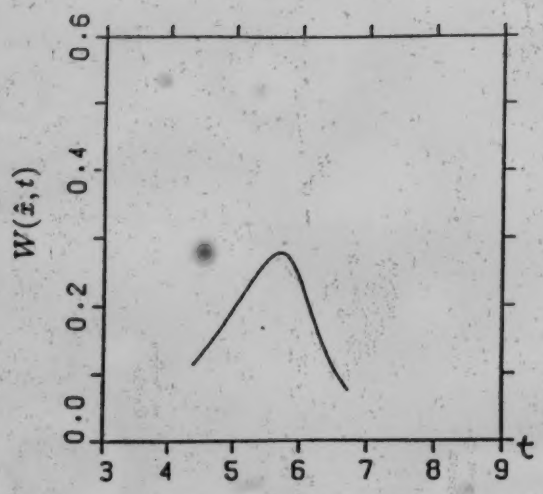

$p = 0.1,\ G_\infty = 0.1,\ \eta = 0.173125.$
$\hat{x}$=6

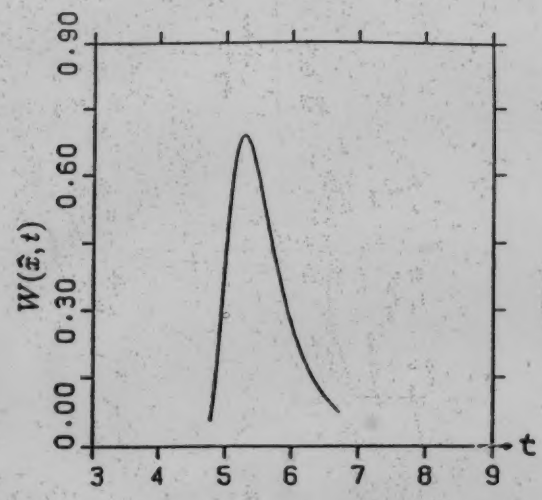

$p = 0.1,\ G_\infty = 0.1,\ \eta = 0.$
$\hat{x}$=6

Fig.[5-5.1]

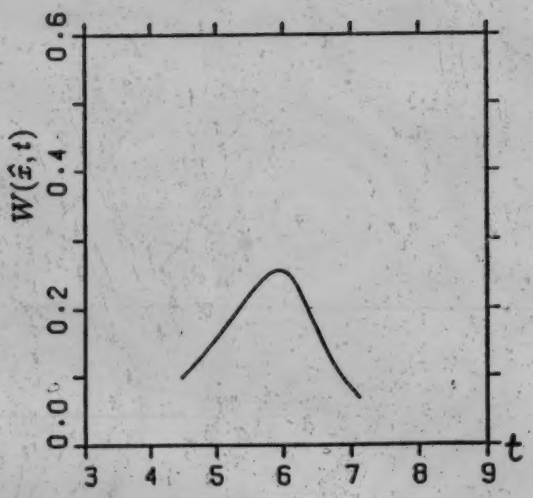

$p = 0.1,\ G_\infty = 0.01,\ \eta = 0.173125.$
$\hat{x}$=6

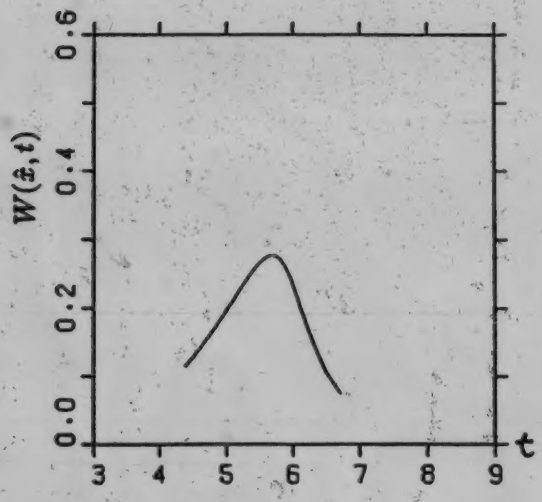

$p = 0.1,\ G_\infty = 0.1,\ \eta = 0.173125.$
$\hat{x}$=6

Fig.[5-5.2]

Fig.[5-5]. Plots of equation (5.53), $W(\hat{x},t)$ for the case $s\overline{G}(s) = G_\infty + \hat{c}s^p, G_\infty > 0$. Fig.[5-5.1] shows that wave is faster at $\eta = 0$ then at $\eta > 0$. Fig.[5-5.2] shows that wave goes faster with the incresing of G_∞.

Chapter 6. Numerical Procedures and Conclusions

In Chapter 4 we summarised the results obtained by Pipkin [19] for wave propagation in viscoelastic rods. For the class of relaxations treated there it was shown that for the basic problem, that is for a step input at $t = 0$, the resulting wave forms are closely connected with stable probability distribution functions. In Chapter 5 we considered the general asymptotic wave forms for wave propagation in a fluid filled viscoelastic tube which differ from the previous situation, in their simplest forms by the addition of a term η due to radial inertia of the tube wall. That is

$$\overline{W}(x,s) = \overline{\Phi}(s)e^{-\frac{sx}{\sqrt{s\overline{G}(s)+\eta s^2}}}, \tag{6.1}$$

with $\eta = 0$ for the rod. Even though one would expect the asymptotic forms to be the same, it is clear from the analysis in Chapter 5 that this is not always so. Thus, in considering those cases where $s\overline{G}(s)$ has an analytic expansion about $s = 0$, a case is typified by the Kelvin-Voigt relaxation function with

$$s\overline{G}(s) = 1 + \tau s, \tag{6.2}$$

it was shown that if

$$\eta \gg \frac{\tau^2}{4}, \tag{6.3}$$

then the asymptotic form of $W(x,t)$ is in the form of Airy function, which is oscillatory and so equation (6.1) with $\overline{\Phi}(s) = \frac{1}{s}$ can not represent the transform of a probability distribution function, unlike the case $\eta = 0$. As η decreases, this conclusion changes. For example if

$$\eta = \frac{\tau^2}{4}, \tag{6.4}$$

then

$$\overline{W}(x,s) = \overline{\Phi}(s)e^{-\Omega(s)x}, \tag{6.5}$$

with

$$\Omega(s) = \frac{s}{1+\tau s}. \tag{6.6}$$

Clearly, $\Omega(s) > 0$, $\Omega'(s)$ is completely monotone for $s > 0$, so for each $x > 0$, $\overline{W}(x,s)$ is completely monotone by Theorem 4, and hence by Theorem 1 is the Laplace transform of a probability distribution function for $\overline{\Phi}(s) = \frac{1}{s}$.

For

$$\eta < \frac{\tau^2}{4}, \tag{6.7}$$

we have employed the numerical method described below to graph the behavior of $W(x,t)$ for a specified pulse input. The graphs are shown in Fig.[6-4], for various values of η.

In the examples corresponding to Pipkin's other cases when , near $s = 0$,

$$s\overline{G}(s) = G_\infty + \hat{c}s^p, \quad 0 < p < 1, \tag{6.8}$$

where G_∞ may be zero or a positive constant. It is not clear whether this case, like the case $\eta = 0$, gives rise to probability distribution and density functions.

Whether or not this last case is so, it is of some importance to determine how the various available parameters affect the propagation of pulses in viscoelastic tubes. If it is true that most materials can be approximated by relaxation functions of the classes considered above, then we can decide how pulses in a wide variety of fluid filled viscoelastic tubes are affected by the tube wall viscoelasticity.

Next we consider a numerical method briefly.

We have the inverse Laplace transform of $\overline{W}(x,s)$ as

$$W(x,t) = \frac{1}{2\pi i}\int_{a-i\infty}^{a+i\infty} e^{st}\overline{W}(x,s)\,ds, \tag{6.9}$$

which may be written as

$$W(x,t) = \frac{e^{at}}{\pi} \int_0^\infty [\Re\{\overline{W}(a+i\omega)\} \cos\omega t - \Im\{\overline{W}(a+i\omega)\} \sin\omega t]\, d\omega. \qquad (6.10)$$

where $\Re$ and $\Im$ are the real and imaginary parts respectively.

Following Crump [18], we can write the series approximation to (6.10) as

$$W(x,t) = \frac{e^{at}}{T} \left[\frac{1}{2}\overline{W}(x,a) + \sum_{k=1}^{\infty} [\Re\{\overline{W}(a+\frac{k\pi i}{T})\} \cos(\frac{k\pi t}{T}) \right.$$
$$\left. -\Im\{\overline{W}(a+\frac{k\pi i}{T})\} \sin(\frac{k\pi t}{T})] \right], \qquad (6.11)$$

where T is chosen so that $2T > t_{\max}$, where $t_{\max}$ is the largest t over a range of t-value, and a is chosen to satisfy that

$$a = \alpha - \frac{\ln E'}{2T}, \qquad (6.12)$$

where E' is the relative error of the computation, and α is a number to be chosen slightly larger than $\max\{\Re(p),\ p \text{ is a pole of } \overline{W}(x,s)\}$.

To calculate (6.11) numerically, we use the Epsilon Algorithm (EPAL) [23]. By this algorithm, the rate of convergence can be significantly improved. The method of EPAL can be described as follows.

To numerically approximate the sum of series $\sum_{n=1}^{\infty} a_n$, we can use its first $2N+1$ partial sums $s_m = \sum_{n=1}^{m} a_n$, $m = 1, 2, \ldots, 2N+1$, and define a nonlinear sequence as

$$\varepsilon_{s+1}^{(m)} = \varepsilon_{s-1}^{(m+1)} + [\varepsilon_s^{(m+1)} - \varepsilon_s^{(m)}]^{-1}, \qquad (6.13)$$

with $\varepsilon_{-1}^{(m)} = 0$ and $\varepsilon_0^{(m)} = s_m$. Then the sequence $\varepsilon_1^{(1)}, \varepsilon_3^{(1)}, \varepsilon_5^{(1)}, \ldots, \varepsilon_{2N+1}^{(1)}$ is a successive approximation to the sum of the series.

An example of both experimental and numerical results for wave propagation in fluid filled distensible tubes is given in [12]. We use the same boundary condition and values here for comparison purposes.

The boundary condition is given as

$$p_m(0,t) = \frac{1}{2}[1 + \cos\frac{\pi}{t_0}(t - t_0)]H(2t_0 - t)H(t), \tag{6.14}$$

with $t_0 = 3ms$, and p_m the mean pressure. The relation between $\overline{W}(x,s)$ and $\overline{p}_m$ is

$$\overline{W}(x,s) = \overline{B}(s)e^{-\Omega(s)x}, \tag{6.15}$$

$$\overline{p}_m = A(s)e^{-\Omega(s)x}, \quad A(s) = \frac{2s^2\overline{B}(s)}{\Omega^2(s)}. \tag{6.16}$$

and

$$A(s) = \overline{p}_m(0,s) = \frac{1 - e^{-2st_0}}{2s}\frac{\pi^2}{\pi^2 + s^2t_0^2}. \tag{6.17}$$

Then

$$\overline{p}_m(x,s) = \frac{1 - e^{-2st_0}}{2s}\frac{\pi^2}{\pi^2 + s^2t_0^2}\exp\{-\frac{sx}{\sqrt{s\overline{G}(s) + \eta s^2}}\}. \tag{6.18}$$

Applying Crump's series approximation and EPAL to equation (6.18), we can get the numerical results of $p_m(x,t)$ for the different choices of $s\overline{G}(s)$.

First consider the case where

$$\Omega(s) = \frac{s}{\sqrt{1 + \tau s + \eta s^2}}, \tag{6.19}$$

where $\tau = 9 * 10^{-5}$ sec, $\eta = 0.173125$. The mean pressure at $x = 6$, 11 cms are shown in Fig.[6-1] and [6-2], and these are in good agreement with [12].

The case $\eta = 0$ is shown in Fig.[6-3].

Next we consider the case where

$$\Omega(s) = \frac{s}{\sqrt{\hat{c}s^p + \eta s^2}}, \quad 0 < p < 1. \tag{6.20}$$

For $\eta = 0$, we have case (IA) of Chapter 4, The graphs are shown in Fig.[6-5].

For $\eta \neq 0$, Figs [6-6], [6-7] and [6-8] illustrate the graphs of p_m for different choices of the parameters of η, p and $\hat{c}$. We can see that η decides the degree of oscillation in the tail. p is related to both the amplitude and the tail of the wave. The value of $\hat{c}$ affects the speed of the wave.

Next we consider

$$\Omega(s) = \frac{s}{\sqrt{G_\infty + s^p + \eta s^2}}, \quad G_\infty > 0, \quad 0 < p < 1. \tag{6.21}$$

Fig.[6-9] is the graph for $\eta = 0$, which is case (IB) of Chapter 4. Fig.[6-10] shows the effect of G_∞ on the speed of the propagating wave, while Fig.[6-11] illustrates the effect of η on the oscillation of the tail.

Fig.[6-12] is the graphs of $p_m(x,t)$ for the three different cases at $\eta = 0$. It is really Figs. [6-3], [6-5] & [6-9] in one axis of coordinates. The graphs display the behavior of wave propagation in viscoelastic rods with a pulse input.

It has been shown in Chapter 4 that for a viscoelastic rod, with $\Phi(s) = \frac{1}{s}$,

$$W(x,t) = \lim_{R\to\infty} \int_{a-iR}^{a+iR} \frac{1}{s} e^{-\frac{sx}{\sqrt{s\overline{G}(s)}}} e^{st}\, ds \tag{6.22}$$

is a probability distribution function for these three cases. Therefore

$$w(x,t) = \frac{\partial W(x,t)}{\partial t} = \lim_{R\to\infty} \int_{a-iR}^{a+iR} e^{-\frac{sx}{\sqrt{s\overline{G}(s)}}} e^{st}\, ds \tag{6.23}$$

is a probability density function.

The graphs in Fig.[6-12] are about $p_m(x,t)$ with

$$\overline{p_m}(x,s) = \frac{1 - e^{-2st_0}}{2s} \frac{\pi^2}{\pi^2 + s^2 t_0^2} e^{-\frac{sx}{\sqrt{s\overline{G}(s)}}}, \tag{6.24}$$

with an input given by the pulse function (6.14), rather than a step function. The behavior of the various equations are connected through the ordinary convolution theorem for Laplace transforms. Since $p_m(0,t) \geq 0$, it follows that if $w(x,t)$ is given by equation (6.23) for any $G(t)$ in the classes described, then

$$p_m(x,t) = p_m(0,t) * w(x,t), \tag{6.25}$$

where the $*$ denotes convolution which is defined as

$$f * g = \int_0^t f(t-\tau)g(\tau)\,d\tau.$$

and so $p_m(x,t) \geq 0$ if both $p_m(o,t)$ and $w(x,t)$ are positive.

Suppose now we consider the perturbed equation with $\eta \neq 0$. If the behavior of the kernel is dominated by the values near $s = 0$, then η should have little effect. In any case continuity arguments should ensure that for η sufficiently small, there should be little effect. The question is whether or not as η increases, the behavior of $p_m(x,t)$ will change and no longer remain completely positive. Fig.[6-4], [6-6] and [6-11] show that for the classes of relaxation functions described above, that this is so. For η sufficiently small, $p_m(x,t) \geq 0$, but as η increases, the tail oscillates. One may then conclude that the radial inertia term η does alter the wave propagation properties for fluid filled tubes from those found for rods.

In certain cases above we have managed to show analytically the occurrence of oscillatory solutions as η increases. For the case described by equation (5.6) we can consider the two extreme cases for step input. If $\xi = 0$, and $\hat{\eta} = \xi + \eta = 0$ in equation (5-1), then following Pipkin, $W(x,t)$ is a probability distribution function for each $0 < x,\ t < \infty$. If on the other hand, $\tau = 0$, $\hat{\eta} = \xi + \eta \neq 0$, we have the standard Love approximation solution for wave propagation in a bar with

$$W(x,t) \sim \left(\int_0^{\tau_1} A_i(-q)\,dq + \frac{1}{3}\right) + O(\frac{1}{\sqrt{t}}), \tag{6.26}$$

where

$$\tau_1 = \frac{(t-x)}{(\frac{3}{2}x\hat{\eta})^{1/3}}, \tag{6.27}$$

see Miklowitz [25] for detail of the equations.

This solution displays oscillation about the elementary step solution.

In the other cases we have to rely on numerical results. There are similarities in the various cases. Suppose we write

$$s\overline{G}(s) + \eta s^2 = a + bs^p + cs^2, \quad 0 < p \leq 1, \tag{6.28}$$

and consider equation (5.1) for a step input. Then, to illustrate the various cases we can in turn set $b = 1,\ c = 0$ to give Pipkin's case and then $b = 0,\ c = 1$ to give oscillatory case. $a = 0,\ 1$ depending on whether we consider $G_\infty = 0$, or not respectively. $0 < p < 1$ and $p = 1$ are considered as separate cases. The results are shown in Fig.[6-13] to Fig.[6-21].

Figs.[6-20] and [6-21] attempt to describe the case $p = 1,\ a = 0$ that $s\overline{G}(s) = bs,\ b > 0$. If $c = 0$, we have

$$\begin{aligned} W(x,t) &= \frac{1}{2\pi i}\int_{Br} e^{st - xs^{1/2}b^{-1/2}}\,\frac{ds}{s} \\ &= Erfc(\frac{x}{2\sqrt{bt}}), \end{aligned} \tag{6.29}$$

where $Erfc$ denotes the complementary error function with

$$Erfc(z) = \frac{2}{\sqrt{\pi}}\int_z^\infty e^{-u^2}\,du. \tag{6.30}$$

Clearly $W(x,t)$ increases monotonically to 1 as $t \to \infty$, but the increase is extremely slow as can be seen from Fig.[6-20]. At the opposite extreme when $b = 0,\ c \neq 0$, the exact solution is

$$W(x,t) = H(t)e^{-x/\sqrt{c}}. \tag{6.31}$$

This last result indicates the infinite wave speed associated with the approximating equation and emphasizes that the signal decays exponentially with x so that at large x the amplitide is negligible.

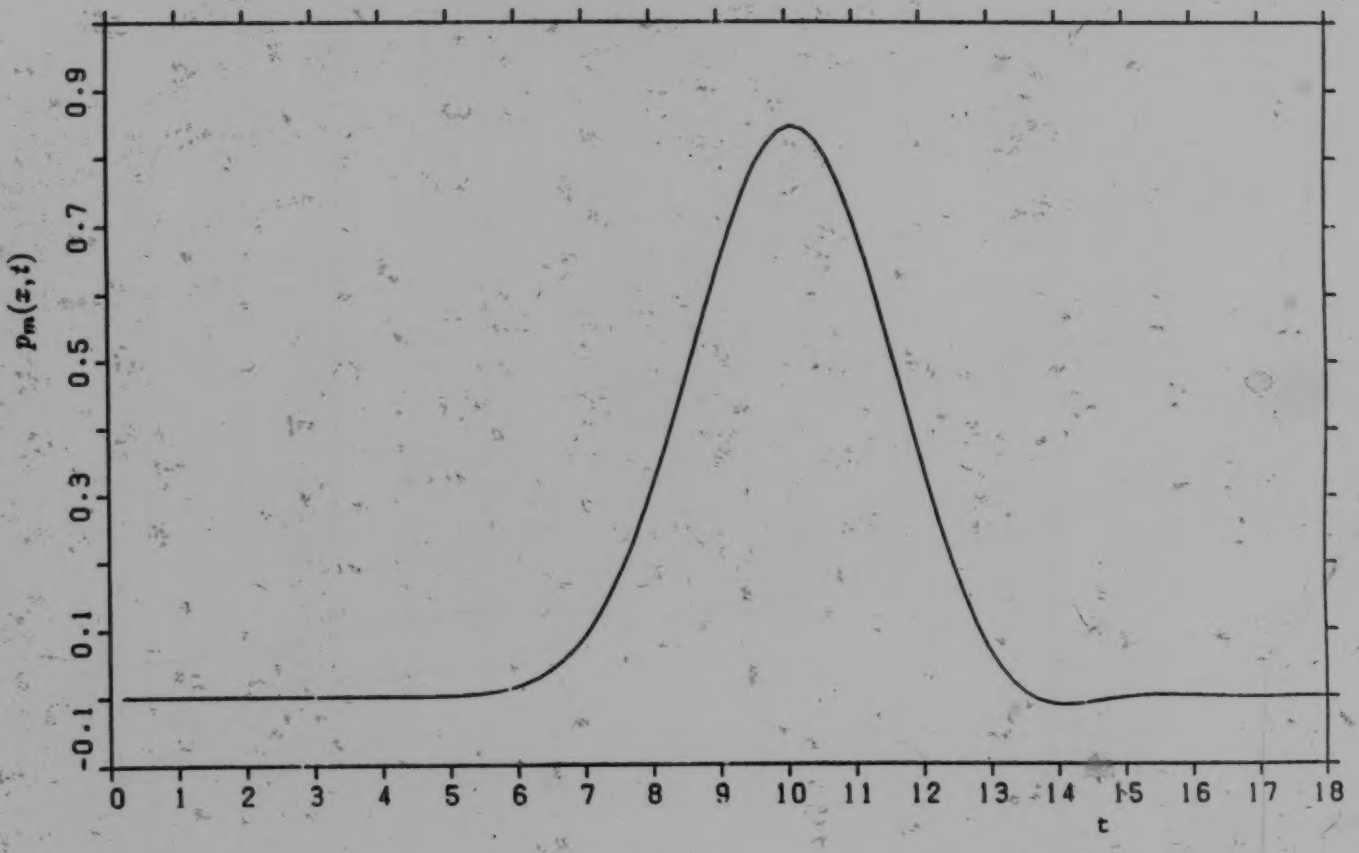

Fig.[6-1]. The graph of $p_m(x,t)$ with $\Omega(s) = \frac{s}{\sqrt{1+\tau s+\eta s^2}}$ at $x = 6cms$, $\tau = 9 * 10^{-5}$, $\eta = 0.173125$.

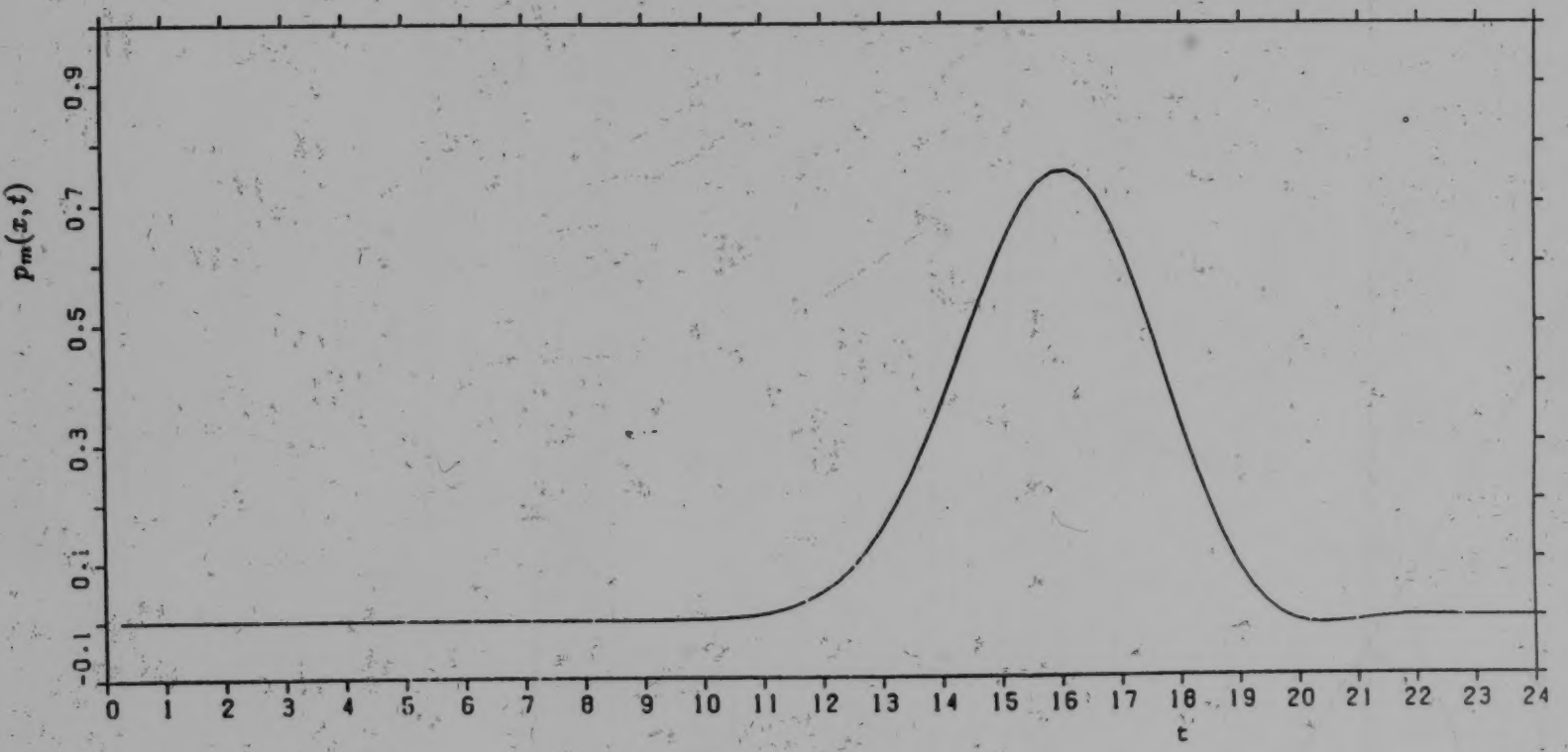

Fig.[6-2]. The graph of $p_m(x,t)$ with $\Omega(s) = \dfrac{s}{\sqrt{1+\tau s+\eta s^2}}$ at $x = 11cms$, $\tau = 9 * 10^{-5}$, $\eta = 0.173125$.

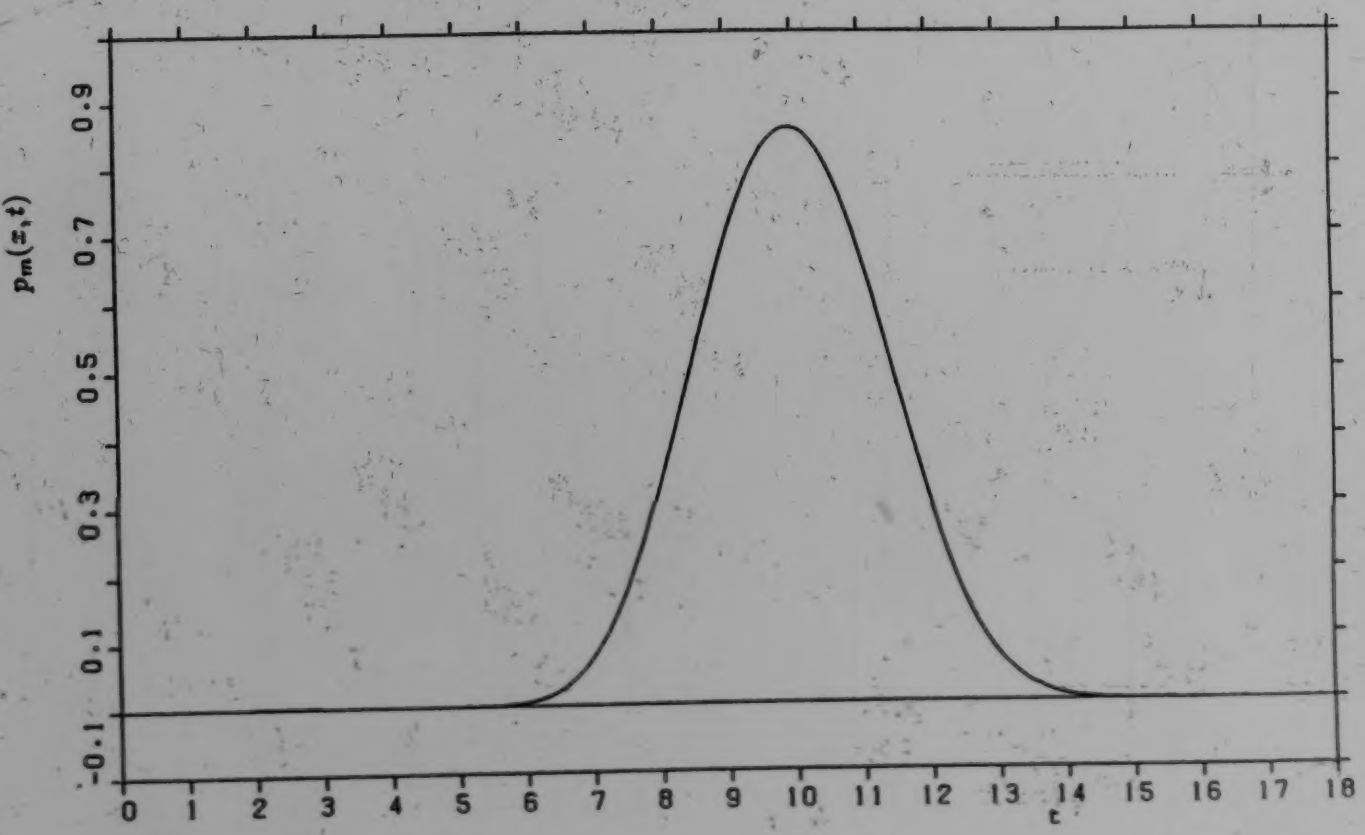

Fig.[6-3]. The graph of $p_m(x,t)$ with $\Omega(s) = \frac{s}{\sqrt{1+\tau s}}$ at $x = 6cms$, $\tau = 9 * 10^{-5}$.

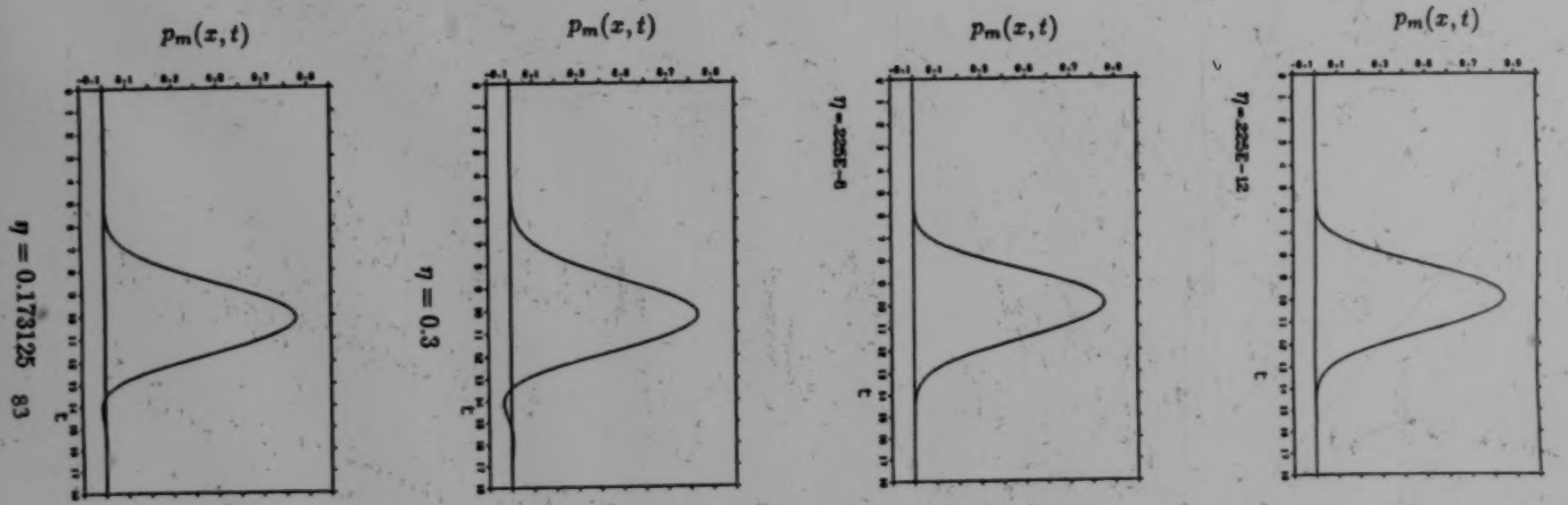

Fig.[6-4]. The graphs of $p_m(x,t)$ with $\Omega(s) = \dfrac{s}{\sqrt{1+\tau s+\eta s^2}}$ at $x = 6cms$, $\tau = 9 * 10^{-5}$, and different choices of η.

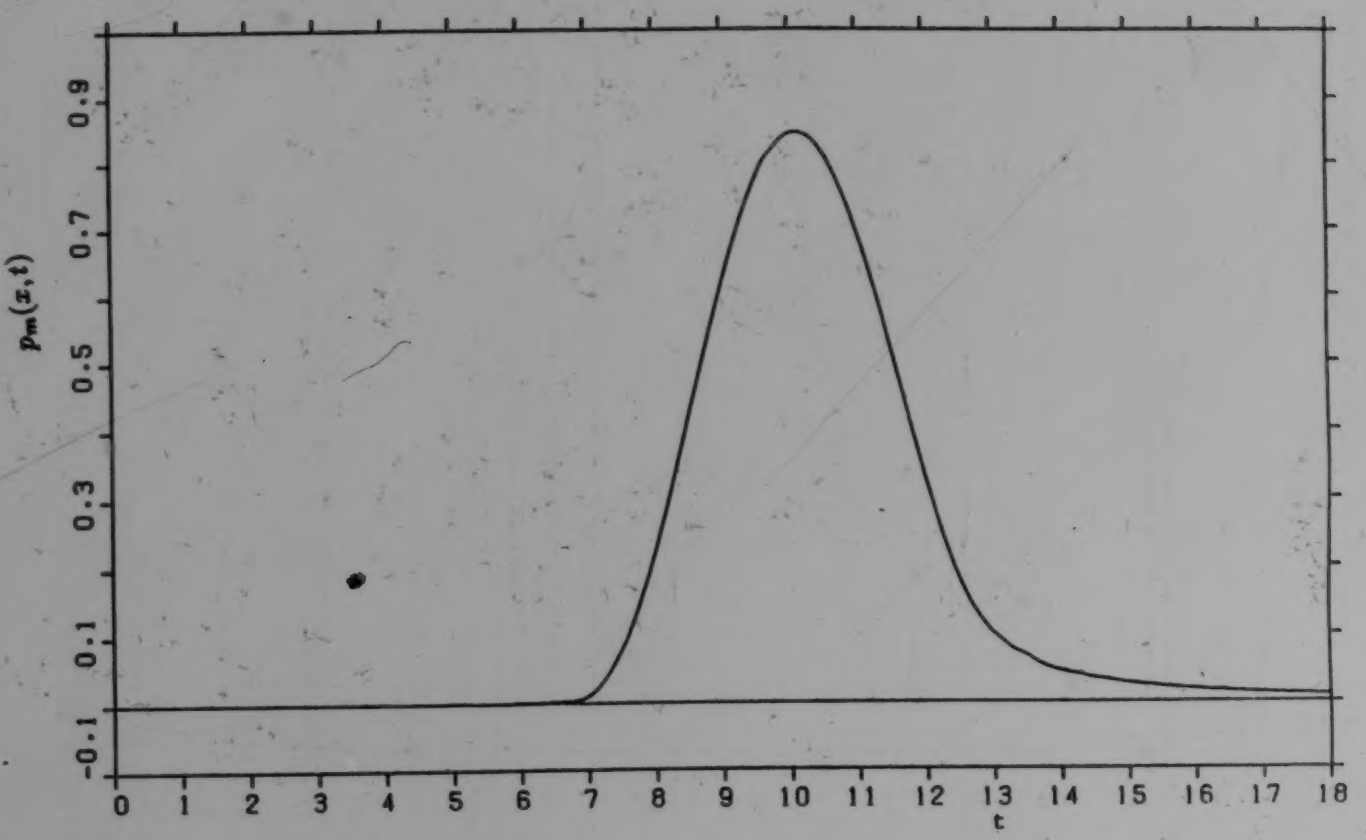

Fig.[6-5]. The graph of $p_m(x,t)$ with $\Omega(s) = \frac{s}{\sqrt{\hat{c}s^p}}$ at x=6cms, $\hat{c}$=1, p=0.05.

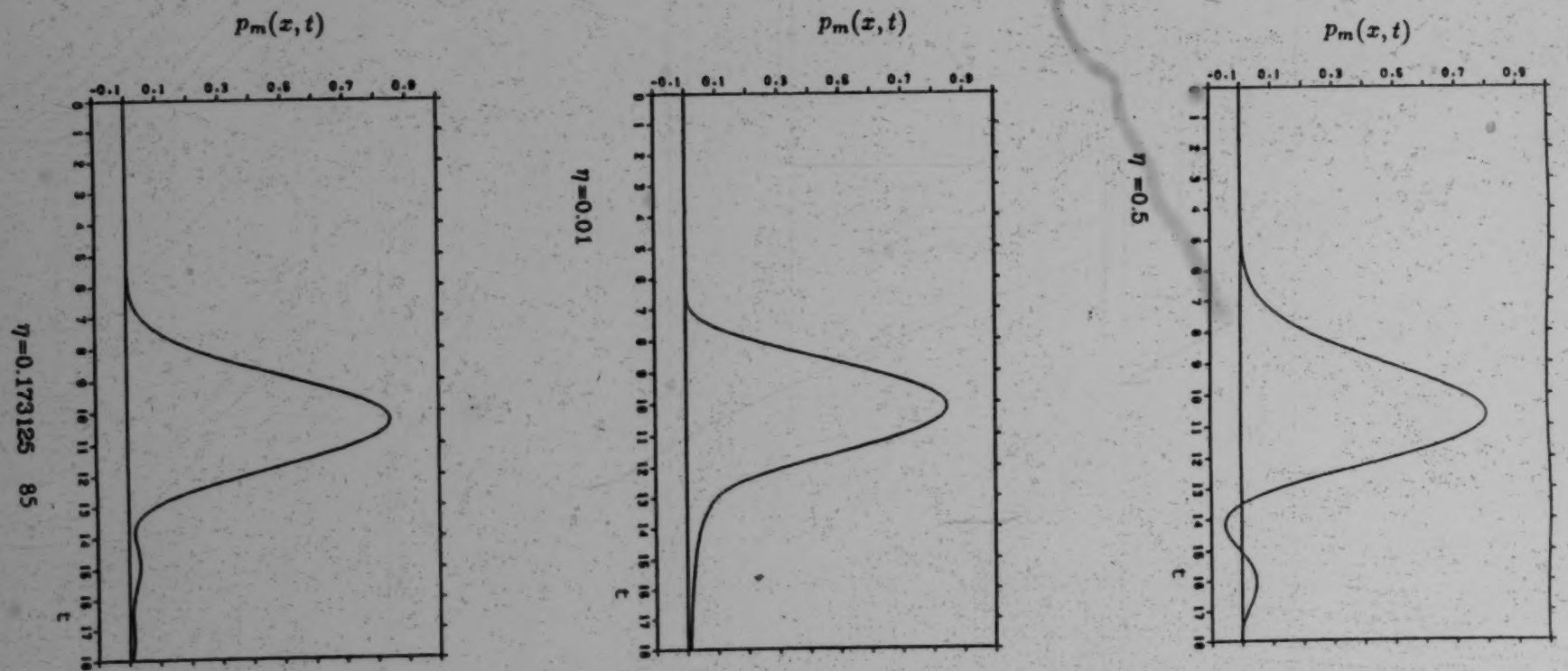

Fig.[6-6]. The graphs of $p_m(x,t)$ with $\Omega(s) = \frac{s}{\sqrt{\hat{c}s^2 + \eta s^2}}$ at x=6cms, $\hat{c}$=1, p=0.05 for various η.

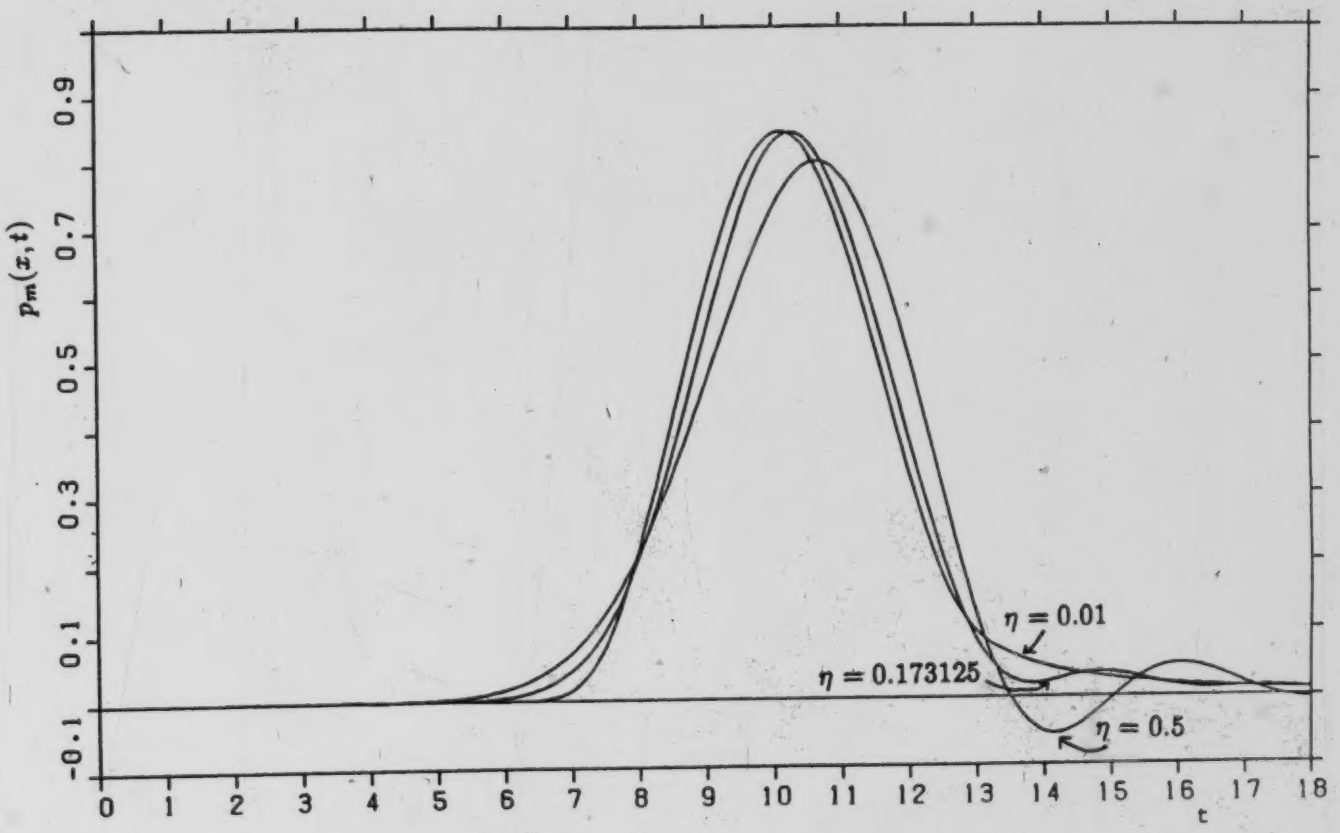

Fig.[6-6]. The graphs of $p_m(x,t)$ with $\Omega(s) = \frac{s}{\sqrt{\hat{c}s^p + \eta s^2}}$ at x=6cms, $\hat{c}$=1, p=0.05 for various η.

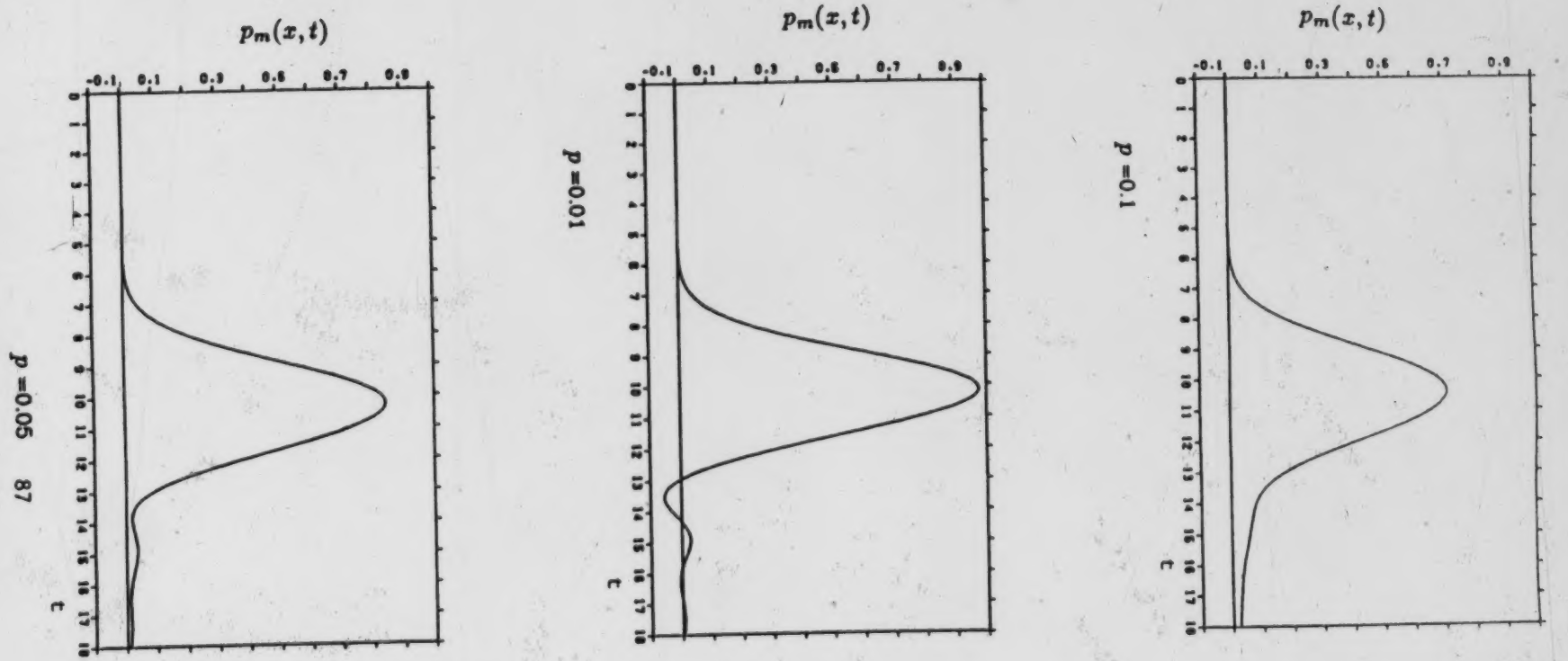

Fig.[6-7]. The graphs of $p_m(x,t)$ with $\Omega(s) = \frac{s}{\sqrt{\hat{c}s^p + \eta s^2}}$ at x=6cms, $\hat{c}$=1, η=0.173125 for various p.

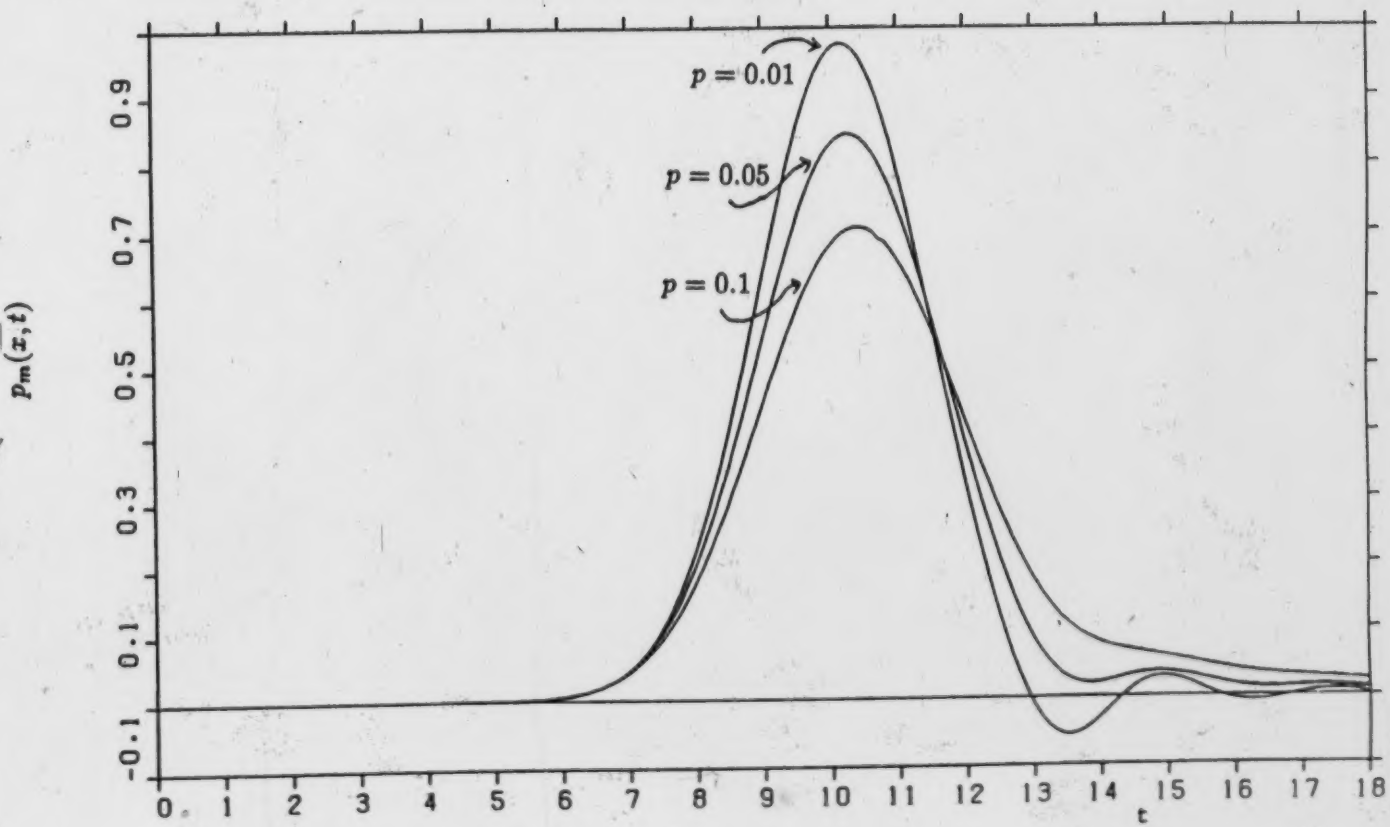

Fig.[6-7]. The graphs of $p_m(x,t)$ with $\Omega(s) = \frac{s}{\sqrt{\hat{c}s^p + \eta s^2}}$ at x=6cms, $\hat{c}$=1, η=0.173125 for various p.

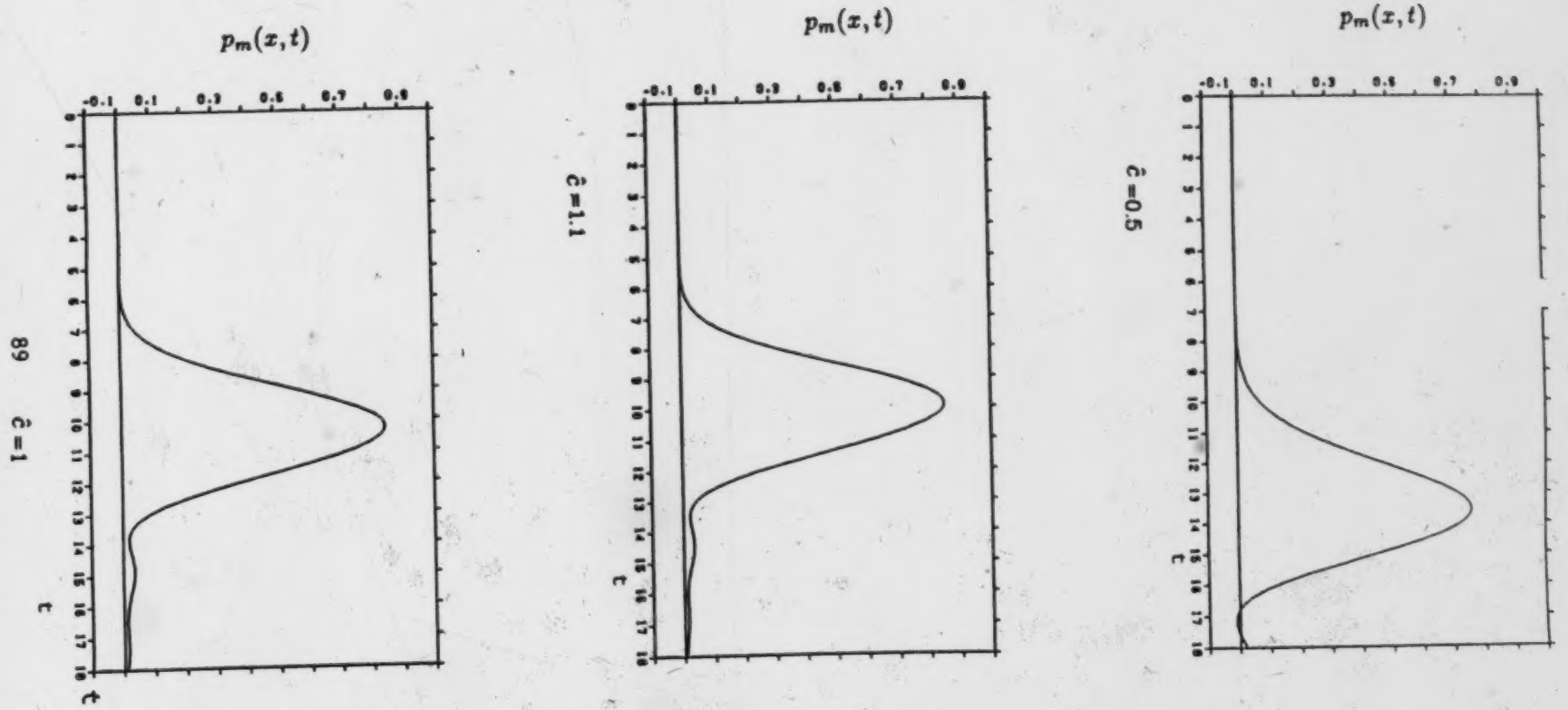

Fig.[6-8]. The graphs of $p_m(x,t)$ with $\Omega(s) = \dfrac{s}{\sqrt{\hat{c}s^p + \eta s^2}}$ at x=6cms, p=0.05, η=0.173125 for various $\hat{c}$.

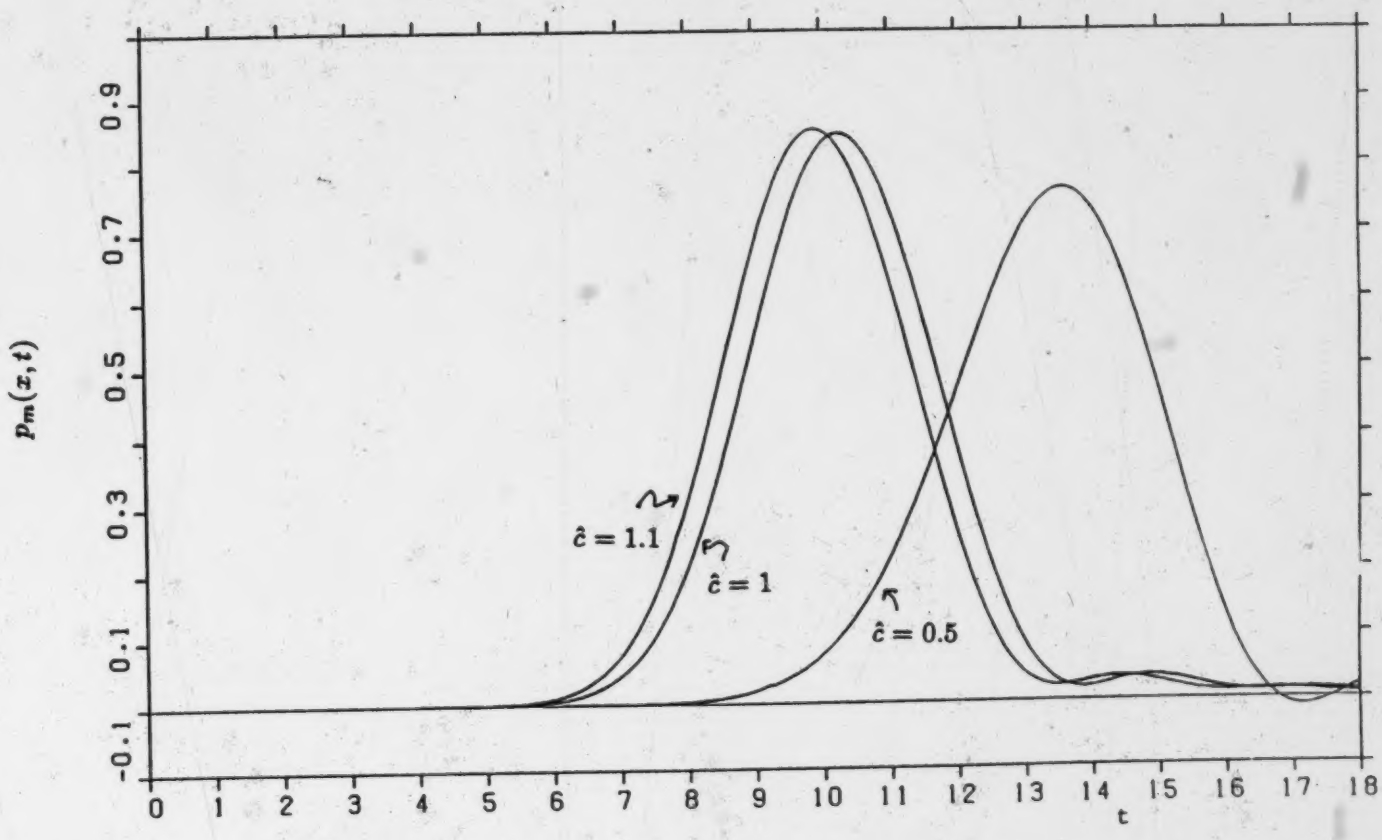

Fig.[6-8]. The graphs of $p_m(x,t)$ with $\Omega(s) = \dfrac{s}{\sqrt{\hat{c}s^p + \eta s^2}}$ at x=6cms, p=0.05, η=0.173125 for various $\hat{c}$.

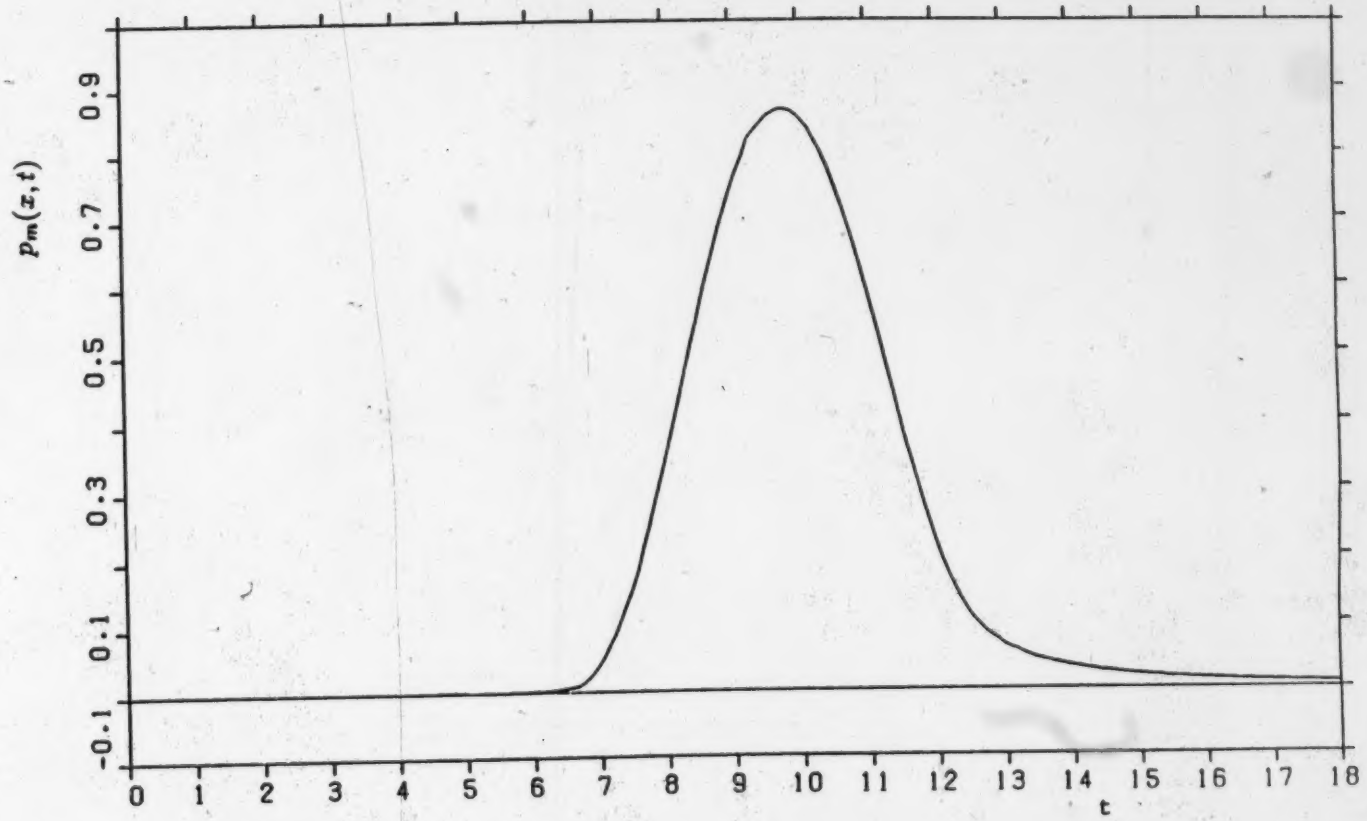

Fig.[6-9]. The graph of $p_m(x,t)$ with $\Omega(s) = \dfrac{s}{\sqrt{G_\infty + s^p + \eta s^2}}$ at x=6cms, p=0.05, G_∞=0.1, η=0.

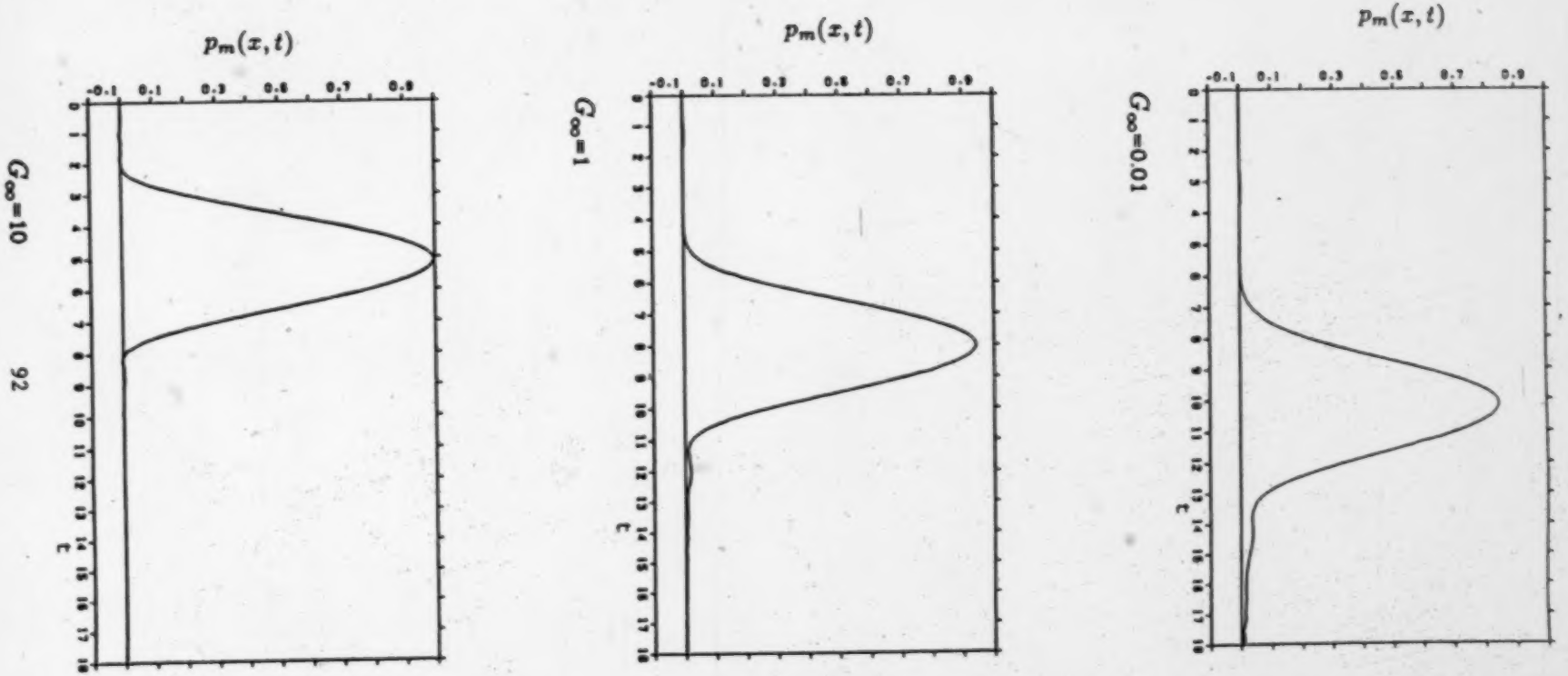

Fig.[6-10]. The graphs of $p_m(x,t)$ with $\Omega(s) = \frac{s}{\sqrt{G_\infty + s^p + \eta s^2}}$ at x=6cms, p=0.05, η=0.1 and various G_∞.

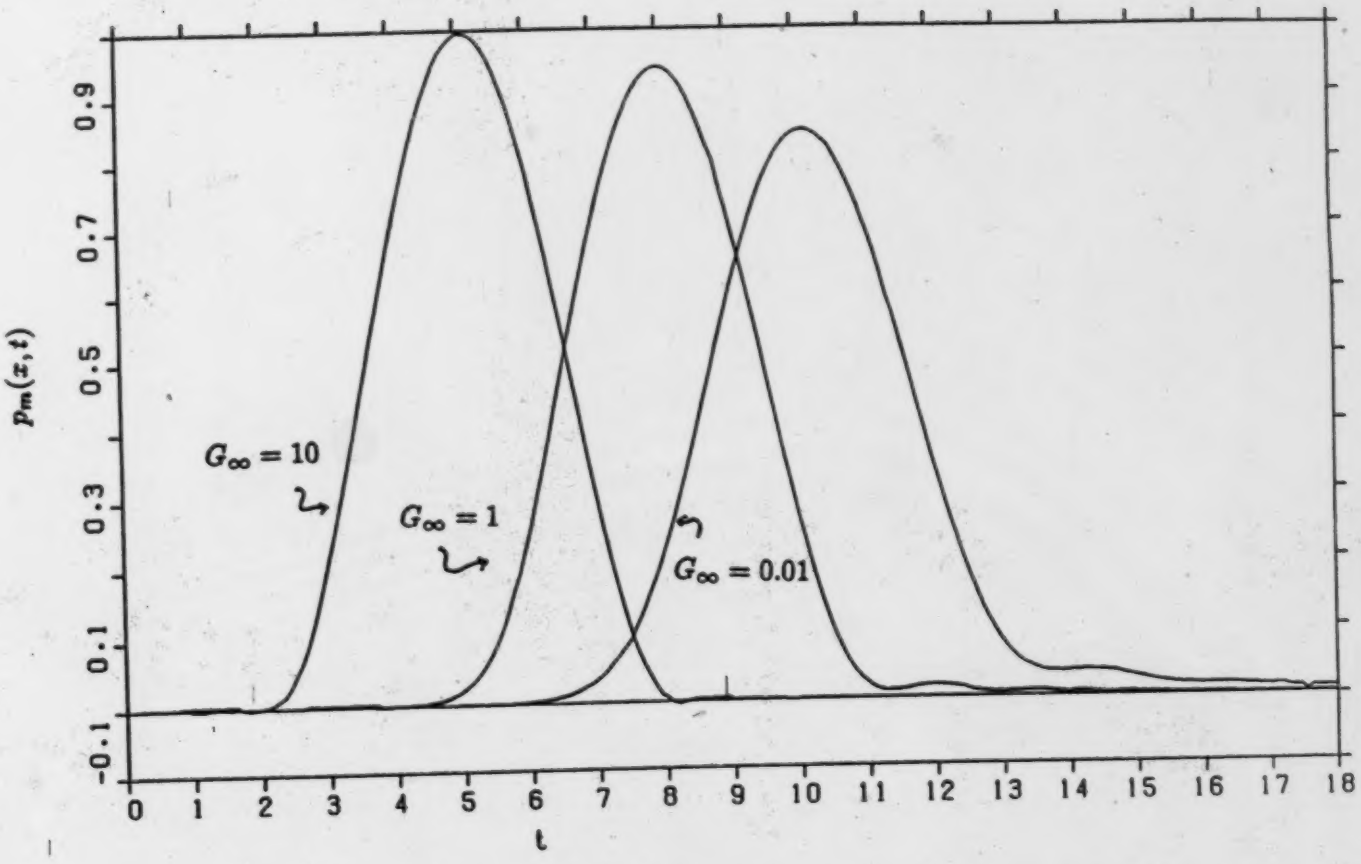

Fig.[6-10]. The graphs of $p_m(x,t)$ with $\Omega(s) = \dfrac{s}{\sqrt{G_\infty + s^p + \eta s^2}}$ at x=6cms, p=0.05, η=0.1 and various G_∞.

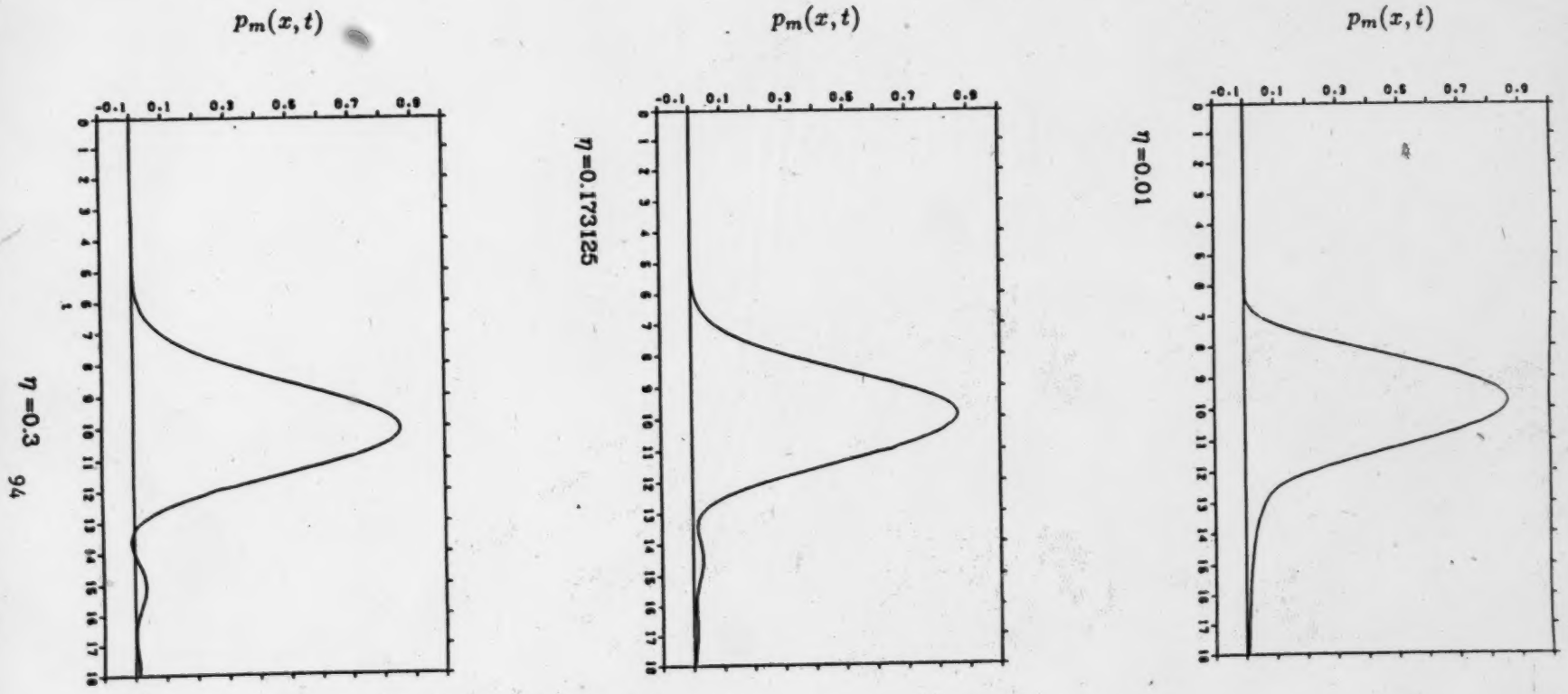

Fig.[6-11]. The graphs of $p_m(x,t)$ with $\Omega(s) = \dfrac{s}{\sqrt{G_\infty + s^p + \eta s^2}}$ at x=6cms, p=0.05, G_∞=0.1 and various η.

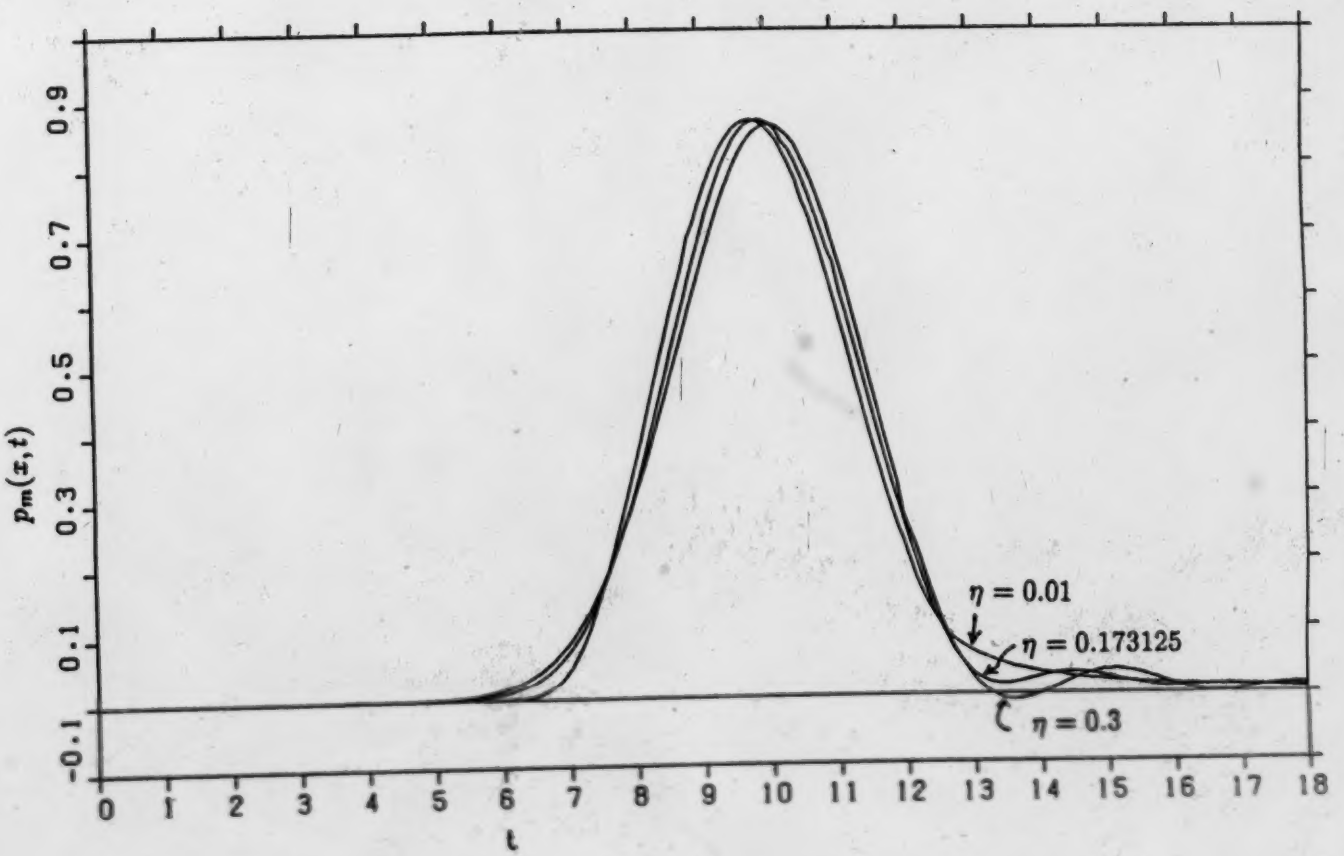

Fig.[6-11]. The graphs of $p_m(x,t)$ with $\Omega(s) = \dfrac{s}{\sqrt{G_\infty + s^p + \eta s^2}}$ at x=6cms, p=0.05, G_∞=0.1 and various η.

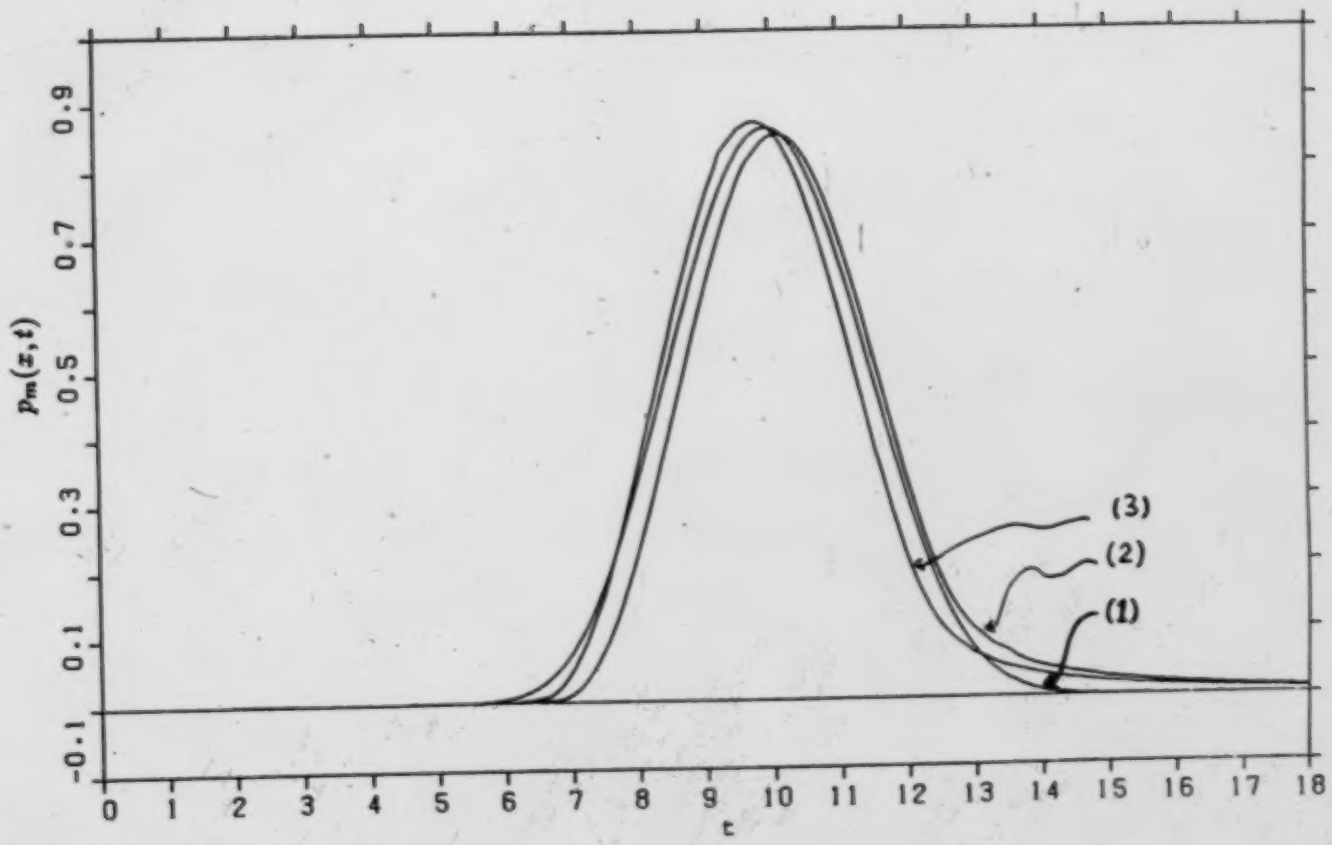

Fig.[6-12]. Figs.[6-3], [6-5] & [6-9] on one axis of coordinates.

(1). $p_m(x,t)$ with $\Omega(s) = \frac{s}{\sqrt{1+\tau s}}$ at $x = 6cms$, $\tau = 9*10^{-5}$.

(2). $p_m(x,t)$ with $\Omega(s) = \frac{s}{\sqrt{\hat{c}s^p}}$ at x=6cms, $\hat{c}$=1, p=0.05.

(3). $p_m(x,t)$ with $\Omega(s) = \frac{s}{\sqrt{G_\infty + s^p + \eta s^2}}$ at x=6cms, p=0.05, G_∞=0.1, η=0.

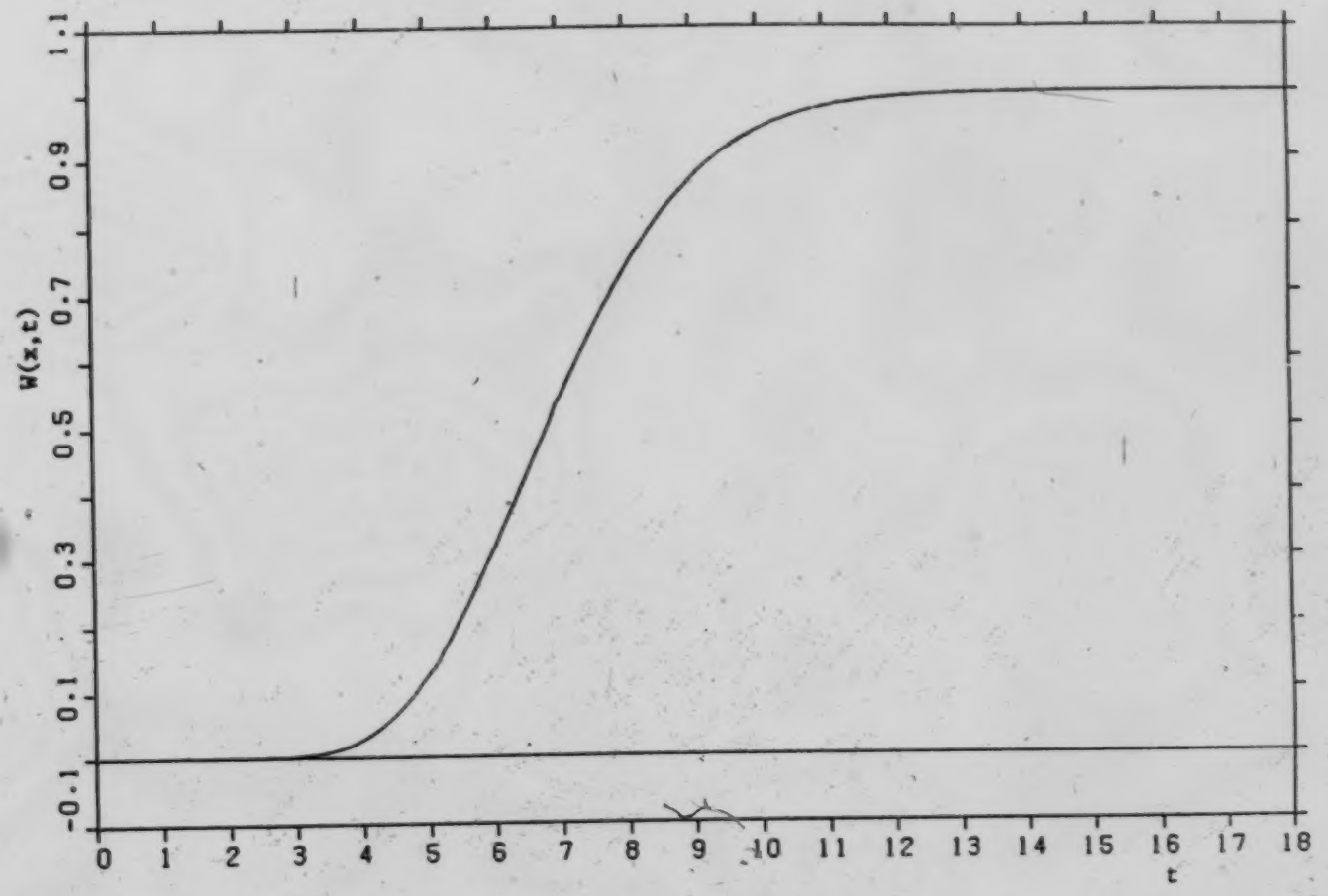

Fig.[6-13]. W(x,t) with step input and $s\overline{G}(s) = 1 + s$, at $x = 6$.

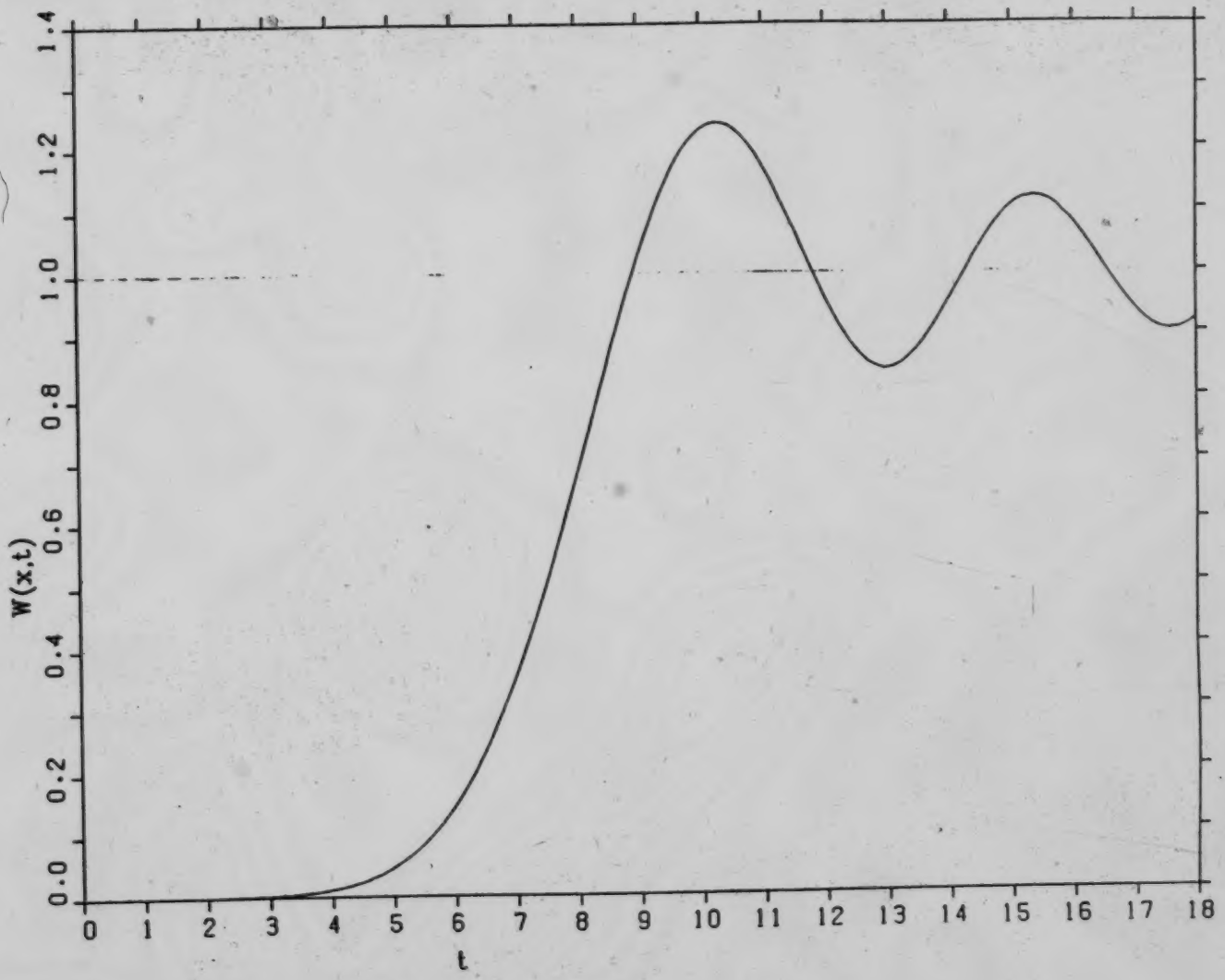

Fig.[6-14]. W(x,t) with step input and $s\overline{G}(s) = 1 + s^2$, at $x = 6$.

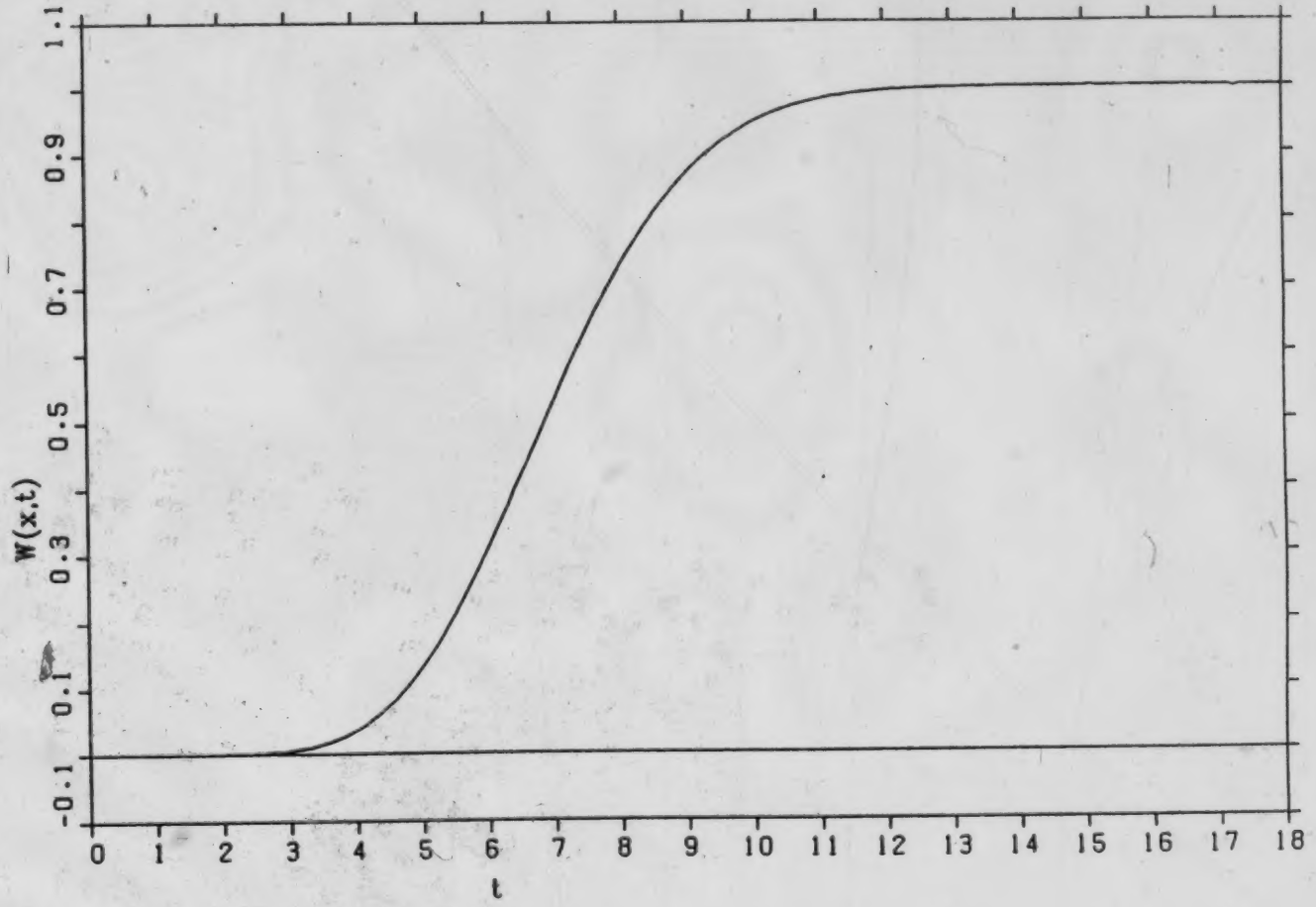

Fig.[6-15]. W(x,t) with step input and $s\overline{G}(s) = 1 + s + \frac{1}{4}s^2$, at $x = 6$.

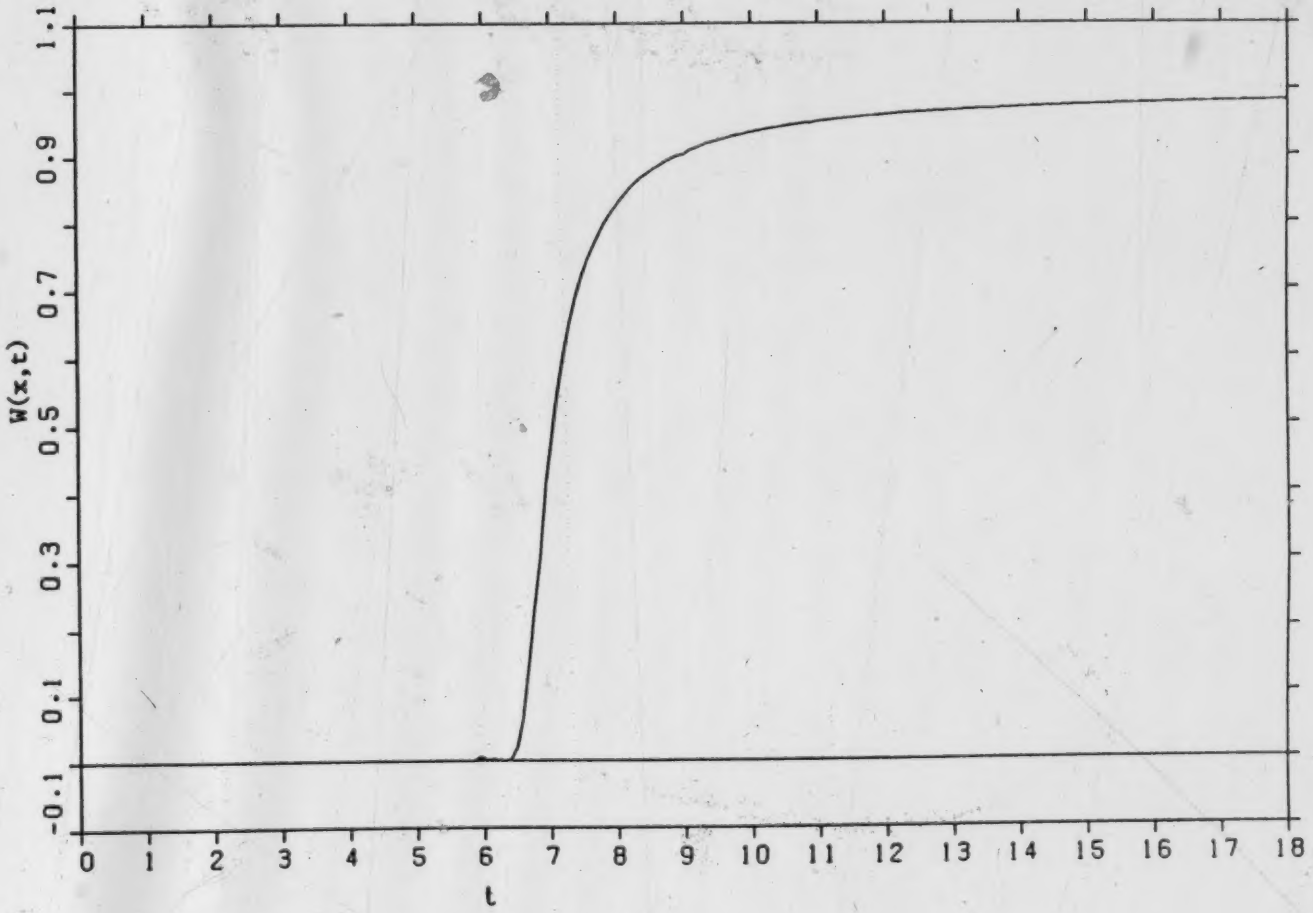

Fig.[6-16]. W(x,t) with step input and $s\overline{G}(s) = s^p$, at $x = 6$. p= 0.05.

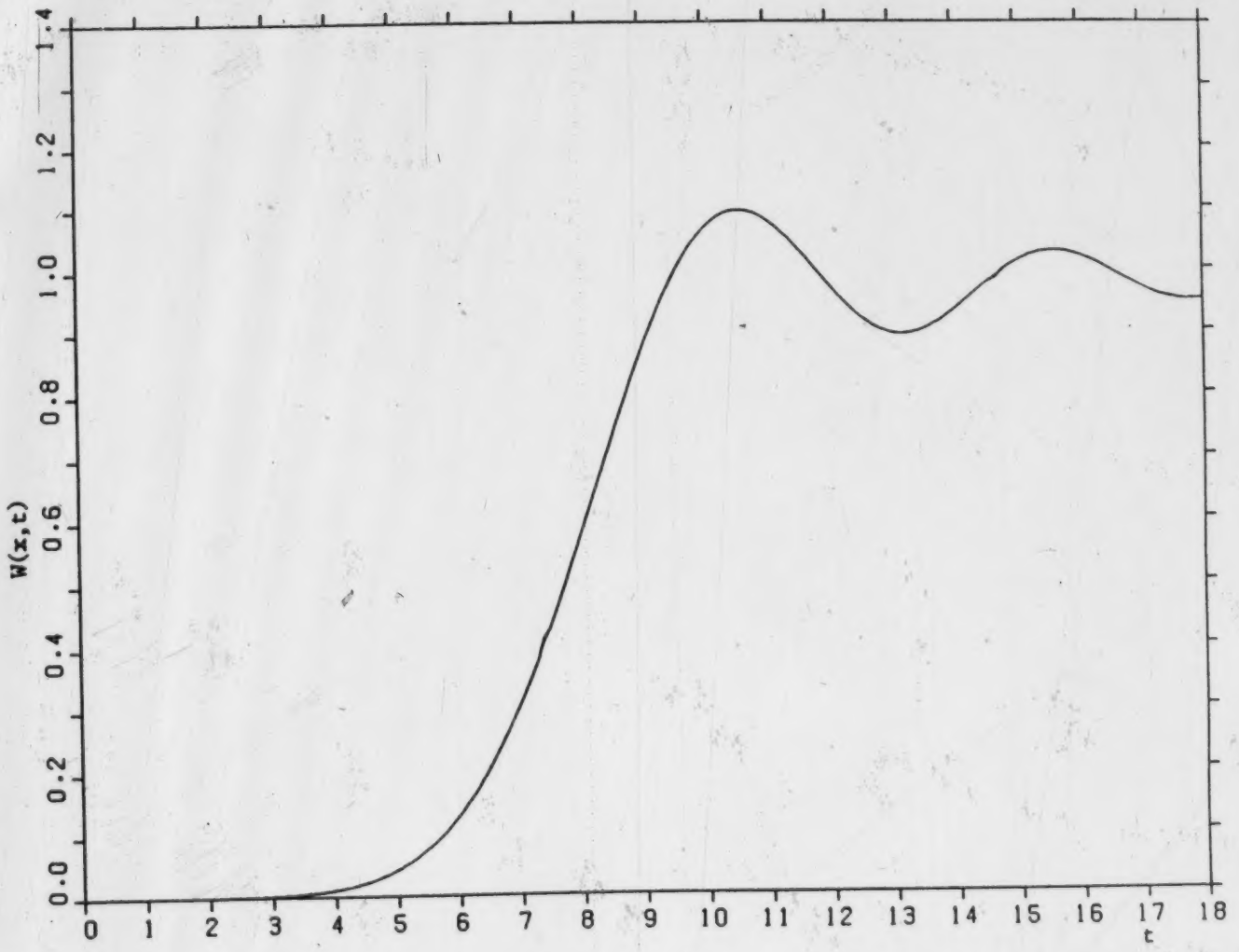

Fig.[6-17]. W(x,t) with step input at $s\overline{G}(s) = s^p + s^2$, $x = 6$, p = 0.05.

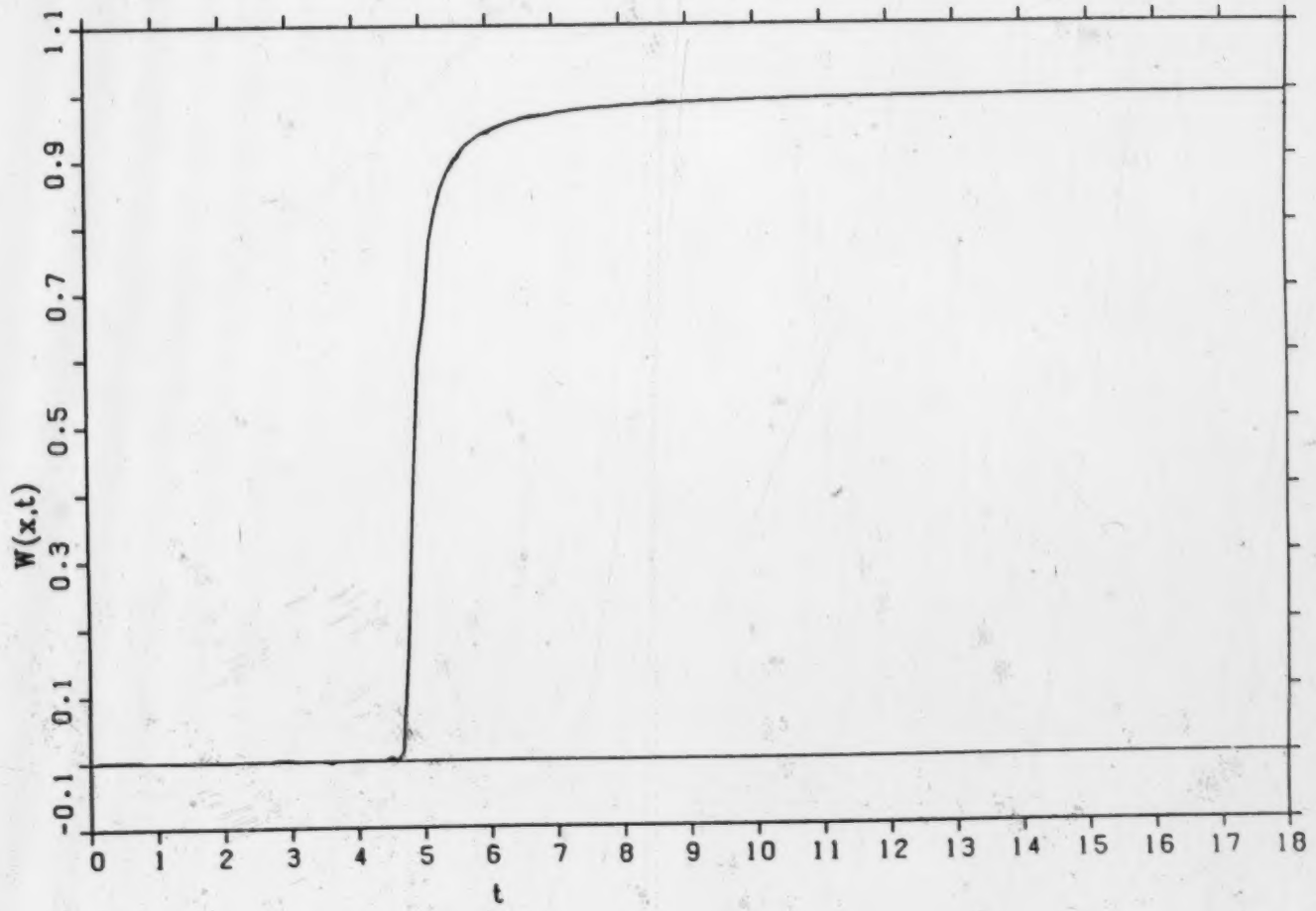

Fig.[6-18]. W(x,t) with step input and $s\overline{G}(s) = 1 + s^p$, at $x = 6$. p = 0.05.

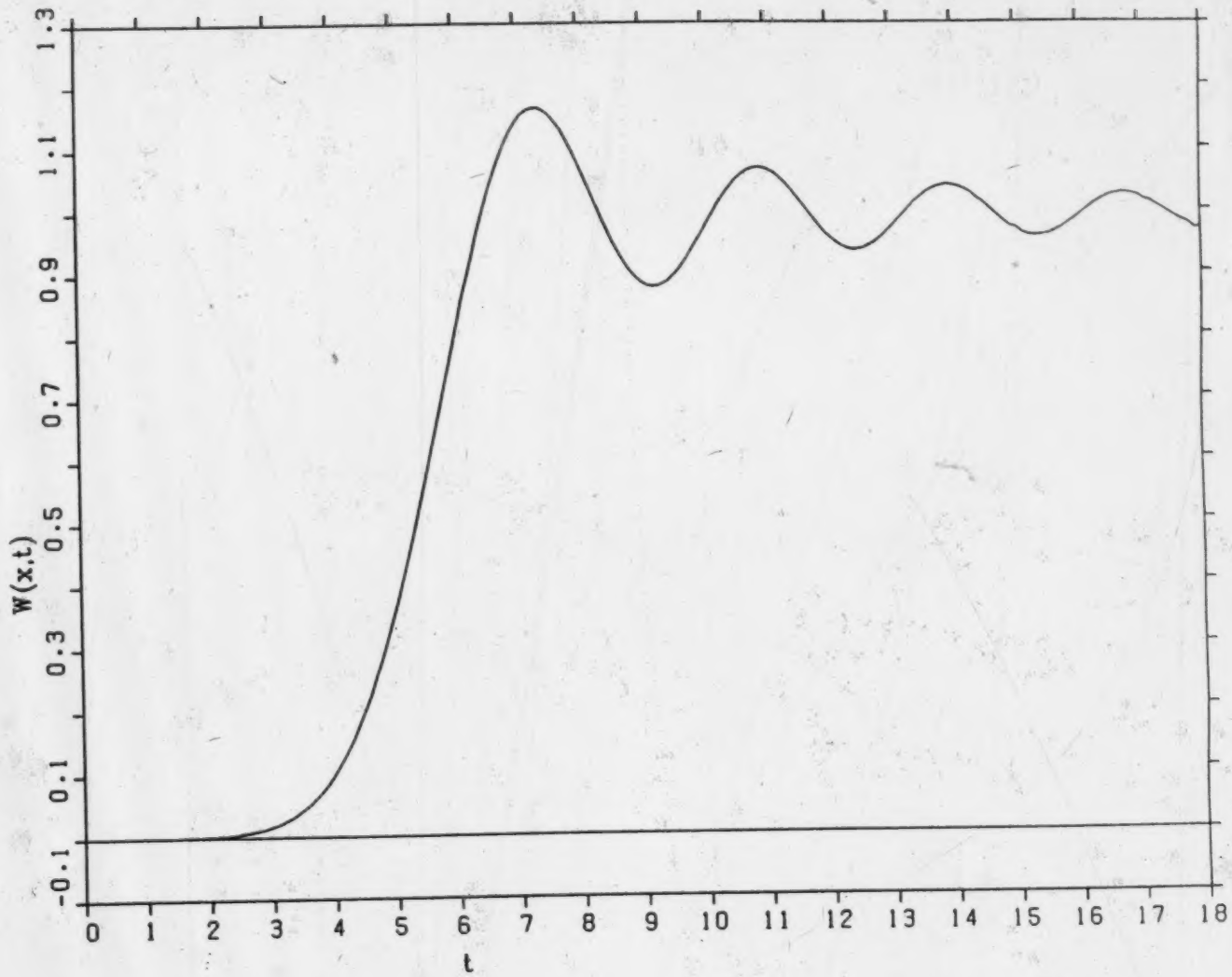

Fig.[6-19]. W(x,t) with step input and $s\overline{G}(s) = 1 + s^p + s^2$, at $x = 6$. p= 0.05.

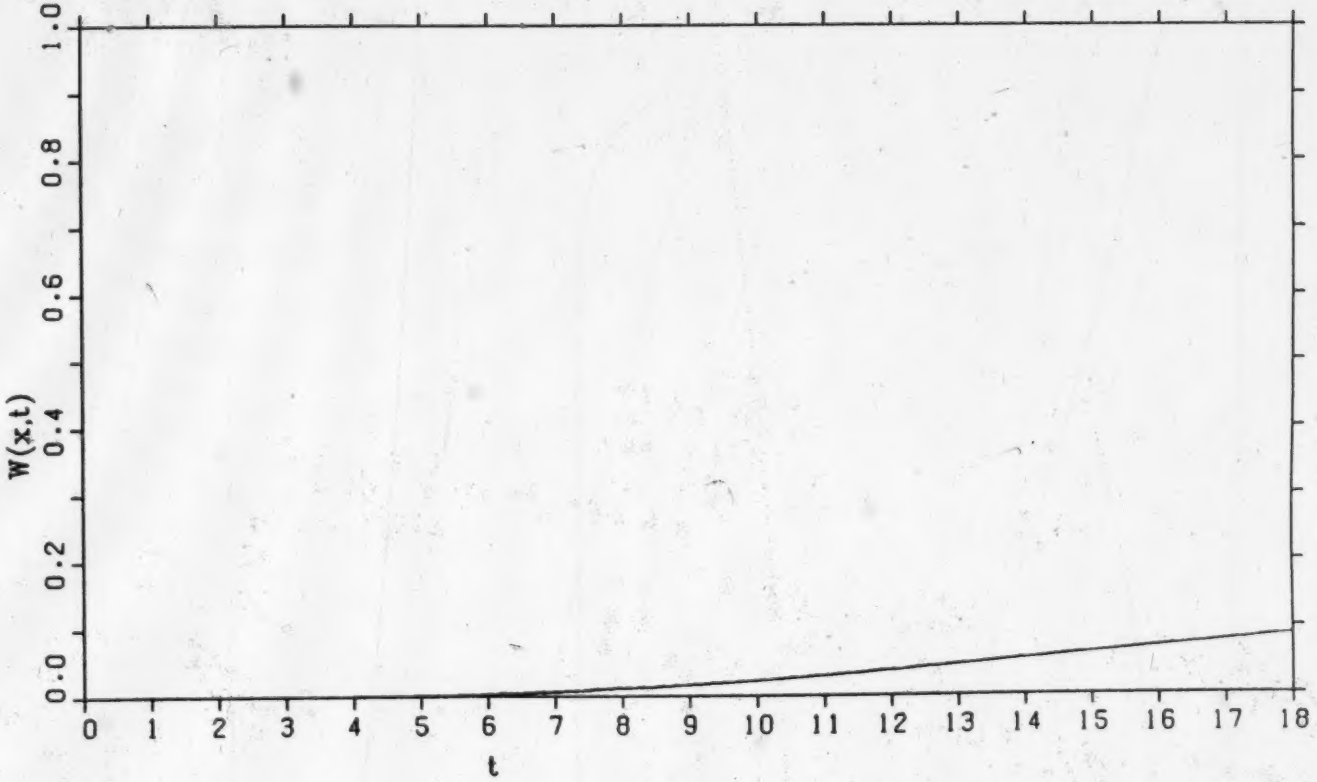

Fig.[6-20]. W(x,t) with step input and $s\overline{G}(s) = s$, at $x = 6$.

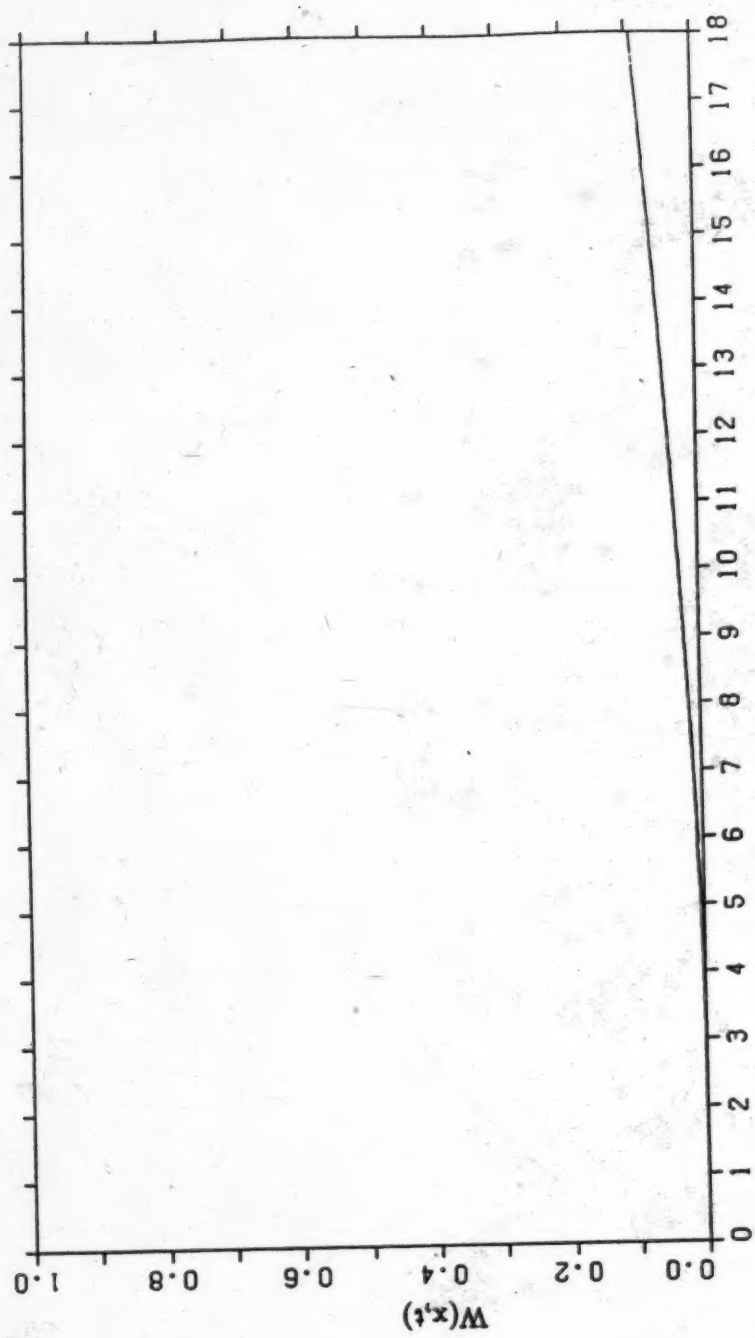

Fig.[6-21]. W(x,t) with step input and $s\overline{G}(s) = s + s^2$, at $x = 6$.

Bibliography

[1]. Euler,L., *Principia pro motu sanguins per arterias determinado,* Opera Posthuma Mathematica et Physica,Vol II, ediderunt P.H. Fess et N.Fess. Petropoli: 1862. Reprinted Nendeln, Liechtenstein: Kraus, 1969, p814-823.

[2]. Skalak,R., *Wave propagation in blood flow biomechanics.* Symp. Appl. Mech. Div. ASME (Fung,Y.C. ed) p20-46.

[3]. Skalak,R., Keller, S.R., Secomb, T.W. *Mechanics of blood flow.* J. Biomech. Engng. V103, 1981, p102-115.

[4]. Fung,Y.C., *Properties of Biological Fluids and Solids; Mechanics of Tissues and Organs.* American Society of Mechanical Engineers, New York, 1973.

[5]. Caro,C.G., Pedley,T.J., Schroter,R.C., Seed,W.A., *The Mechanics of the Circulation.* Oxford University Press, 1978.

[6]. Lighthill,M.J., *Waves in Fluids.* Cambridge University Press, 1978.

[7]. Tait,R.J, Moodie,T.B., Haddow,J.B., *On radial motion of a non-linear viscoelastic tube.* Quarterly Appli. Math. Vxiii. Jan.1985. No.4.

[8]. Swaters, G.E., *Resonant three-wave interactions in non-linear hyper-elastic fluid-filled tubes.* ZAMP 39, p668-681, 1988.

[9]. Rubinow,S.I., Keller,J.B., *Wave propagation in a fluid-filled tube.* J. Acoust. Soc. Am. 50, 198(1971).

[10]. Rubinow,S.I., Keller,J.B., *Wave propagation in a viscoelastic tube containing a viscous fluid.* J. Fluid Mech. 88, 181(1978).

[11]. Moodie,T.B., Tait,R.J., Haddow,J.B., *Wave propagation in a fluid filled elastic tube.* Acta Mechanica. 38, p123-134 (1982).

[12]. Moodie,T.B., Barclay,B.W., Greenwald,S.E., *Impulse propagation in liquid filled distensible tubes: Theory and experiment for intermediate to long wavelengths.* Acta Mechanica 59, p47-58 (1986).

[13]. Greenwald,S.E., Newman,D.L., *Impulse propagation in normal and stenosed vessels.* Cardiovasc. Res. 15, 190(1981).

[14]. Pipkin,A.C., *Lectures on Viscoelastic Theory.* Springer, New York, 1972.

[15]. Kolsky,H., *The propagation of stress pulses in viscoelastic solids.* Phil. Mag. 8 (ser. viii) 1(1956) p693-710.

[16]. Sawatzky,R.P., *Wave phenomena in fuild-filled distensible tube: dispersion, dissipation and reflection.* Ph.D. Thesis in Department of Mathematics, University of Alberta, 1987.

[17]. Lockett,F.J., *Nonlinear Viscoelastic Solid.* Academic Press, 1972.

[18]. Crump,K.S., *Numerical inversion of Laplace transforms using a Frouier series approximation.* J. of Associ. for Cmput Mach. V23, No.1, Jan. 1976, p89-96.

[19]. Pipkin,A.C., *Asymptotic behavior of viscoelastic waves.* Q. J. Mech. Appl. Math., V41, Pt.1, 1988.

[20]. Feller,W., *An Introduction to Probability Theory and its Applications.* Vol.II, Wiley, New York, 1957.

[21]. Bleistein,N., Handelsman,R.A., *Asymptotic Expansions of Integrals.* Holt, Rinehart and Winston, 1975.

[22]. Widder.D.V., *The Laplace Transform.* Princeton University Press, 1946.

[23]. Macdonald,J.R., *Accelerated convergence, divergence, iteration, extrapolation, and curve fitting.* J. of Appl. Phys. V35, No.10, Oct. 1964, p3034-3041.

[24]. Boas,R.P., *Invitation to Complex Analysis.* Random House, New York, 1987.

[25]. Miklowitz,J., *The Theory of Elastic Waves and Waveguides.* North Holland, 1987.